

Improved initial design through better initial assumptions regarding load distribution

A study of analytical and numerical methods for structural systems of buildings

Master's Thesis in the Master's Programme Structural engineering and building technology

AXEL HARALDSSON
SVANTE SEVERINSSON

MASTER'S THESIS BOMX02-16-45

Improved initial design through better initial assumptions regarding load distribution

A study of analytical and numerical methods for structural systems of buildings

Master's Thesis in the Master's Programme Structural engineering and building technology

AXEL HARALDSSON

SVANTE SEVERINSSON

Department of Civil and Environmental Engineering

Division of Structural engineering

Concrete structures

CHALMERS UNIVERSITY OF TECHNOLOGY

Göteborg, Sweden, 2016

Improved initial design through better initial assumptions regarding load distribution
A study of analytical and numerical methods for structural systems of buildings

Master's Thesis in the Master's Programme Structural engineering and building technology

AXEL HARALDSSON

SVANTE SEVERINSSON

© AXEL HARALDSSON & SVANTE SEVERINSSON, 2016

Examensarbete BOMX02-16-45/ Institutionen för bygg- och miljöteknik,
Chalmers tekniska högskola 2016

Department of Civil and Environmental Engineering
Division of Structural engineering
Concrete structures
Chalmers University of Technology
SE-412 96 Göteborg
Sweden
Telephone: + 46 (0)31-772 1000

Cover:

Distribution of vertical reaction forces in initial and final calculations.

Department of Civil and Environmental Engineering, Göteborg, Sweden, 2016

Improved initial design through better initial assumptions regarding load distribution

A study of analytical and numerical methods for structural systems of buildings

Master's thesis in the Master's Programme Structural engineering and building technology

AXEL HARALDSSON

SVANTE SEVERINSSON

Department of Civil and Environmental Engineering

Division of Structural engineering

Concrete structures

Chalmers University of Technology

ABSTRACT

If a prefabrication manufacture is involved in the design of the structural system of a building it is common that the design process is divided into an initial and a final phase. In *Pyramiden* differences were observed between the reaction forces in the foundation in the initial and the final design. In an attempt to reduce the timespan of the building process the construction phase was initiated before the design phase was completed. As a result of this the foundation was based on initial and simplified calculations instead of the final structural design, which could result in a need to strengthen the foundation or find another structural solution to redirect the load path.

The purpose of this thesis was to identify uncertainties in the design of the structural system for buildings and their influence on the load distribution.

Through a case study of the building project *Pyramiden* horizontally loaded bracing members were identified as critical structural members with uncertainties regarding stiffness estimations in the initial calculation. Further investigations of the uncertainties influence on the load distribution were carried out through a parametric study. The result of the parametric study was a comparison of stiffness calculations performed by analytical methods based on Timoshenko beam theory and by numerical calculations in *FEM-design*. A comparison of wall elements with opening resulted in recommendations for estimating the stiffness of various configurations. In the parametric study it was also briefly investigated how interaction between wall elements influence the load distribution.

It was concluded that there existed possibilities to improve the stiffness estimation and the assumptions regarding distribution of reaction forces that should be considered in calculations of the horizontal load distribution. It was also concluded that there existed possibilities to improve the design process. The feasibility of using the accuracy of the FE-analysis to estimate stiffness of wall configurations together with the time efficient design process of the initial calculations should be considered. Finally, it was concluded that an increased collaboration between the involved parties would be beneficial for the design process and that the problem discussed in this thesis would be eliminated if the construction process were initiated after the completion of the final design of both the foundation and the structural system.

Key words: Assumptions, initial design, load distribution, stiffness, wall with openings, FEM-design, Rymdknäckning

Förbättrad initial design genom bättre initiala antaganden angående last fördelning
En studie av analytiska och numeriska metoder för bärande system i byggnader

Examensarbete inom masterprogrammet Structural engineering and building
technology

AXEL HARALDSSON

SVANTE SEVERINSSON

Institutionen för bygg- och miljöteknik

Avdelningen för Konstruktionsteknik

Betongbyggnad

Chalmers tekniska högskola

SAMMANFATTNING

Om en Prefab tillverkare är involverad i konstruktionen av det bärande systemet i en byggnad är det vanligt att konstruktionsprocessen delas upp i en inledande och en slutlig fas. I *Pyramiden* observerades skillnader mellan reaktionskrafterna som uppstod i grundläggningen för den inledande och den slutliga konstruktionen. I ett försök att reducera byggtiden påbörjades uppförandet av byggnaden innan den slutliga dimensioneringen var avslutad. Detta resulterade i att grundläggningen dimensionerades utifrån förenklade beräkningar istället för den slutliga konstruktionen, vilket skulle kunna ha lett till behov av förstärkningar av grundläggningen eller förändringar i stomsystemet för att omfördela lasten.

Detta arbete syftade till att identifiera osäkerheter i utformningen av det bärande systemet för byggnader samt deras inverkan på lastspridningen.

Genom en fallstudie av projektet *Pyramiden* kunde det fastslås att det fanns osäkerheter kring uppskattningen av styvheten av horisontellt belastade konstruktionselement i de inledande beräkningarna. Vidare studier kring osäkerheternas inverkan på lastspridningen genomfördes via en parameterstudie. Resultat av parameterstudien var en jämförelse mellan styvhetsberäkningar med analytiska metoder baserade på Timoshenkos balkteori och numeriska beräkningar utförda i *FEM-design*. En jämförelse av väggelement med öppningar ledde till rekommendationer för styvhetsuppskattningar av olika konfigurationer. Det genomfördes även en kortfattad undersökning kring samverkan mellan väggelement och dess inverkan på lastfördelning.

Det konstaterades att det fanns vissa möjligheter att förbättra styvhetsuppskattningen och de antaganden som gjorts kring fördelningen av reaktionskrafter, vilket borde tas hänsyn till i beräkningar av den horisontella lastfördelningen. Det kunde även konstateras att det fanns förbättringsmöjligheter i konstruktionsprocessen. Möjligheten att utnyttja FE-analysers noggrannhet för uppskattningen av väggkonfigurationers styvhet tillsammans med den tidseffektiva konstruktionsprocess som används i de inledande beräkningarna borde utvärderas. Slutligen kunde det konstateras att ett utökat samarbete mellan de involverade parterna skulle vara fördelaktigt för konstruktionsprocessen och att problemet som diskuterats i denna rapport skulle undanröjas om byggnation påbörjades först efter färdigställandet av den slutliga dimensioneringen av både grund- och stomkonstruktionen.

Nyckelord: Antaganden, initial design, lastfördelning, styvhet, vägg med öppningar, FEM-design, Rymdknäckning

Contents

ABSTRACT	I
SAMMANFATTNING	II
CONTENTS	III
PREFACE	VII
NOTATIONS	VIII
1 INTRODUCTION	1
1.1 Background	1
1.2 Aim and objectives	1
1.3 Limitations	1
1.4 Method	2
1.5 Outline	2
2 CASE STUDY: PYRAMIDEN	4
2.1 Background	4
2.2 Description of project <i>Pyramiden</i>	6
2.2.1 Description of Building 3	7
2.3 Initial calculations	8
2.3.1 Vertical loads – Vertical program and truss analysis	9
2.3.2 Horizontal loads - <i>Rymdknäckning</i>	11
2.4 Final calculations	15
2.4.1 <i>FEM-Design</i>	15
2.4.2 Modelling choices	16
2.5 Results	17
2.5.1 Vertical loads	17
2.5.2 Horizontal loads	18
2.5.3 Identified Assumptions	18
2.6 Discussion	18
3 CASE STUDY: SIMPLIFIED BUILDING	20
3.1 Method of the study	20
3.1.1 Building geometry	20
3.2 <i>Rymdknäckning</i>	22
3.2.1 Geometry input	22
3.2.2 Loading	23
3.3 <i>FEM-Design</i>	23

3.3.1	Analysis	23
3.3.2	Element types	23
3.3.3	Material	24
3.3.4	Mesh density	24
3.3.5	Supports and boundary conditions	24
3.3.6	Loading	25
3.3.7	Output	25
3.4	Results	26
3.5	Discussion	28
4	STABILIZING ELEMENTS	29
4.1	System of columns	29
4.2	Shear walls	30
4.3	Shear walls with openings	31
4.3.1	<i>Method 1</i>	32
4.3.2	<i>Method 2</i>	33
4.3.3	<i>Method 3</i>	33
5	PARAMETRIC STUDY – WALL ELEMENTS	37
5.1	Method of the study	37
5.1.1	Aspect ratio	37
5.1.2	Placement of opening	38
5.1.3	Width of openings	38
5.1.4	Height of openings	39
5.1.5	Distribution of vertical reaction forces	39
5.1.6	Interaction between wall elements	39
5.1.7	Position of wall elements with reduced stiffness	39
5.1.8	Number of wall elements with reduced stiffness	40
5.2	Analytical calculations	40
5.2.1	Aspect ratio	40
5.2.2	Wall elements with openings	40
5.2.3	Interaction between wall elements	41
5.2.4	Positions of wall elements with reduced stiffness	41
5.2.5	Number of wall elements with reduced stiffness	41
5.3	Numerical calculations	41
5.3.1	Analysis	41
5.3.2	Element types	41

5.3.3	Material	41
5.3.4	Mesh density	42
5.3.5	Supports and boundary condition	42
5.3.6	Loading	42
5.3.7	Output	42
5.4	Results	43
5.4.1	Aspect ratio	43
5.4.2	Wall elements with openings	45
5.4.3	Distribution of vertical reaction forces	50
5.4.4	Interaction between wall elements	50
5.4.5	Position of wall elements with reduced stiffness	52
5.4.6	Number of wall elements with reduced stiffness	53
5.5	Discussion	55
5.5.1	Aspect ratio	55
5.5.2	Individual wall elements	55
5.5.3	Connected wall elements	57
6	PARAMETRIC STUDY – LOAD DISTRIBUTION	58
6.1	Method of study	58
6.2	Analytical calculations	58
6.3	Numerical calculations	58
6.4	Results	59
6.5	Discussion	63
7	CONCLUSION	65
7.1	Recommendations	66
8	REFERENCES	67

APPENDIX A: Theory

APPENDIX B: Convergence study

APPENDIX C: Results of parametric study

Preface

This thesis studied the possibility to improve stiffness estimations of wall elements and assumptions regarding load distribution in the initial phase of the design process. The problem was formulated by the Building department at ELU konsult AB in Gothenburg, Sweden and the thesis was carried out at the same department from January to June 2016.

First of all, we would like to thank our supervisors Hans Lindewald and Johannes Lundgren at ELU konsult AB for their enthusiasm and willingness to assist and direct this project. Hans and Johannes provided guidance regarding the structural behaviour of buildings and a deep understanding of the design process. We would also like thank Amanda Sagemo and Bo Jansson together with the other structural engineers at the building department for providing insight in the design process of the project *Pyramiden* and a pleasant environment to conduct our research.

Assistance, for which we are very thankful, with the structure of the report and the implementation of the studies has been provided by the Division of Structural Engineering at the Department of Civil and Environmental Engineering of Chalmers University of Technology that was part of the collaboration in conducting this research. A special thanks to associate professor Mario Plos for supervising and assisting in the development of this report. Finally, we wish to show our gratitude to our examiner professor Kent Gylltoft for valuable discussions and advices that enabled the completion of this thesis.

Göteborg, June 2016

Axel Haraldsson & Svante Severinsson

Notations

Roman upper case letters

A	Area of structural member
A_{pier}	Area of pier located within a wall element with openings
A_{shear}	Shear area of structural member
A_{truss}	Cross-sectional area of the diagonal bar in a truss
$A_{solid\ strip}$	Cross-sectional area of solid strip
$A_{solid\ wall}$	Cross-sectional area of solid wall
E	Elastic modulus
E_c	Elastic modulus of concrete
E_s	Elastic modulus of steel
G	Shear modulus
H	Height of structural member
H_{pier}	Height of pier located within a wall element with openings
H_{red}	Reduced height of structural member
$H_{solid\ strip}$	Height of solid strip
$H_{solid\ wall}$	Height of solid wall
I	Second moment of area of structural member
I_{pier}	Second moment of area of pier located within a wall element with openings
$I_{solid\ strip}$	Second moment of area of a solid strip
$I_{solid\ wall}$	Second moment of area of a solid wall
I_{truss}	Second moment of area of a truss
K	Stiffness of structural member
K_i	Stiffness of individual structural member in a system of structural members
K_{pier}	Stiffness of pier located within a wall element with openings
$K_{wall.el.}$	Stiffness of wall element
L	Length of structural member
L_{truss}	Length of the diagonal bar in a truss
M	Moment
P	Horizontal point load
P_i	Horizontal point load acting on an individual structural member
V	Vertical reaction force

Roman lower case letters

a	Distance
h	Height of pier within a wall element with openings
h_b	Height of pier located in the bottom within a wall element with openings
h_t	Height of pier located in the top within a wall element with openings
p	Variable defined in <i>Method 3</i>
q	Variable defined in <i>Method 3</i>
r	Variable defined in <i>Method 3</i>

s	Variable defined in <i>Method 3</i>
t	Thickness of structural member

Greek Upper case letters

Δ	Horizontal deformation of structural member
$\Delta_{bending}$	Horizontal bending deformation of structural member
$\Delta_{cantilever}$	Horizontal deformation of structural member with cantilever boundary condition
Δ_{fixed}	Horizontal deformation of structural member with fixed boundary condition
Δ_{frame}	Horizontal deformation of frame structure
Δ_{pier}	Horizontal deformation of pier located within a wall element with openings
Δ_{shear}	Horizontal shear deformation of structural member
$\Delta_{solid\ strip}$	Horizontal deformation of solid strip
$\Delta_{solid\ wall}$	Horizontal deformation of solid wall element
$\Delta_{wall.el.}$	Horizontal deformation of wall element

1 Introduction

1.1 Background

The design process of the structural system of buildings is full of uncertainties. In the initial design simplified calculations of the structural system is carried out. At this stage the structural engineer has to make assumptions regarding the calculations since a lot of aspects of the final design are still not defined and since the current building process allows the client to make changes in the structural system as the project proceeds. Most of the uncertainties the structural engineer is faced with, such as material properties and capacities of structural members, are considered in design codes. But there are also uncertainties in the choice of structural models and how well they represent the real behaviour of the building. How detailed the initial structural design should be and how rigorously the behaviour of the elements needs to be analysed are often based on the judgement of the structural engineer (Bulleit, 2008).

If a prefabrication manufacture is involved in the design of the structural system it is common that design process is divided into an initial and a final phase. The structural engineer is responsible for a static evaluation of the structural system to determine how the loads are transferred through the building and the prefabrication manufacture is responsible for the detailed design of the structural system and its members. The static evaluation is often based on simplified analytical calculations while the detailed design is based on more advanced numerical calculations. In both the initial and the final design assumptions are made that affects the load paths through the structural system such as boundary conditions, material models and stiffness of structural members. The above-mentioned uncertainties combined with the different calculation methods may cause differences between the load distributions in the initial and final design.

1.2 Aim and objectives

This thesis aims to identify uncertainties in design and modelling of the structural system for buildings. Different assumptions and choices made by the structural engineer as well as their influences on the load distribution will be investigated.

The thesis has the following specific objectives

- Identify critical structural members and possible assumptions made regarding their behaviour that leads to different results in simplified analytical calculations compared to more advanced numerical calculations.
- Evaluate and compare the uncertainties in the assumptions regarding the structural members behaviour.

1.3 Limitations

The focus of the thesis will be on how self-weight, imposed vertical loads, deviation loads and wind loads are transferred through the structural system to the foundation and their vertical reaction forces. Linear elastic analysis will be carried out with

analytical hand calculations according to Timoshenko Beam Theory and the software *Rymdknäckning* and *FEM-design* only considering horizontal loads.

1.4 Method

In order to identify critical structural members and possible assumptions regarding their behaviour in simplified analytical calculations compared to more advanced numerical calculations a case study of an existing building and its design process is carried out. The project *Pyramiden* is chosen as the study due to the extent of the project. *Pyramiden* consists of several different structural member types and structural solutions. Both structural calculations and blueprints from the initial and final design are studied in order to identify differences in load paths and vertical reaction forces. To be able to find the reasons for the different results the study includes interviews with the involved structural engineers and a literature study regarding theory behind the identified assumptions. The case study results in a number of specified assumptions that leads to differences in the load distribution.

To further investigate the assumptions identified in the case study of *Pyramiden* and to verify that the response is not specific for *Pyramiden* a simplified building is designed. The response of this building when loaded with horizontal loads is calculated using the analytical software *Rymdknäckning* and the numerical software *FEM-design*. The output of the calculations is the reaction moments at the foundation. It is also interesting to study the response of the building on a structural level.

By performing a parametric study on various configurations of wall elements with openings the stiffness estimation of four analytical methods is compared to *FEM-design*. The varying parameters are the number of openings, the height of the openings, the width of the openings and the placement of the openings. The parametric study investigates the limitations in the four analytical methods and results in recommendations for which configurations of openings the methods are applicable. Similar comparisons of the different calculation methods are performed to investigate what influence the stiffness of the individual wall element have when connected to other wall elements on a structural level.

1.5 Outline

Chapter 2 describes the case study of *Pyramiden*. First of all a brief description of the building process and the problem associated with differences between initial and final calculations are presented. The chapter then describes the studied building, the design process of the initial and the final design and the results of the case study followed by a discussion.

Chapter 3 describes the case study of a simplified building designed for this thesis. The chosen method of study is presented followed by descriptions of analytical and numerical calculations. Finally the results are presented together with a discussion.

Chapter 4 comprises the theory necessary to perform stiffness estimations of wall elements and wall elements with openings.

Chapter 5 describes the parametric study carried out on wall elements. The study includes stiffness estimations of wall elements with varying aspect ratio, wall elements with various dimensions and locations of openings and interaction between wall elements. The chosen method of study is presented followed by descriptions of analytical and numerical calculations. Finally the results are presented together with a discussion.

Chapter 6 describes the parametric study of load distribution of a building. The study includes stiffness reduction in one of the exterior walls of a simplified building. The chosen method of study is presented followed by descriptions of analytical and numerical calculations. Finally the results are presented together with a discussion. Chapter 7 presents the conclusions of this thesis.

2 Case study: Pyramiden

During the design process of the project *Pyramiden* it was noted that the reaction forces in the foundation differed in the final calculations compared to the initial calculations. In *Pyramiden* the differences were noted in an early phase and could be investigated and evaluated without any major influence on the construction process. The initial calculations included the design of the structural system based on drawings from the architect. Vertical and horizontal calculations were made to determine preliminary dimension of vertical and horizontal load carrying members and stability of the structural system. Based on the preliminary dimension the structural members were designs in detail by the prefabrication manufacture¹. This case study intended to show what different assumptions that could be made in the design and modelling process and what diverse results they may lead to depending on the used calculation method. Both the initial and the final calculations was described and analysed to increase the understanding of their possibilities and limitations. The results of the study was a number of assumptions that could influence the load distribution.

2.1 Background

In order to understand the problem associated with different result of the structural design at different phases in the design process it is important to have basic understanding of the building process.

The building process, including planning, design, procurement and construction, varies with each specific project and often involves several parties. However, common for all types of building processes is the time aspect. A shorter building process reduces the total cost of the project significantly which often is a high priority of the client. The time aspect therefore influences the way of managing building projects.

One way of trying to achieve a short design and construction process is exemplified by describing the process involving a general contractor, see Figure 2.1.a. The process involving a general contractor is here considered a good representation of the process in traditional contracts as well as novation contracts.

When the building process is based on a general contractor the involved parties could generally be divided in to three stages. The first stage involves the client and the design consultant. The client is the person or organisation that wants to build the building. In order to do so the design consultant is hired as a structural engineer to produce procurement document. In stage two a general contractor is hired based on the procurement documents to be responsible for the construction process and to hire subcontractors. The third stage consists of the subcontractors that are responsible for specific parts of the building, such as the foundation or the structural system. (Nordstrand, 2008)

¹ Amanda Sagemo (ELU konsult AB Göteborg) interview 08 02 2016

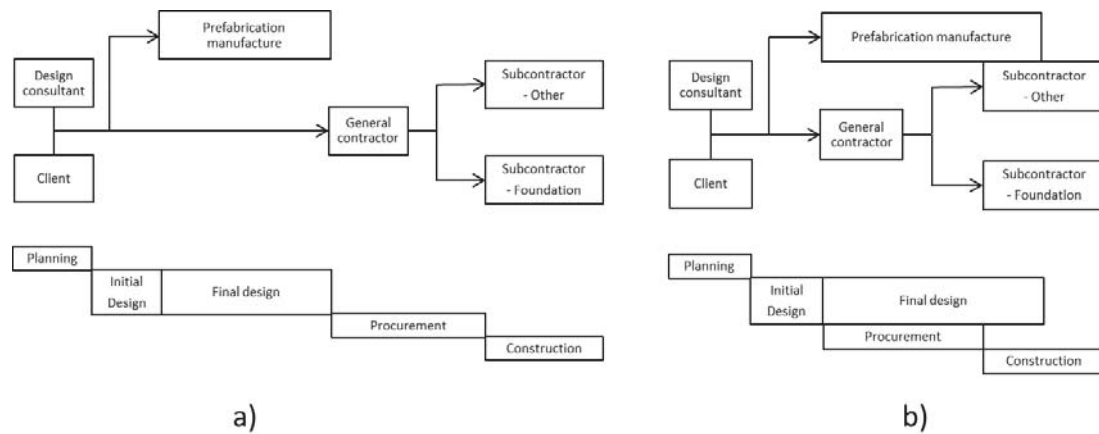


Figure 2.1 a) The building process involving a general contractor with ideal time schedule. b) The building process involving a general contractor with reduced time schedule.

If a prefabrication manufacture is involved in the design of the structural system it is often chosen to hire the prefabrication manufacture in the same stage as the general contractor. The design consultant is then responsible for a static evaluation of the structural system to determine how the loads are transferred through the building. An initial design of the structural system containing recommendations and limitations of the structural members dimensions is then handed over to the prefabrication manufacture that is responsible for the detailed design of the structural system. Ideally, the design of the foundation is then based on the result of the detailed design of the structural system.

However, in order to get advancing and time efficient design and construction processes it is common that the construction of the foundation is initiated based on the initial structural evaluation before the final details of the structural system is designed. The design of the foundation is then based on the calculations from the design consultant while the calculations from the prefabrication manufacture are used as validation of the foundation. This is a problem since the final design of the structural system from the prefabrication manufacturer in some cases leads to a different load distribution and consequently requires a different design of the foundation.

The reason behind the problem with different load distribution in the initial design compared to the final design can partly be explained by the time aspect. In an ideal building process the planning and the design is completed before the procurement and construction starts, see Figure 2.1.a. To reduce the total time of the project the procurement and the construction often start before the design phase is completed, see Figure 2.1.b, this also enables the general contractor to influence the design process. If this is the case changes to the structural system often occur after the initial design is completed and are therefore only accounted for in the final structural design².

Another reason to the problem with different load distribution is the different calculation methods used in the initial and the final calculations. The initial calculations are often based on analytical calculations that require assumptions and simplifications of the structural behaviour made by the structural engineer and the final design is based on numerical calculations. Even if the final design is based on

² Bo Jansson (ELU konsult AB Göteborg) interview 26 01 2016

numerical calculation and therefore should be able to perform more detailed analysis it should be noted that assumptions has to be made regarding the structural behaviour also in this phase. In cases where the final structural design of the foundation differs from the initial design measures need to be taken by either strengthening the foundation or finding another structural solution to redirect the load paths. These measures increase both the cost and the construction time. The choice to design the slab based on the initial calculations may therefore lead the opposite of the desired effect ³.

2.2 Description of project *Pyramiden*

The studied building is located within the block *Pyramiden* in Solna adjacent to Solna Station and Mall of Scandinavia. Due to the lively environment in the surroundings the building is designed as three separate buildings connected by footbridges to allow pedestrian passages between the buildings on the ground level. The three buildings are also connected through an underground parking garage. (Schramm, 2014)

The building referred to as *Pyramiden Building 1*, see Figure 2.2, consists of two parts with different heights. The lower part has seven storeys and the higher part rises to ten storeys. *Pyramiden Building 2*, see Figure 2.3, consists of one part with seven storeys and two parts with ten storeys. The lower part of *Pyramiden Building 3*, see Figure 2.4, rises to seven storeys and the higher part rises to fourteen storeys. The common parking garage is not considered as a storey.

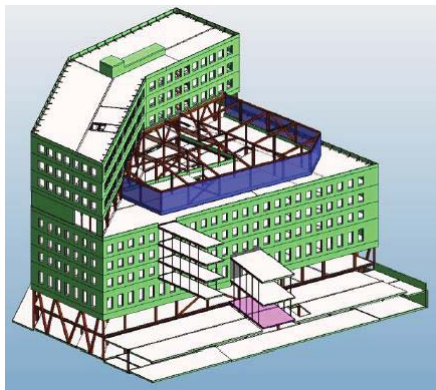


Figure 2.2 *Pyramiden Building 1* (ELU konsult AB, 2015)

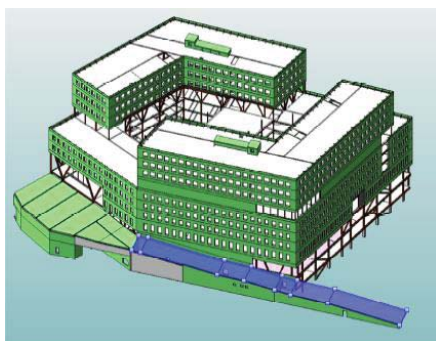


Figure 2.3 *Pyramiden Building 2* (ELU konsult AB, 2015)

³ Bo Jansson (ELU konsult AB Göteborg) interview 26 01 2016

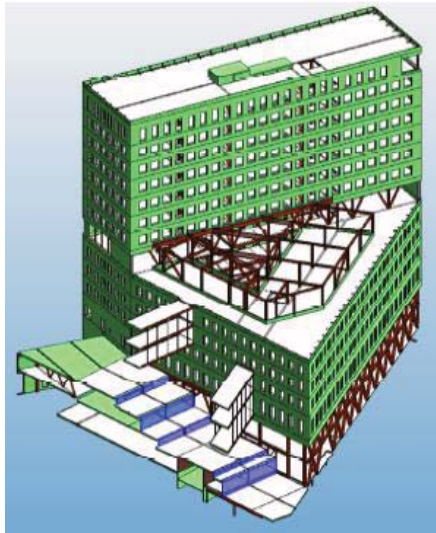


Figure 2.4 Pyramiden Building 3 (ELU konsult AB, 2015)

The structural system of the three buildings consists mainly of prefabricated structural members. Vertical loads are transferred through the exterior walls and an interior beam column system with steel beams and columns made of either concrete or steel. The exterior walls are prefabricated concrete sandwich elements except in the floors 1, 2 and 7 where load carrying and stabilizing steel trusses are used. Prefabricated hollow core slabs of the type HD/F 32 are used as slab elements where possible. In parts of the building with long spans or high imposed loads hollow core slabs with greater dimensions or homogeneous concrete slabs are used. All slab elements are designed as stiff slabs that transfer and distribute the horizontal loads to the vertical stabilizing members. The stability of the buildings is obtained through the exterior walls, concrete elevator shafts and internal steel trusses. The three buildings are connected through expansion joints such that they are free to move independently of each other. (ELU konsult AB, 2015)

Due to similarities in the design and construction of *Pyramiden Building 1* and *Pyramiden Building 3* the calculation methods were similar for the two buildings. The construction and calculations of *Pyramiden Building 2* deviated to some extent due to its exterior shape and interior spaces such as a gym and an assembly hall located on floor 1-2. *Pyramiden Building 1* and *Pyramiden Building 3* were therefore considered to be better representations of a common building. It was chosen to only study *Pyramiden Building 3* in detail with the motivation that it is the highest one and therefore is subjected to the largest loads and variation in reaction forces.

2.2.1 Description of Building 3

The lower part of *Pyramiden Building 3*, storey 1-7, has triangular floor plans with an atrium located in the centre, see Figure 2.5.a. The higher part of *Pyramiden Building 3*, storey 8-14, has rectangular floor plans, see Figure 2.5.b. Due to possible future extensions the structural system in the higher part of the building is designed to carry the load from an additional storey.

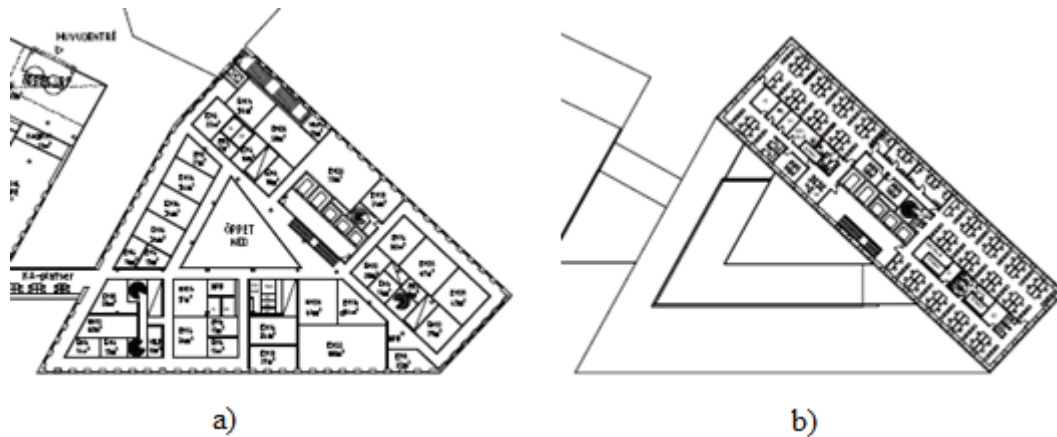


Figure 2.5 a) Floor plan storey 1-7(ELU konsult AB, 2015) b) Floor plan storey 8-14(ELU konsult AB, 2015)

Load carrying concrete sandwich elements that transfer vertical loads and provide stability to the building are used as exterior walls in most of *Pyramiden Building 3*. Exceptions are floor 1, 2 and 7 where steel trusses constitute the load carrying wall elements. A steel column-beam system is also used as load transferring members in the façades facing the atrium on floor 1-7.

The dimensions of *Pyramiden Building 3* enable a slab system consisting of hollow core slab elements of the type HD/F 32 supported by an interior load carrying column-beam system and the exterior walls.

In addition to the exterior walls the building is stabilized by an elevator shaft. The elevator shaft is located in the higher part of *Pyramiden Building 3* and contains 5 elevators designed as a single concrete structure. To provide additional stability to the elevator shaft steel trusses are attached between the elevator and the column-beam system.

Figure 2.6 shows a simplification of the floorplan of the parking garage and the structural members that transfers vertical and horizontal loads to the foundation.

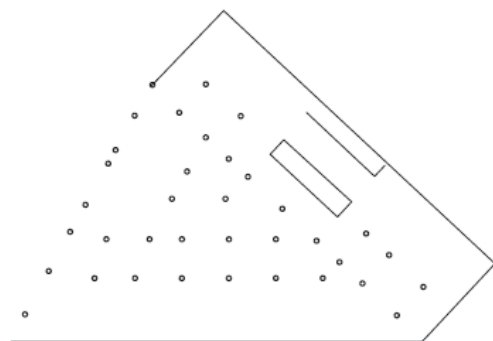


Figure 2.6 Simplified arrangement of exterior load carrying walls, interior column and elevator shaft. Adopted from (ELU konsult AB, 2015)

2.3 Initial calculations

The initial calculations could be divided into two main categories; one for the vertical loads and one for the horizontal loads. Vertical loads and the corresponding vertical reaction forces were determined using a programmed excel sheet, further referred to as *Vertical program*. The stability of the building and the vertical reaction forces corresponding to horizontal loads were determined using the software

Rymdknäckning. To obtain the total vertical reaction forces the principle of superposition was applied⁴.

2.3.1 Vertical loads – Vertical program and truss analysis

The *Vertical program* for the vertical loads is a programed matrix used internal by ELU konsult AB where a specific element; column or wall could be analysed separately. The requested numbers of stories was added to the *Vertical program* and the engineer was allowed to add different loads; snow, variable load, installations and self-weight to each floor in the building. The influence area of each load was also an input and the *Vertical program* then calculated the vertical load in the element for the load combinations in ULS and SLS according to (Eurocode 1, 2002). The load was summed up for each floor, giving the total load in the element at the foundation. This load would either be a point load [kN], if a column was studied; or a line load [kN/m] if a wall was studied. The *Vertical program* did not take any wind load or inclination into account. Figure 2.7 shows an example of the excel program where 2 storeys (8-7) were calculated.

INDATA																			
Plan	Lastbeskrivning	Lastyta			Lastvärde				Formfaktorer, Belastad area, ψ -faktorer										
		Bredd (m)	Längd (m)	Yta / L (m ² / m)	Permanent		Variabel	Snölast	Ff / BA	γ_d	ψ_0	ψ_1	ψ_2	α_A	α_n kategorivis				
	Säkerhetsklass 3				tjocklek	densitet	värde	värde	Kategori						A	B	C	D	
8	Snö fläktrum	(3,6)	(6,2)	22,32						2		1	0,7	0,4	0,2				
8	Tak fläktrum	(3,6)	(6,2)	22,32	1	3,5	3,5					1							
7	NL Terrass	(5,6)	(6,2)	34,72				5	C			1	0,7	0,7	0,6	1		1,00	
7	Överbyggnad, Terrass	(5,6)	(6,2)	34,72	1	4	4					1							
7	Terrass, HDF38	(5,6)	(6,2)	34,72	1	4,6	4,6					1							
7	Installationer	(5,6)	(6,2)	34,72			1					1							

RESULTAT								
Tillskott			Lastsummering					
Permanent koeff-fri	Variabel koeff-fri	Snölast koeff-fri	Brottgränstillstånd			Bruksgränstillstånd		
			0,9 EGV	Ekv 6.10a	Ekv 6.10b	Ekv 6.14b	Ekv 6.15b	Ekv 6.16b
		44,6		46,9	67,0	44,6	17,9	8,9
78,1			70,3	152,3	160,7	122,8	96,0	87,0
	173,6			334,6	421,1	296,4	217,5	191,2
138,9			195,3	522,1	587,8	435,2	356,4	330,1
159,7			339,0	737,7	779,4	595,0	516,1	489,8
34,7			370,3	784,6	821,1	629,7	550,8	524,5

Figure 2.7 Example of in-data and results in Vertical program

The imposed loads were reduced by a factor α_n based on the number of storeys within the same load category, in accordance with (Eurocode 1, 2002). If a vertical load carrying element was placed between two areas with different live loads, but within the same load category; the program treated the two loading areas as separate floor resulting in a smaller reduction factor. To avoid this error the imposed loads acting on the vertical load carrying element were recalculated into a mean value load⁵.

⁴ Hans Lindewald (ELU konsult AB Göteborg) interview 10 02 2016

⁵ Amanda Sagemo (ELU konsult AB Göteborg) interview 08 02 2016

2.3.1.1 Design choices and assumptions

In *Pyramiden* the *Vertical program* was used to calculate the loads acting in the columns, exterior walls, elevator shafts and internal walls. The loads that had to be accounted for were the variable load for each floor, often designed for offices or meeting rooms; the self-weight of a HDF slab, including a cast-in situ concrete layer and loads from various installations. The self-weight of the vertical load carrying elements was neglected except for the load carrying exterior walls elements. The columns were treated as point loads and the walls were treated as line loads.

In order to simplify the calculations and due to uncertainties of the actual structural behaviour the spans in the column-beam system supporting the slab elements were treated as simply supported resulting in a 50% contribution from the adjacent spans to the vertical member. Spans where it was uncertain whether to treat them as simply supported or as continuous spans were treated as a combination of the two support conditions. The vertical members that should get a 60% contribution from the adjacent spans were treated as continuous and obtain 60% of the load while the members that should get 40% contribution from the adjacent spans were treated as simply supported and obtain 50% of the load, see Figure 2.8. By this assumption a portion of the span was accounted for twice which was considered to be on the safe side with regard to dimensioning loads on the foundation⁶.

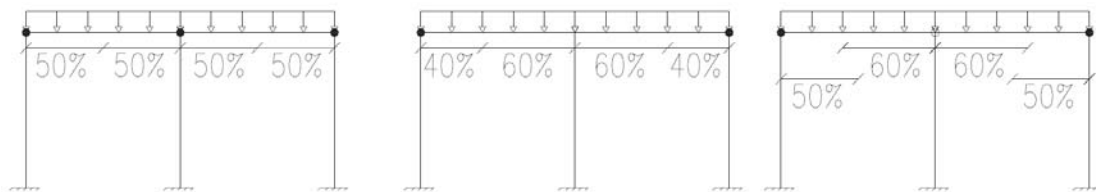


Figure 2.8 Assumption regarding load distribution in span with uncertain support condition

Since the lower parts of the exterior walls were made of a steel framework and thereby demanded another calculation approach a second analysis were carried out in the program *Frame analysis* as a complement to the excel calculation. *Frame analysis* analyses arbitrary plane structures of steel, timber or concrete according to first- or second order theory according to Eurocode. The analysis carried out was finite element analysis using the displacement method. (Strusoft, 2009) The façade

⁶ Amanda Sagemo (ELU konsult AB Göteborg) interview 08 02 2016

frameworks were analysed separately as a two-storey frame, see Figure 2.9

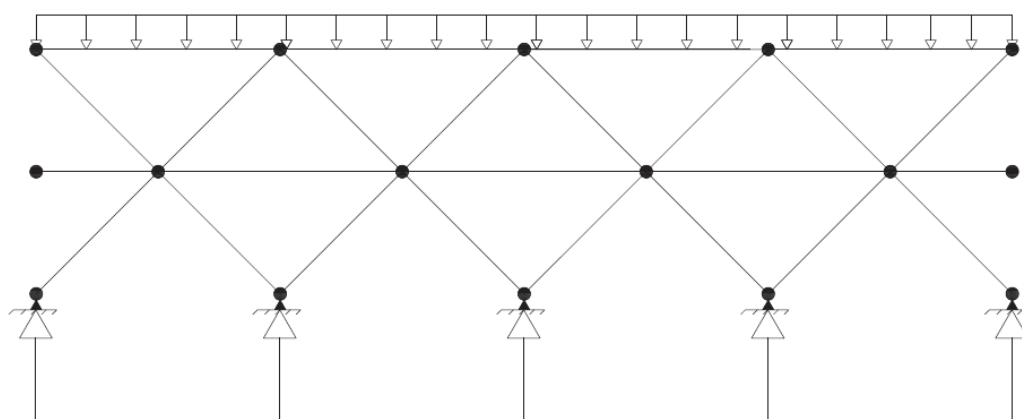


Figure 2.9 Visualisation of reaction forces obtained in Frame analysis

The frame was loaded with the loads acting on the structure, including self-weight, variable load, wind load and unintended inclination. To capture the real behaviour of the frame resultants from the loads originating from the storeys above the frame were added as line-loads to the top member. The output from the *Frame analysis* was point loads at each of the supports instead of the line-loads provided by the *Vertical program*, which was a more accurate description of the actual load distribution⁷.

2.3.2 Horizontal loads - *Rymdknäckning*

The horizontal loads and the stabilizing system was analysed in the software *Rymdknäckning*. *Rymdknäckning* only consider horizontal loads. The software calculated the displacement of the shear centre in local x- and y-direction, rotation of shear centre, shear forces and moments in all the walls and normal forces in the floor slabs according to 2:nd order theory. Calculations were performed under the assumptions of totally stiff floor slabs that transferred the vertical loads to walls located within the same floor. The software is text based and doesn't have any visual interface, instead an input file is written which holds all input data. The input file contained information about the number of storeys, the height of storeys, young's modulus, loads and more detailed information about the different walls and slabs.

Each wall was defined to run the entire height of the building. The geometry of the walls was defined by a position within a coordinate system, a moment of inertia and a cross-section area. It was possible to define different moment of inertia and shear area for different storeys of a wall if it for example didn't run the entire height of the building or had local reductions of stiffness on some storeys. The different slabs were defined with corner coordinates.

Rymdknäckning only considered unintended inclination and wind load in the calculations. The imposed load was defined as an input, but it was only used to obtain the deviation load and did not contribute directly to the vertical reaction forces. Imposed loads were defined as an average load [kN/m^2] acting on a specific floor. The wind load was defined as a resulting point load [kN] for each floor with an eccentricity from the origin of the coordinate system. (SSI Byggkonsult, u.d.)

⁷ Amanda Sagemo (ELU konsult AB Göteborg) interview 08 02 2016

2.3.2.1 Design choices

Pyramiden Building 3 was designed as eleven separated stabilizing walls, see Figure 2.10. *Wall 1-4* ran the entire height of the building, *5-6* covered the lower part of the building, *wall 9-11* existed only in the basement, and *7-8* represented the elevator shaft. Openings in the slab for elevators and other installations were neglected.

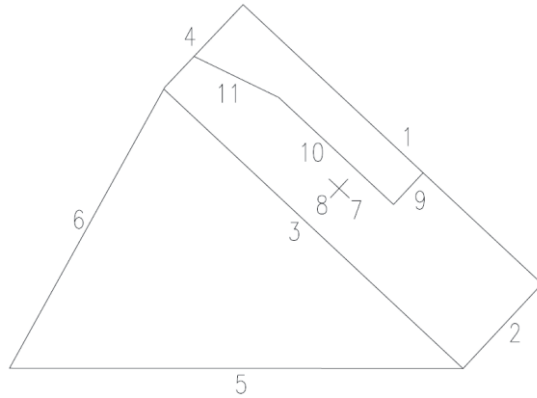


Figure 2.10 Stabilizing walls of *Pyramiden Building 3* in *Rymdknäckning*

2.3.2.2 Assumptions regarding elevator shaft

The elevator shaft was designed as two equivalent stiff walls, *Wall 7-8*, in order to be able to implement in *Rymdknäckning*. These walls represented the stiffness of the elevator shaft in local *x*- and *y*- direction and were placed in the centre of gravity of the elevator shaft. The moment of inertia and the shear area of the actual elevator shaft were obtained by modelling the actual geometry in the software RFEM. (ELU konsult AB, 2015)

2.3.2.3 Assumptions regarding walls

Wall 1-6 and *9-11* contained several prefabricated wall elements with various configurations on different storeys. The shear area and moment of inertia for these walls were calculated by adding up the stiffness for the individual prefabricated wall elements on each storey in the respective wall. The stiffness of a wall was therefore obtained as the stiffness of the individual wall elements.

Three different types of bracing elements were used in *Pyramiden*; solid wall elements, wall elements with openings and steel trusses.

Solid wall elements were calculated according to the basic equation for moment of inertia and shear area for a beam, see equation 2.1-2.2.

$$I = \frac{tL^3}{12} \quad (2.1)$$

$$A = tL \quad (2.2)$$

Where L = length of the wall element
 t = thickness of the wall element

The calculations of wall elements with openings took the reduced stiffness due to the discontinuity region into account. This was achieved by assuming that wall elements with openings could be treated as a system of columns and that wall elements with

openings could be replaced by a equivalent stiff solid wall element. The force required to deflect the piers between the openings 1 unit length horizontally can be determined, see Figure 2.11.

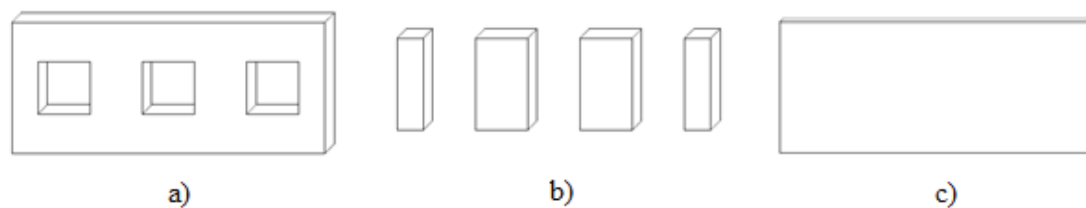


Figure 2.11 a) Wall element with openings b) System of piers c) Equivalent stiff wall element with reduced thickness

The pier was assumed to be fixed in the bottom and partially fixed in top. The force P was calculated according to bending deformations of the Timoshenko beam, see equation 2.3 and Figure 2.12.

$$P = \frac{12EI\Delta}{H^3} \quad (2.3)$$

Where $E = \text{modulus of elasticity of pier}$
 $I = \text{second moment of area of pier}$
 $H = \text{height of the pier}$
 $\Delta = \text{horizontal deformation at the top of the pier}$

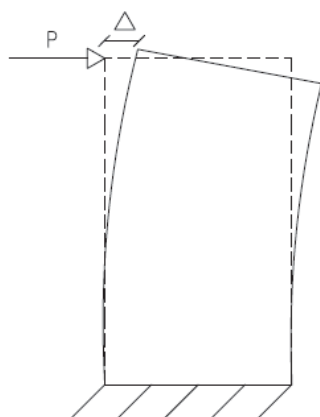


Figure 2.12 Bending deformation of pier due to point load P

The stiffness of the piers was increased by reducing the height of the piers according to equation 2.4 and Figure 2.13. This was considered a good approximation of the additional stiffness due to the interaction between the piers⁸.

$$H_{red} = H - \frac{h_1 + h_2}{2} \quad (2.4)$$

⁸ Hans Lindewald (ELU konsult AB Göteborg) interview 10 02 2016

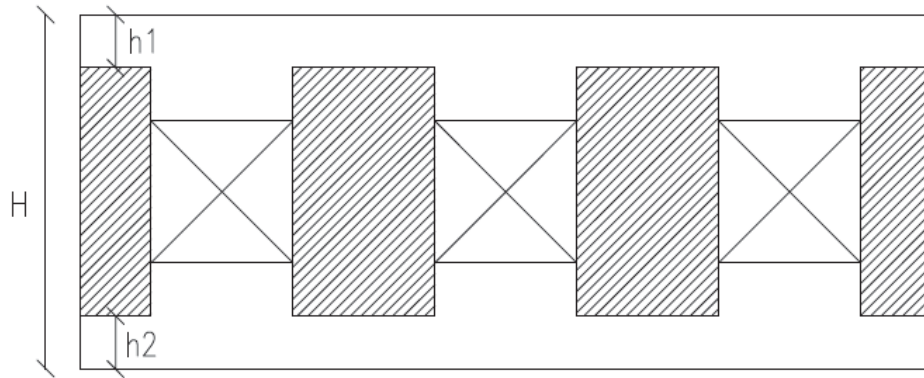


Figure 2.13 Discretization of wall element with openings according to assumption

The same calculated force and prescribed displacement was then used in the equation for shear deformation of a Timoshenko beam to calculate the area of an equivalent stiff wall element, equation 2.5.

$$A_{shear} = \frac{1.2HP}{G\Delta} \quad (2.5)$$

Where A_{shear} = shear area of equivalent stiff wall element
 G = shear modulus

From A_{shear} the thickness of the equivalent stiff wall was calculated by dividing with the length L .

The truss elements were also transformed into a wall element with moment of inertia and shear area to fit the input in *Rymdknäckning*. In the same way as for wall elements with openings truss element were calculated for how much force it took to displace the top 1 unity length in horizontal direction, see Figure 2.14.

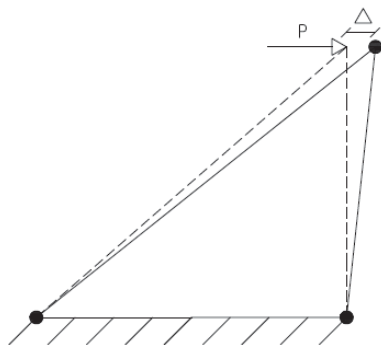


Figure 2.14 Deformation of truss system due to applied load P

This was done in the program *Frame analysis* where the reaction force in horizontal direction was calculated according to 1:st order analysis. These values were used in the equation for shear deformation and the shear area of an equivalent stiff wall element was solved; see equation 2.5.

The moments of inertia were calculated according to equation 2.6.

$$I_{truss} = \frac{E_s}{E_c} * A_{truss}(0.5L_{truss})^2 \quad (2.6)$$

Where A_{truss} = cross – sectional area of the diagonal bar in the truss
 L_{truss} = length of the diagonal bar in the truss

2.3.2.4 Assumptions regarding cracking

Cracking was taken into consideration through an iterative process where the stiffness of walls subjected to large forces or moments were reduced by multiplying with 0.4. If the load distribution did not change after the reduction of stiffness the iterative process was cancelled.

2.4 Final calculations

The final structural system was designed using a Finite-element analysis in the software *Strusoft FEM-design 3D Structure 14*, further referred to as just *FEM-design*. In the FE-analysis both vertical and horizontal loads were considered via various load combinations.

2.4.1 FEM-Design

FEM-design is a FE-software suitable for analysis of load-carrying structures made of concrete, steel or timber according to Eurocode. (Strusoft, 2015)

2.4.1.1 Analysis

FEM-design performs linear static analysis according to second order theory taking global stability, buckling shapes and critical load into consideration. Through active choices non-linear analysis is performed considering uplift and cracking. Non-linear behaviour of supports and connections describes uplift by detaching the stiffness of the supports or connection when load is acting in a chosen direction making them resistant to compression only. The calculation process is iterative where the stiffness in tension is decreased in each step. Cracked analyses are performed as iterative calculation by increasing the load and modifying the stiffness in each step. The smallest principal moment for each load step is compared to the crack moment of the plate. If the plate is cracked the direction of the crack is calculated and the stiffness of the plate is reduced in the direction perpendicular to the crack lines.

2.4.1.2 Structural elements

The *FEM-design* module *3D-structure* implements 3D shell elements and 3D beam elements. Both elements are capable of describing membrane displacements in plane and bending perpendicular to plane. 3D shell elements are isoparametrical with eight or six nodes and can be used to model structures with plane centre surfaces. Each node has six degrees of freedom; displacements in local coordinates and rotations in global coordinates. 3D beam elements have a straight axis with a node at each end. Each node has six degrees of freedom; displacements in local coordinates and rotations in global coordinates. (Strusoft, 2015)

2.4.1.3 Mesh

The built in function *Prepare* generates a mesh with an average element size optimized for the structure based on geometry, support and loading conditions. By using the setting *Region by region* the program optimizes the element size for each model region. The manual recommends this setting if discontinuity regions such as walls with openings are modelled. It is also possible to use *Accurate* element types instead of *Standard* element types, which increases the number of active nodes. As a result the computational time increases but the analysis provides a more accurate result.

2.4.1.4 Supports and boundary conditions

Supports can be modelled using the predefined support groups *Line support group* and *Point support group*, which define the stiffness against displacement, $[kN/m]$, and rotation, $[kNm/^\circ]$, in local coordinates. In *FEM-designs* predefined support type *rigid* the stiffness against displacements is $1 * 10^7 [kN/m]$ and the stiffness against rotation is $1.745 * 10^7 [kNm/^\circ]$. The connections between elements are defined via *Boundary connection*, which prevent deformations in the same way as support groups. When connecting two elements the *Boundary connection* with the lowest stiffness will govern the behaviour of the connection.

2.4.2 Modelling choices

Based on the initial design the structural system of *Building 3* was modelled only considering the prefabricated elements. The prefabricated elements included the concrete exterior walls, elevator shafts, concrete slabs, internal trusses and the steel frame on storey 1-2. These were modelled with the built in objects in *FEM-design*, plane wall, profiled plate, beam, column and truss elements, for which it was possible to choose standard profiled cross-sections and material properties. The foundation and cast-in situ concrete structures connected to the structural system where modelled as supports⁹.

The walls were modelled as equivalent stiff solid plane walls with a thickness determined in a similar way as in the method described in Chapter 2.3.2. The solid walls were divided into elements with a length of $4.8m$ and where considered as hinged along the edge connection between each other. In the transformation of the equivalent stiff walls the self-weight was reduced. Adding additional line load acting within the wall compensated the reduction of the self-weight¹⁰.

The slab was assumed to act as a stiff plate and was modelled as a predefined HDF-slab available in *FEM-design* with boundary condition such that vertical loads only where transported in a one-way action to the supporting structural members.

The analysis of the final structural model considered both horizontal and vertical loads and the reaction forces were extracted from the foundation supports. Both columns and walls were assigned *point supports* representing the locations of the load carrying piles of the foundation.

⁹ Emelie Granberg (Ramböll) interview 26 04 16

¹⁰ Emelie Granberg (Ramböll) interview 26 04 28

2.5 Results

By comparing the load distribution and the resulting vertical reaction forces in the foundation obtained from the initial and final calculation methods some specific problems in the design process were identified. This chapter describes the situations where differences in the load distribution were observed and explains why they occurred.

2.5.1 Vertical loads

In a section of the building where two spans of slab elements were supported by an intermediate column-beam system differences were observed in the vertical forces in the columns, see Figure 2.15. These differences originated in uncertainties whether to treat the spans of the supporting column-beam system as continuous or simply supported as described in Chapter 2.3.1¹¹. The initial calculations were also based on a simplified load distribution of the two adjacent slab elements. The two slabs were subjected to different imposed loads that were treated as a single mean value load according to Chapter 2.3.1.

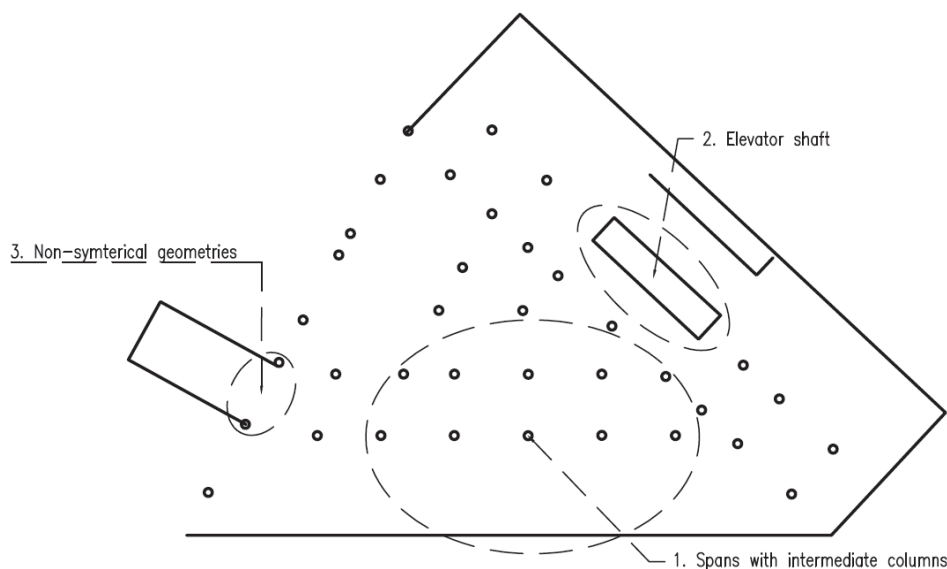


Figure 2.15 Areas with observed local differences in vertical reaction forces

It was observed that load carrying walls and columns arranged in non-symmetrical geometries leads to differences between the initial and the final calculations. The initial calculations also suggested that the area around the elevator shaft was subjected to greater vertical load than in the final calculations. Differences in the areas with non-symmetrical arranged columns occurred due to definitions and choices of how the structural members were defined in the final phase. The increased loading in the area around the elevator shaft was explained by an additional safety factor in the initial calculations since the details of the final design were still unknown. As an example of the additional precaution in the initial calculations the cast-in-situ concrete

¹¹ Amanda Sagemo (ELU konsult AB Göteborg) interview 08 02 2016

cover of the HD/F slab elements was assumed to have the maximum standard measurement¹².

2.5.2 Horizontal loads

The comparison of the horizontal loads contribution to the vertical reaction forces indicated that the initial and final calculations treated the stabilizing members differently and consequently obtained different load distributions. In the initial calculations a greater part of the horizontal loads was absorbed in the elevator shafts than in the final calculations where a majority of the horizontal loads were absorbed in the exterior walls¹³. The stiffness was assumed, in accordance with (Westerberg, 1997), to influence the load distribution. Stiffness estimations of wall elements with openings according to Chapter 2.3.2 and the assumption regarding solid wall elements with equivalent stiffness were assumed to be the main reason for the differences found in the calculations of the stabilizing members.

2.5.3 Identified Assumptions

Differences regarding vertical loads occurred due to additional safety factors and the structural engineer had little possibility to influence the result of the calculation. It was therefore chosen to focus on the following assumptions regarding horizontal loaded wall elements:

- Wall elements with openings can be treated as a system of columns
- Wall elements with openings can be replaced by a equivalent stiff solid wall element
- The stiffness of a wall is the sum of the stiffness of the individual wall elements

2.6 Discussion

Performing a case study of a building project the size of *Pyramiden* comprised studying and evaluating documents from different stages of the project that spanned over a relative long time. Some calculations were performed several times since more details of the final design of the building became available as the building project proceeded. The discussion that occurred between ELU konsult AB and the prefabrication manufacture during the design process also involved updating previous calculations in order to reduce eventual differences. This, in combination with the large number of available documentation, implied that there most likely existed assumptions regarding the structural behaviour that were not examined in this thesis. A more detailed and comprising study could have been performed if more time had been dedicated. Some assumptions were neglected in this thesis that might have been interesting to investigate further. The case study would probably also have benefitted from studying the FE-model of the final design of the structural system. However, considering that the main focus of the case study was to identify differences in the load distribution the studied differences of the reaction forces in the foundation provided a sufficiently accurate depiction of the structural behaviour.

¹² Amanda Sagemo (ELU konsult AB Göteborg) interview 08 02 2016

¹³ Hans Lindewald (ELU konsult AB Göteborg) interview 10 02 2016

Some of the identified differences in the load distribution were brought up in the discussion between ELU konsult AB and the prefabrication manufacture and were evaluated to some extent. The performed evaluation considered reasonable differences in the reaction forces to be acceptable as long as the initial calculations overestimated the reaction force and thereby would not exceed the capacity of the foundation. It was chosen to not value the sign of the differences in the reaction forces in this thesis. It should be noted that generally an overestimation in the initial calculations were preferable compared to an underestimation as long as all forces were overestimated evenly.

The identified differences suggested that most of the assumptions were made regarding stabilizing members subjected to horizontal load. It was chosen to consider the identified differences that originated from vertical loads as active choices instead of assumptions since the involved structural engineers had little or no possibility to influence the outcome. Through continuous interviews with the involved structural engineers the observations and results of the case study were confirmed and elaborated. Thus, the assumptions regarding horizontally loaded bracing members were considered the most interesting subject for further studies in this thesis.

Analytical calculations could be used to estimating the stiffness of steel trusses and elevator shafts, see Appendix A. The initial calculations of the stiffness of steel trusses were obtained using the numerical software *Frame analysis*, which were expected to provide a more accurate result and a shorter computational time. Analytical assumptions regarding steel trusses were therefore not studied further in this thesis. Stiffness calculations of the elevator shaft would be interesting to investigate further. However, the analytical stiffness calculations were considered too uncertain for estimating the stiffness at a specific floor and were problematic to implement in the methodology of this thesis. It was therefore chosen to focus on the assumptions regarding stiffness estimations of wall elements.

3 Case study: Simplified Building

A building with a rectangular and symmetrical structural system was designed in order to investigate if the observed assumptions from the case study of *Pyramiden* had similar effects in a simplified building. The investigation comprised three versions of the building where the stiffness of wall elements in one of the exterior walls was altered. Both *Rymdknäckning* and *FEM-design* were used to determine the reaction moments of the horizontal loads.

3.1 Method of the study

The stiffness of the exterior walls was altered by using three types of wall elements with configurations similar to those in *Pyramiden Building 3* studied in Chapter 2; solid wall element, wall elements with openings and steel truss element.

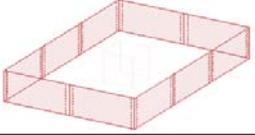
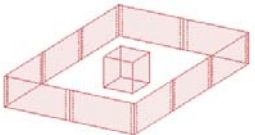
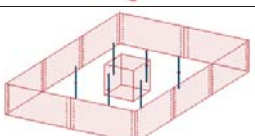
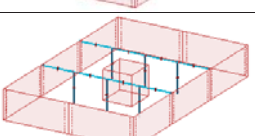
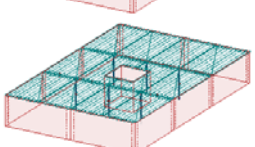
Besides the reaction moments in the foundation the buildings captured the behaviour of different configurations of wall elements on a structural level. It was of interest to investigate how the interaction between the wall elements was influenced by irregular stiffness. The distribution of loads between wall elements with different stiffness within the same wall as well as between walls with different stiffness within the same storey was also of interest.

The buildings were subjected to wind load and deviation loads from unintended inclination acting together. Since *Rymdknäckning* did not consider self-weight or imposed load, other than to calculate the deviation loads, these were not applied in the FE-models of the buildings.

3.1.1 Building geometry

All three buildings had the same dimensions and load carrying system. It was chosen to use a structural system similar to that in *Pyramiden Building 3* studied in Chapter 2. The structural system consisted of prefabricated exterior concrete walls, a concrete elevator shaft located in the centre of the building, an interior concrete beam-column system and hollow core slab elements. The dimensions were chosen according to (Betongelementföreningen, 1998) and in consultation with structural engineers at ELU konsult AB and are presented in Table 3.1.

Table 3.1 Description of structural system in Simplified building

Structural element	Length [m]	Height [m]	Width [m]	Visualisation
Exterior wall elements	7.2	3	0.2	
Elevator shaft wall elements	3	3	0.2	
Columns with quadratic cross section	0.2	3	0.2	
Beams with rectangular cross section	3.6	0.3	0.12	
Slab HD/F 120-27 elements	7.2	0.265	1.197	

The buildings had 5 storeys and a total height of 15 meters. There were two wall elements in the width of the building and three wall elements in the length of the building resulting in floor plans with dimension $13.6 * 20.4 m^2$.

Building 1, Figure 3.2, had solid exterior walls and an equally distributed stiffness through the structural system. In *Building 2*, Figure 3.3, and *Building 3*, Figure 3.4, the solid wall elements in one of the exterior walls were replaced by wall elements with openings which thereby reduced the stiffness of the wall. The openings had the dimensions $1.2 * 1.2 m^2$ and were placed symmetrically in the wall element. The distance between the openings was twice the distance from the opening to the edge of the wall element. In addition the wall elements in the bottom floor of the wall with reduced stiffness in *Building 3* were replaced by steel trusses. The truss was in VKR profile with dimensions $0.2 * 0.2 * 0.0063 m^3$ and steel class S 355. Figure 3.1 illustrates the three different wall elements and their configurations.

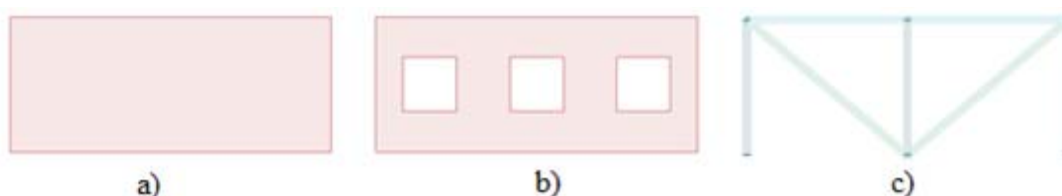


Figure 3.1 a) Solid wall element b) Wall element with openings c) Truss element.

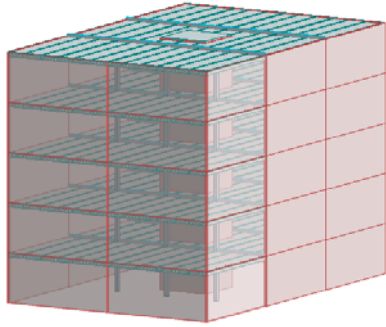


Figure 3.2 Building 1 – solid wall elements.

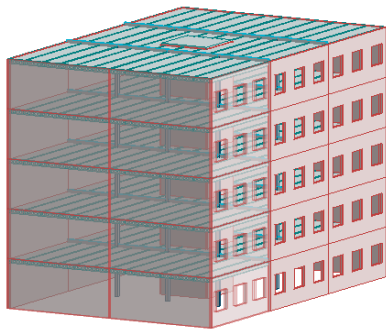


Figure 3.3 Building 2 – wall elements with openings.

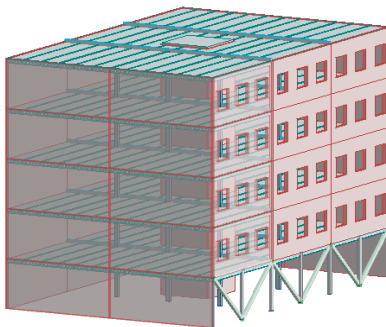


Figure 3.4 Building 3 – truss elements.

3.2 Rymdknäckning

The *Rymdknäckning* calculation were done in similar way as in *Pyramiden* and resulted in a moments and shear forces in each wall according to second order theory of the three buildings. A more detailed description of the software can be found in Chapter 2.3.2.

3.2.1 Geometry input

The three buildings were designed as 6 walls, where the elevator shaft was simplified into two walls in accordance with the method used in the case study of *Pyramiden*. Figure 3.5 shows the configuration of the walls. It should be noted that wall number 4 was the one that was altered in the study.

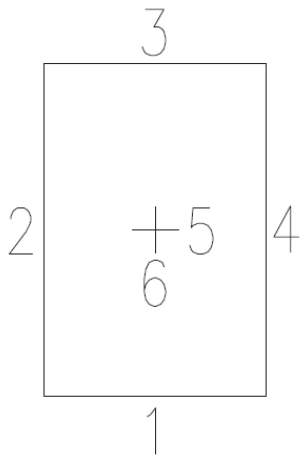


Figure 3.5 Configuration of stabilizing walls in Rymdknäckning.

The stiffness of the different wall elements was calculated according to Chapter 2.3.2. Table 3.2 shows the calculated values that were used as input in *Rymdknäckning*:

Table 3.2 Input data of wall elements in *Rymdknäckning*

Structural member	$I [m^4]$	$A [m^2]$
Solid wall elements	6.205	1.420
Wall elements with openings	1.742	0.403
Truss elements	0.156	0.027
Elevator shaft	2.913	2.000

3.2.2 Loading

The values of the wind load obtained from the *FEM-design* analysis, see section 3.3.6, were used as input data in *Rymdknäckning* to make sure that the same loads were applied. Loads from unintended inclination were derived from the applied imposed loads.

3.3 FEM-Design

FEM-design was used to calculate the reaction moment in the three buildings. The input data were chosen to imitate the one from *Pyramiden* and this chapter will describe the choices made for the analysis of *Building 1-3*. More general information about *FEM-design* can be found in Chapter 2.4.1.

3.3.1 Analysis

It was chosen to perform linear analyses taking second order effects into consideration. Cracking or uplift was not considered.

3.3.2 Element types

The interesting output of the models in this study was the global response of the structural system and the reaction moments at the foundations. Since the desired

output was the global behaviour of the structural system it was sufficient to use structural type finite elements and FE-models on structural level. (Broo, et al., 2008).

3.3.2.1 Exterior walls and Elevator shafts

Exterior walls and elevator shafts were modelled using the *FEM-design* built in object *Plane wall*, which in the *3D-structure* module created a structural wall consisting of 3D shell elements.

3.3.2.2 Columns and Beams

Beam and columns were modelled using *FEM-designs* build in objects *Beam* and *Column*, which in the *3D-structure* module created structural beams consisting of 3D beam elements.

3.3.2.3 Slabs

Slabs were modelled using the *FEM-design* built in object *Profiled plate*, which in the *3D-structure* module created 3D shell elements. The profile was chosen to HD-F 120-27 and the analytical model was chosen to *individual panels*.

3.3.2.4 Truss members

The web members of truss structures were modelled using the *FEM-design* built in object *Truss member*. It models bars that were limited to describe compression, tension and deformations along their own axis.

3.3.3 Material

All concrete members were assigned the material isotropic Concrete C35/45 and the creep and shrinkage factor were set to zero. The steel members were assigned the material Steel S 355 with predefined values of gamma factors according to (Eurocode 3, 2005).

3.3.4 Mesh density

The mesh of the structure was generated using the *FEM-design* built in function "Prepare" and selecting *Region by region* and *Accurate* element types. For bar elements the minimum number of line elements was set to five, which with the "Accurate" element type divided columns, beams and truss members into ten elements.

3.3.5 Supports and boundary conditions

3.3.5.1 Foundation

It was chosen to model the structures connection to the model space by supports. The bottom wall elements were assigned the support *Line support group* with the support type *rigid*. In order to model totally stiff foundations the stiffness against displacement and rotation were set to the maximum allowed values, $1 * 10^{15}$ [kN/m] and $1.745 * 10^{13}$ [kNm/°] respectively. The rotation around the wall elements axis

was released under the assumption that wall elements only transfer membrane forces. The columns located on the bottom floor were assigned *Point support groups* with maximum allowed stiffness against displacement and zero stiffness against rotation.

3.3.5.2 Exterior walls and Elevator shafts

Wall elements were assigned the predefined values for the boundary connection condition *rigid* at the top and the bottom edge. The longitudinal connections between individual wall elements were assigned maximum stiffness against displacement and zero stiffness against rotation creating a hinged *Boundary connection*.

3.3.5.3 Columns and Beams

Columns and beams were assigned the maximum stiffness against displacement and zero stiffness against rotation at their ends.

3.3.5.4 Slabs

Plate elements were assigned the predefined values for the boundary connection condition *Hinged* at all edges.

3.3.5.5 Truss members

Truss members end connections were predefined as *Hinged* and could not be modified.

3.3.6 Loading

The wind load and deviation loads in Table 3.3 were generated by *FEM-design* built in functions for generating loads according to (Eurocode 1, 2002).

Table 3.3 Horizontal loads applied in FEM-design for each floor

Floor	Wind load [kN/m]	Deviation load [kN]
1	3.60	11.7
2	3.60	11.7
3	3.60	11.7
4	3.60	11.7
5	1.99	7.51

3.3.7 Output

The output of the analysis was the resultant moment in the foundation for each wall. Due to the chosen boundary condition the structural system acted like a box structure and vertical resultant forces occurred in the walls perpendicular to the applied load. These resultant forces were converted to moment by multiplying them with their distance to the centre of gravity. The converted moment was when distributed between the walls parallel to the applied load with the same proportion as the resultant moment distribution, see Figure 3.6.

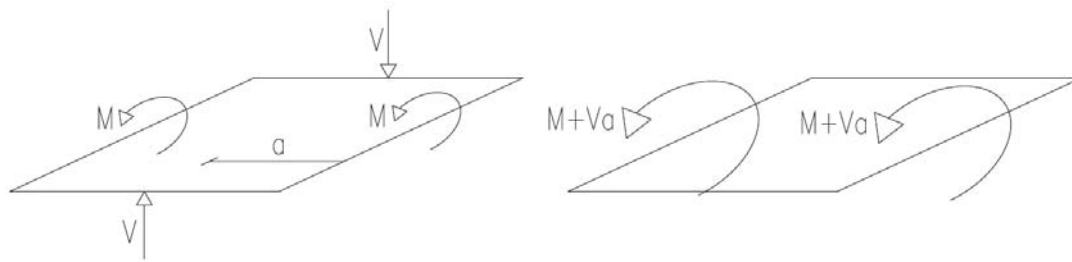


Figure 3.6 Exemplification of method to convert vertical reaction forces to moments.

3.4 Results

The results of the calculations performed on the three buildings was plotted as the resulting moment in each wall as percentage of the total resulting moment for each building respectively, see Figure 3.7-Figure 3.9

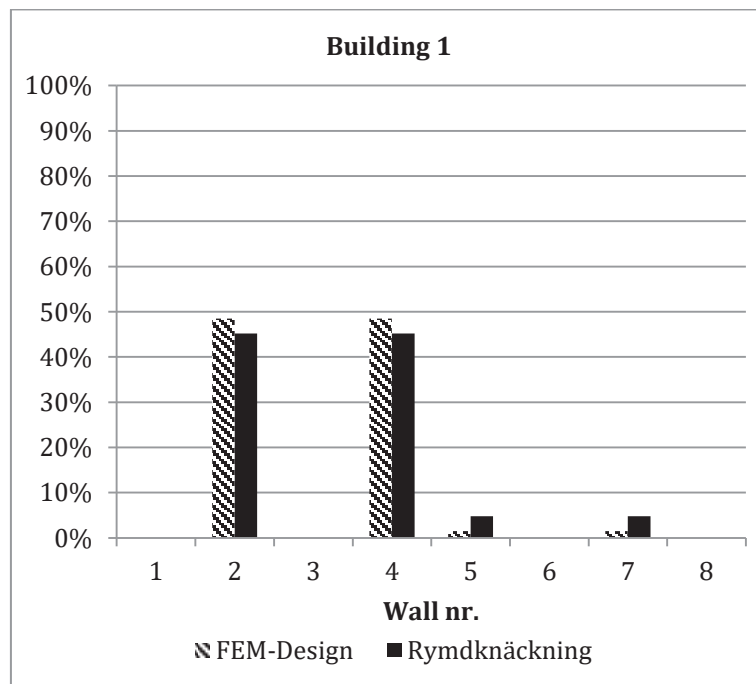


Figure 3.7 The amount of total moment in Wall 1-8 for Building 1.

In *Building 1*, with only solid wall elements, the results in *FEM-design* and *Rymdknäckning* were similar. As showed in Figure 3.7 the external walls attracted a larger moment in *FEM-design* than *Rymdknäckning*. *Rymdknäckning* attracted a larger amount of moment in the elevator shaft.

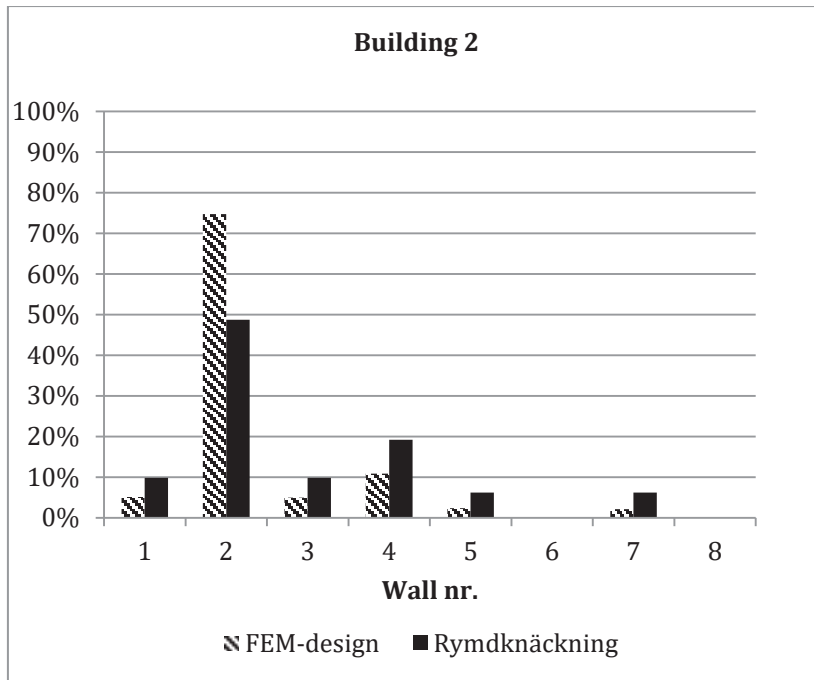


Figure 3.8 The amount of total moment in Wall 1-8 for Building 2.

In *Building 2* the reduced stiffness of *Wall 4* resulted in torsion of the structural system and therefore additional resultant moments in *Wall 1* and *Wall 3*, see Figure 3.8. The FE-analysis suggested that a majority of the applied horizontal load was attracted by *Wall 2* while the loads were divided more equally between the walls in *Rymdknäckning*.

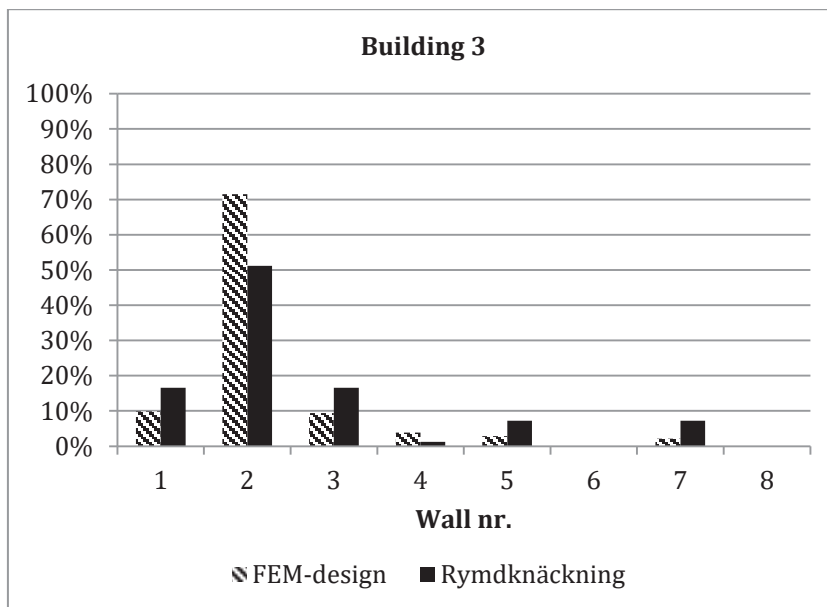


Figure 3.9 The amount of total moment in Wall 1-8 for Building 3.

In Figure 3.9 it was noted that the distribution of moment in *building 3*, with trusses, were similar as for *Building 2* in Figure 3.8. It was found that almost no moment where attracted to *Wall 4* in *Rymdknäckning* while the FE-analysis still attracted some

moment. The moment distribution also increased in *Wall 1* and *Wall 3* compared to the results in *Building 2*.

The overall results of the case study of the simplified building showed that there occurred a redistribution of the reaction moment between the walls as the stiffness of *Wall 4* was reduced. In *Rymdknäckning* the percentage of the attracted moment in *Wall 2* remained constant while *Wall 1* and *Wall 3* attracted a larger amount of the induced total moment. The moment distribution obtained from FE-analysis instead attracted a majority of the induced total moment in *Wall 2*. It could also be seen that the walls of the elevator shaft attracted more moment compared to FE-analysis. The case study therefore suggested that the observed differences in load distribution were not specific for the structural system of *Pyramiden* and that reduced stiffness of exterior wall influenced the load distribution.

3.5 Discussion

In order to gain a deeper understanding of the influence of the horizontal loads on the load distribution it was chosen to not consider vertical loads, neither permanent nor variable, in the FE-analysis of the simplified building. By this simplification the behaviour of the building probably became further from reality compared to the case of both horizontal and vertical loads. For example, it could be argued that the global rotational deformation of the building would be smaller in the presence of vertical loads. The opportunity to investigate the differences related to vertical loads observed in the case study of *Pyramiden* influence on the load distribution and the load path of vertical loads through wall elements with openings were also neglected by this choice. However, the choice was well motivated considering the comparison to the initial calculations and the use of the superposition principle of horizontal and vertical loads. Some deviation in the load distribution between the walls were expected since *Rymdknäckning* only considered the load to act in the stabilizing elements located parallel to the applied load while *FEM-design* considers load transferring in the connections between the exterior walls.

It should be noted that the input of deviation loads in *Rymdknäckning* was limited to the number of vertically loaded members and the imposed load per storey while *FEM-design* uses a built in function to obtain the deviation load and that it therefore was problematic to apply the exact same loads in the two software. To reduce the differences the self-weight of the building in *FEM-design* was used as the imposed load in *Rymdknäckning*. The differences in the applied load were therefore assumed to have little influence on the results, which was supported by the results of the parametric study of the load distribution discussed in Chapter 6. As an additional precaution the values of the resultant moments were rounded up and thereby reducing the accuracy of the study. However, the accuracy of the results was still considered sufficient to show the global behaviour of the building and the tendency of the load distribution.

The result also suggested that a larger amount of the total moment was resisted in the elevator than in the exterior wall in *Rymdknäckning* compared to FE-analysis. A similar behaviour was observed in the case study of *Pyramiden* and it was therefore chosen to investigate the assumptions regarding stiffness estimations of wall elements further.

4 Stabilizing elements

The stability of a building is defined as the buildings capacity to transfer horizontal loads through the structural system and down into the foundation. Stability is obtained through a sufficient number of bracing members that are stiff with regard to the horizontal loads. The vertical structural elements used to transfer horizontal loads include shear walls, braced frames, moment resisting frames or a combination of these. (Dickey & Schnider, 1994) This chapter describes analytical methods for estimating the stiffness of stabilizing elements.

4.1 System of columns

Individual columns are often assumed to provide little or none stability, however, a system of columns interacting in one plane can be considered to act as a stabilizing system. The stiffness of the system as well as the deformed shape of the system is determined by the individual stiffness of members and the connections between columns and beams. As shown in Figure 4.1 the deformation of a system of column can be governed by bending deformation of the columns and beams and axial deformations of the columns.

In a frame system it is usually assumed that the columns are connected at the top and that the connecting member is rigid. The deflection at the top will therefore be the same for all columns in the frame system. (Westerberg, 1997)

The horizontal force acting on the system of columns is distributed between the columns in proportion to their individual stiffness according to equation 4.1.

$$P_i = P \frac{K_i}{\sum K_i} \quad (4.1)$$

The total deflection of the frame system can then be determined as the total horizontal force divided by the sum of all stiffness according to equation 4.2. (Westerberg, 1997)

$$\Delta_{frame} = \frac{P}{\sum K_i} \quad (4.2)$$

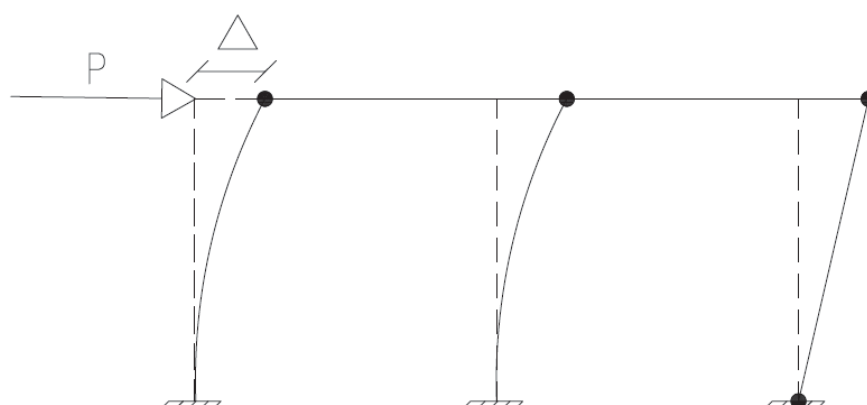


Figure 4.1 Deformation of system of columns due to applied load P

4.2 Shear walls

Shear walls are, as the name implies, a commonly used structural element to stabilize the building against horizontal loads and shear deformation. How the building and the shear walls deform depends on the configuration of the structural system. Buildings with a height to width ratio smaller than one will mainly act as shear structures and the shear walls can be designed on a floor-to-floor basis. In taller buildings with a height to width ratio larger than one the dominant deformation will be bending and the shear walls should be designed as building height cantilevers. (Dickey & Schnider, 1994) However, assuming fixed boundary condition at each storey the wall rigidities of high rise buildings could be computed at each story under the following conditions:

- Relatively uniform arrangement of shear walls
- Relatively long and shear walls with fairly constant size from ground to roof
- Reasonably symmetrical wall arrangement
- Sufficient restraint is provided at each floor level by floors that are stiff relative to walls
- Openings in walls are small enough to have negligible effect on shear distribution

If the shear walls have varying size or in the presence of large openings relative rigidities might be computed at roof level under the assumption of infinitely stiff diaphragms, an assumption that is often questionable. (Dickey & Schnider, 1994)

As mentioned above that there are some uncertainties in how boundary conditions of shear walls should be chosen to provide a good representation of the real behaviour of the structure and that the result is highly dependent on the buildings configuration. According to (Dickey & Schnider, 1994) it is generally conceded that wall elements in one- and two-storey structural systems can be considered to have cantilevered boundary conditions. As the number of storeys increases the boundary conditions of the walls above the first storey might be considered fixed at both the bottom and the top depending on the relationship between the rigidities of the walls and the floor diaphragms.

To determine the lateral stiffness of prismatic shear wall it is suitable to use the structural model for a deep beam. The total deformation of a shear wall subjected to force along the top edge is determined as the sum of shear and bending deformations, see equation 4.3-4.4 and Figure 4.2. (Neuenhofer, 2006) For derivation of equation 4.3-4.4, see Appendix A.

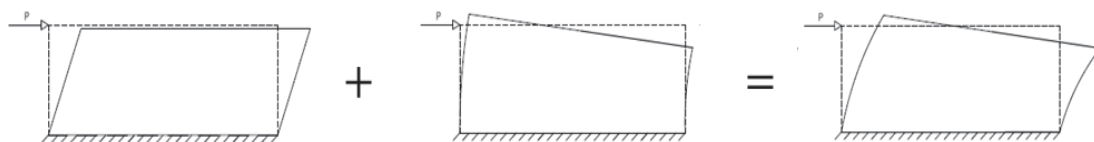


Figure 4.2 Total deformation as the sum of shear and bending deformations due to applied point load P .

For the case of both ends fixed (restrained against rotation) the total deformation at the top of the shear wall is expressed by equation 4.3.

$$\Delta_{fixed} = \Delta_{bending} + \Delta_{shear} = \frac{PH^3}{12EI} + \frac{1.2PH}{GA} \quad (4.3)$$

For the case of cantilever boundary condition (bottom end fixed) the total deformation at the top of the shear wall is expressed by equation 4.4.

$$\Delta_{cantilever} = \Delta_{bending} + \Delta_{shear} = \frac{PH^3}{3EI} + \frac{1.2PH}{GA} \quad (4.4)$$

By using the relationship between the elastic and shear modulus and cross-sectional constants for rectangular cross-sections the relative contribution of bending and shear deformations can be determined according to equation 4.5-4.6. For concrete it is reasonable to use 0.25 as a value of Poisons ratio resulting in a shear modulus of $G = 0.4E$.

$$\Delta_{fixed} = \frac{P}{Et} \left(\left(\frac{H}{L} \right)^3 + 3 \frac{H}{L} \right) \quad (4.5)$$

$$\Delta_{cantilever} = \frac{P}{Et} \left(4 \left(\frac{H}{L} \right)^3 + 3 \frac{H}{L} \right) \quad (4.6)$$

From equation 4.5-4.6 it is seen that for small aspect ratios where $H < L$ shear deformations will be dominant and that the bending deformations increases with the aspect ratio. (Neuenhofer, 2006)

4.3 Shear walls with openings

The presence of openings with significant large dimension in comparison to the dimensions of the shear walls governs disturbed regions that occur where the stress flow is irregular. Standard deep beam theory is therefore not applicable to determine the lateral stiffness of shear walls with openings. (Balasubramanian, et al., 2011)

In (Dickey & Schnider, 1994) three analytical methods are presented which could be used to determine the stiffness of shear walls with openings. All three methods treat the shear wall with openings as a system of piers and spandrels which are more or less connected. The basic principles of these methods are:

1. The stiffness of the shear wall with openings is obtained by adding and subtracting the deflection for shear walls with different dimensions.
2. The stiffness of the shear wall with openings is obtained by treating the wall as a system of piers and summarizing the stiffness of the individual piers.
3. The stiffness of the shear wall with openings is obtained by dividing the wall into systems of piers and spandrels based on their load carrying interaction and summarizing their stiffness or deflection.

A refined version of *Method 3* in (Dickey & Schnider, 1994) is developed and compared to the three methods as well as FE-analyses in (Balasubramanian, et al., 2011). By comparing the results of the stiffness of five typical shear wall configurations it is shown that the results from the refined method deviates less from the results of the FE-analysis than the previous three methods. Based on the result presented in (Balasubramanian, et al., 2011) it is chosen to consider the refined method, referred to as *Method 3* in this thesis.

4.3.1 Method 1

This approach to determine the relative rigidity of a wall consisting of connected piers was suggested in a publication from Concrete Masonry Association of California. It is assumed that the wall should be located within a one- or two-storey building and therefore have cantilever boundary conditions. There are uncertainties in determining the actual stress distribution and the degree of end rotations, which indicates that the deformation should be determined with rather low degree of precision. It is further recommended to not apply this method for shear walls with large openings. (Dickey & Schnider, 1994)

Method 1 can be divided into four calculation steps, see Figure 4.3. (Quamaruddin, 1999)

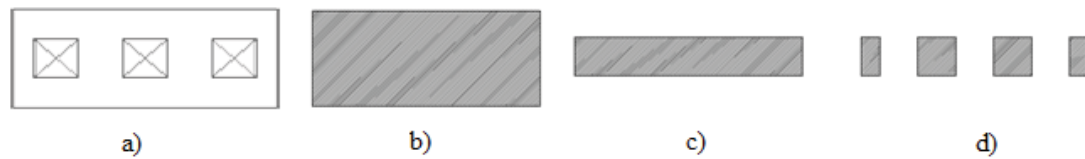


Figure 4.3 a) Wall element with openings. b) Solid wall element. c) Interior strip element. d) System of piers.

The deflection of a cantilever wall is calculated according to deep beam theory, see equation 4.7, without considering the opening, i.e. considering the shear wall as solid, see Figure 4.3.b.

$$\Delta_{solid\ wall} = \frac{PH_{solid\ wall}^3}{3EI_{solid\ wall}} + \frac{1.2PH_{solid\ wall}}{GA_{solid\ wall}} \quad (4.7)$$

The deflection of an interior strip, with a height equal to that of the highest opening, is calculated according to deep beam theory, see equation 4.8, and subtracted from the deflection of the solid wall. Conflicting information regarding the boundary conditions of the interior strip exists in the literature. The interior strip is treated as a cantilever wall according to (Quamaruddin, 1999) while (Neuenhofer, 2006) considers the end conditions of the strip to be fixed-fixed, see Figure 4.3.c.

$$\Delta_{solid\ strip} = \frac{PH_{solid\ strip}^3}{3EI_{solid\ strip}} + \frac{1.2PH_{solid\ strip}}{GA_{solid\ strip}} \quad (4.8)$$

or

$$\Delta_{solid\ strip} = \frac{PH_{solid\ strip}^3}{12EI_{solid\ strip}} + \frac{1.2PH_{solid\ strip}}{GA_{solid\ strip}}$$

The deflection of all the piers within the interior strip is determined individually according to deep beam theory, see equation 4.9, assuming fixed-fixed boundary conditions and summarized as the reciprocal of the stiffness and added to the total wall deflection, see equation 4.10 and Figure 4.3.d.

$$\Delta_{pier} = \frac{PH_{pier}^3}{12EI_{pier}} + \frac{1.2PH_{pier}}{GA_{pier}} \quad (4.9)$$

$$\Delta_{piers} = \frac{1}{\frac{1}{\Delta_{pier}} + \frac{1}{\Delta_{pier}}} \quad (4.10)$$

The stiffness of the total wall, considering the opening, is then calculated as the reciprocal of the deflection of the total wall, see equation 4.11-4.12.

$$\Delta_{wall} = \Delta_{solid\ wall} - \Delta_{solid\ strip} + \Delta_{piers} \quad (4.11)$$

$$K_{wall.el.} = \frac{1}{\Delta_{wall}} \quad (4.12)$$

4.3.2 Method 2

Method 2 is a simplified approach that treats the wall as a strong spandrel-weak pier system where the piers are the portions of the wall framed between the openings. The flexibility of the spandrels is thereby neglected and the stiffness of the wall is calculated as the sum of the stiffness of each individual pier with fixed-fixed end conditions, see equation 4.13-4.14. (Balasubramanian, et al., 2011) In this method the height of the piers is taken as the height of adjacent opening. If the pier is located between two openings with different height the smallest dimension should be used. (Dickey & Schnider, 1994)

By concentrating the stiffness of the wall to the system of piers this method is expected to overestimate the stiffness. In order to get a more realistic behaviour of the wall the stiffness of the spandrels is approximated by increasing the height of the piers and thereby decreasing their stiffness. In accordance with the calculations carried out by ELU konsult AB it is chosen to increase the height of the piers with half the height of the spandrels at each end. The stiffness of each pier is calculated with regard to both bending and shear.

$$K_{pier} = \frac{12EI_{pier}}{H_{pier}^3} + \frac{GA_{pier}}{1.2H_{pier}} \quad (4.13)$$

$$K_{wall.el.} = \sum K_{pier} \quad (4.14)$$

4.3.3 Method 3

Method 3 discretizes the wall into a system of piers. Even the parts of the wall located above and beneath the openings are treated as piers. The stiffness of each pier is calculated and summarized, creating horizontal subsystems within the wall. The final stiffness of the wall is then obtained as the sum of the subsystems stiffness. By dividing the spandrels into subparts their lateral deformation and thereby possible failure is taken into consideration.

Four different types of piers can be distinguished depending on their end conditions, see Figure 4.4.

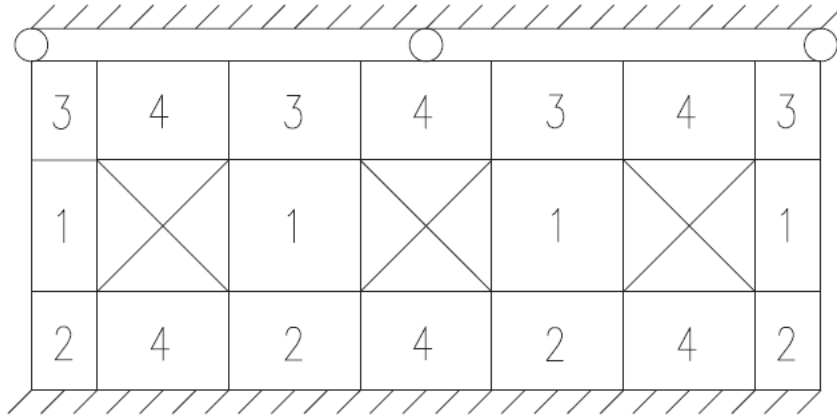


Figure 4.4 The four different pier types in Method 3.

The stiffness of each type is determined according to equation 4.15. (Balasubramanian, et al., 2011)

$$K = \frac{Et}{pq^3+3q} \quad (4.15)$$

This expression for the stiffness is derived under the assumptions that:

- Lateral deflection of individual pier is the sum of deflection due to bending and shear.
- Plain sections before deformation remain plane even after deformation under applied loads.
- Rotation of the cross section normal to the longitudinal axis of the pier is equal to the rotation due to bending only.
- Top edge of the wall is assumed to be restrained against vertical movement.
- Shear interaction between the adjacent piers in horizontal direction is neglected.

It is also assumed that the junction between piers and spandrels are partially fixed which allows rotational deformations in the spandrel, which the previously two methods do not take into consideration. (Balasubramanian, et al., 2011)

It is recommended that the width of the pier shall be at least 3 times the thickness of the pier and that the height of the pier shall be less than five times the width of the pier.

The variables in equation 4.15 are derived differently for the four possible boundary conditions

Piers with both ends partially fixed (type 1), see Figure 4.4.

$$p = \frac{q^4+4q^3r+4q^3s+3q^2r^2+3q^2s^2+14q^2rs+12qr^2s+12qrs^2+12r^2s^2}{q^4+q^3r+q^3s+2q^2rs} \quad (4.16)$$

$$q = \frac{h}{t} \quad (4.17)$$

$$r = \frac{h_b}{t} \quad (4.18)$$

$$s = \frac{h_t}{t} \quad (4.19)$$

Where $h = \text{height of middle pier}$
 $h_b = \text{height of bottom pier}$
 $h_t = \text{height of top pier}$

Piers with bottom end fixed and top end partially fixed (type 2), see Figure 4.4.

$$p = \frac{q+3s}{q} \quad (4.20)$$

$$q = \frac{h_b}{t} \quad (4.21)$$

$$s = \frac{h+h_t}{t} \quad (4.22)$$

Piers with top end fixed and bottom end partially fixed (type 3), see Figure 4.4.

$$p = \frac{q+3r}{q} \quad (4.23)$$

$$q = \frac{h_t}{t} \quad (4.24)$$

$$r = \frac{h+h_b}{t} \quad (4.25)$$

Cantilever piers (type 4), see Figure 4.4.

$$p = 4 \quad (4.26)$$

$$q = \frac{h}{t} \quad (4.27)$$

The piers are then arranged into subsystems depending on if they resist force in parallel action or in series action. The methodology is exemplified by the wall element in Figure 4.5.

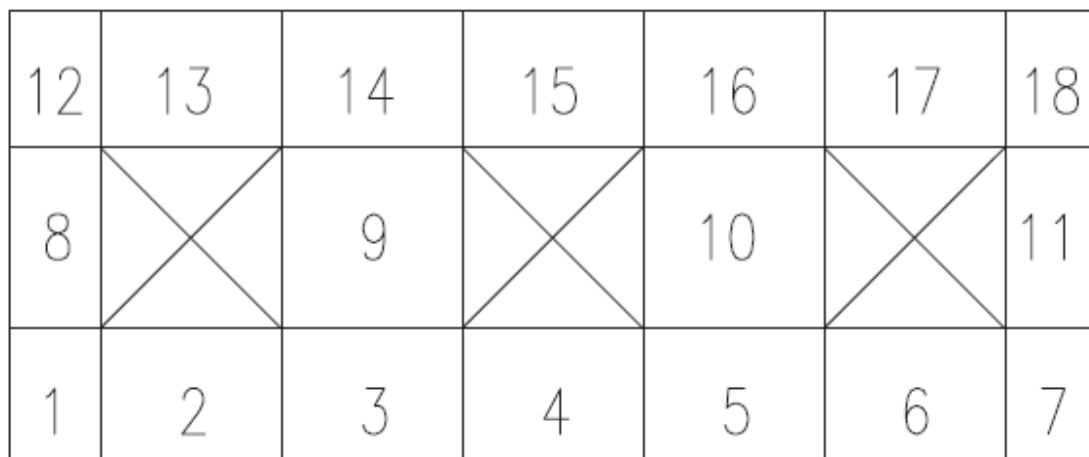


Figure 4.5 Discretization of wall element with openings according to Method 3.

Piers that resist forces in parallel action are arranged into a subsystem where the stiffness of the subsystem is the sum of the stiffness of each pier, see equation 4.28-4.30. Three subsystems that resist forces in parallel action can be identified in Figure 4.5.

$$K_{1-7} = K_1 + K_2 + K_3 + K_4 + K_5 + K_6 + K_7 \quad (4.28)$$

$$K_{8-11} = K_8 + K_9 + K_{10} + K_{11} \quad (4.29)$$

$$K_{12-18} = K_{12} + K_{13} + K_{14} + K_{15} + K_{16} + K_{17} + K_{18} \quad (4.30)$$

Subsystems that resist forces in series actions are merged using relationships related to the flexibility of the structure. The flexibility of *System 1-18* is the sum of the flexibility of *Subsystem 1-7*, *8-11* and *11-18*. The stiffness of *System 1-18* is obtained as the reciprocal of the flexibility, see equation 4.31.

$$K_{wall.et.} = \frac{1}{\frac{1}{K_{1-7}} + \frac{1}{K_{8-11}} + \frac{1}{K_{11-18}}} \quad (4.31)$$

5 Parametric Study – Wall Elements

In order to further investigate what influence assumptions regarding the stiffness of walls have on the horizontal and vertical loads in a building it was preferable to get a deeper understanding of the behaviour of an individual wall element. How the stiffness of one element is calculated and how the stiffness from several elements connected in a row is calculated will be investigated in this chapter through several parametric studies.

5.1 Method of the study

To get better understanding of the influence of the ratio between height and width and whether shear or bending is the governing deformation for a certain ratio a parametric study was performed. Further a study of wall elements with different configurations of openings was performed to determine the stiffness of individual elements. The influence of the width, height and the placement of the openings were chosen to be the varying parameters in these studies. In order to investigate the assumption that a wall element with openings can be replaced by an equivalent stiff solid wall element the presence of openings influence on the vertical load distribution were studied. The wall elements were then studied when connected to each other in horizontal direction and how the amount of elements in a wall is influencing the total stiffness of that wall. Also the effect of where the elements with openings were placed in a wall containing several elements without openings, and how the amount of elements with openings that were placed in the wall would affect the stiffness was studied.

The parametric studies were all done in several steps where one or more parameters were changed and the stiffness was calculated using both analytical and numerical methods. For every step the stiffness was calculated by dividing the force applied at the top of the wall elements with the displacement at the same level. All studies were performed for cantilevered and fixed boundary conditions, see Figure 5.1. All wall elements except those in the aspect ratio study had a constant dimension of $3m$ height, $7.2m$ length and $0.2m$ width.

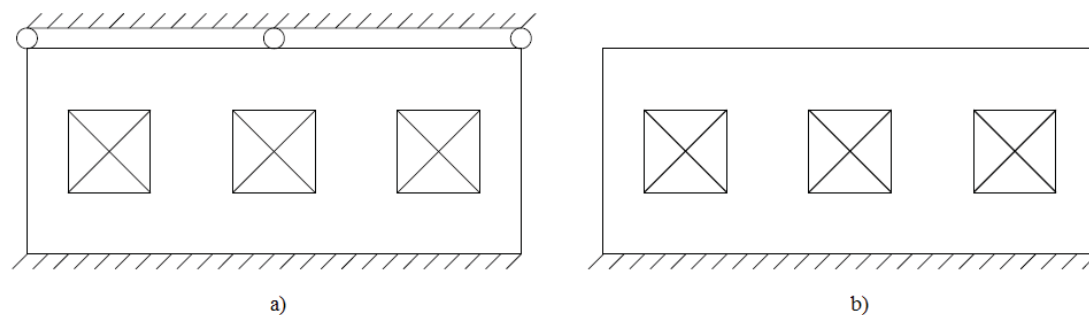


Figure 5.1 a) Fixed boundary condition. b) Cantilever boundary condition.

5.1.1 Aspect ratio

The study of the aspect ratio was done in eleven steps where the ratio, height of wall element divided by length of wall element [H/L], goes from $1/3$ to 3 . The limits were chosen based on the definition of a wall according to (Eurocode 2, 2005). This was done by keeping the height of the wall element at $1m$ for the first six steps while the

length was decreasing from $3m$ towards $1m$, and then increasing the height from $1m$ to $3m$ over the five last steps while the length was constant at $1m$. This is illustrated in Figure 5.2.

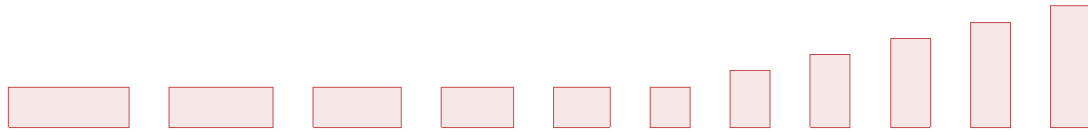


Figure 5.2 Wall elements studied in the parametric study of aspect ratio.

In Figure 5.2 it is also illustrated that this study was done without openings.

5.1.2 Placement of opening

To study the effects of the placement of openings in height the location of the openings were moved from the bottom to the top over eleven steps, with one step equal to $0.18m$. It's also chosen to do this for one-three openings to increase the amount of parameters in the study. The openings were quadratic with a dimension of $1.2 * 1.2 m^2$ and were placed in a symmetrical way over the wall element. The distance between the openings were set to be twice the distance from opening to edge of the wall element. All positions of openings can be seen in Figure 5.3.

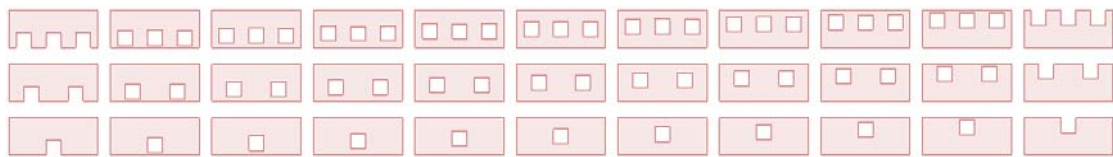


Figure 5.3 Wall elements studied in the parametric study of placement of openings.

5.1.3 Width of openings

In this study was the width of the openings increasing over eleven steps. In the same manner as for placement of openings, was the study done for wall elements with one-three openings placed symmetrical with a distance between the openings set to be twice the distance from opening to the edge of the wall element. The total width of the openings in each step was equal between one-three openings, giving the same area for all three wall elements in each step. The first step has a total opening width of $0.6m$ and step 11 has $6.6m$, giving each step an increase of total opening width of $0.6m$. The heights of the openings were set constant to $1.2m$ for all steps. Figure 5.4 show the different positions of openings in this study.

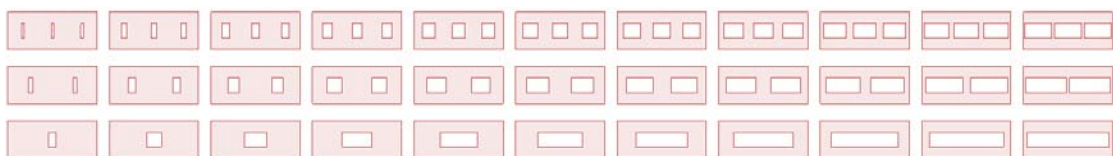


Figure 5.4 Wall elements studied in the parametric study of width of openings.

5.1.4 Height of openings

Also the parametric study of the height of openings was done over eleven steps and with one-three openings placed symmetrically with a distance between the openings set to be twice the distance from opening to the edge of the wall element, see Figure 5.5. The height of the openings was increased from 0.25m to 2.75m with a step of 0.25m, while the width was set constant to 1.2m.

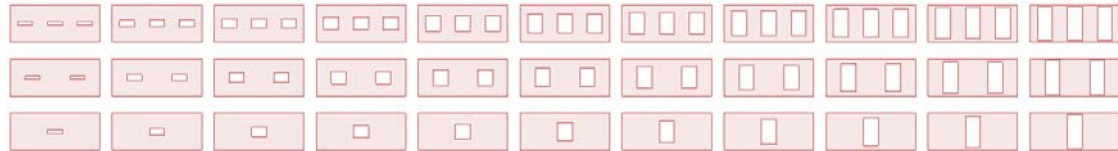


Figure 5.5 Wall elements studied in the parametric study of height of openings.

5.1.5 Distribution of vertical reaction forces

The presence of openings influence on the distribution of vertical reaction forces were investigated by plotting the vertical reaction forces for the different wall element configurations.

5.1.6 Interaction between wall elements

To study how the interaction between wall elements influences the stiffness of a wall of several elements two studies were performed. In the first study the boundary between the elements was prevented from translational deformation in all directions. In the second study the wall elements were treated as individual wall elements without any connection in-between. Both studies were performed over ten steps, where the number of wall elements was increased from one to ten, see Figure 5.6.

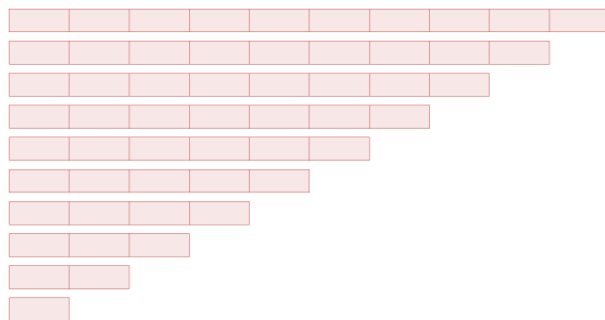


Figure 5.6 Walls studied in the parametric study of interaction between wall elements.

5.1.7 Position of wall elements with reduced stiffness

This study was done in five steps, where three elements with three openings in each were moved from one side of a wall, containing ten elements, towards the centre of it, this is visualized in Figure 5.7. Because of symmetry it was only necessary to step five times. The study was only done for the free boundary between the wall elements since there is no hand calculation method for the fixed boundary when the wall consists of different elements.

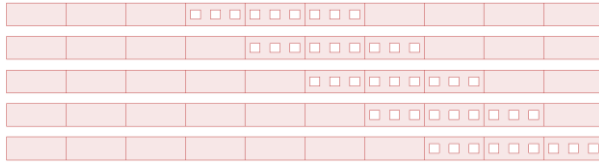


Figure 5.7 Walls studied in the parametric study of position of wall elements with reduced stiffness.

5.1.8 Number of wall elements with reduced stiffness

To study how the stiffness of a wall containing several wall elements was influenced by the amount of wall elements with reduced stiffness a study over ten steps were performed. For each step the number of elements with reduced stiffness were increased, from one element in the first step to ten in the last one. The wall contained ten wall elements in total. Figure 5.8 shows the configurations of elements in each step. This study was only done for the free boundary for the same reason as for Chapter 5.1.7.

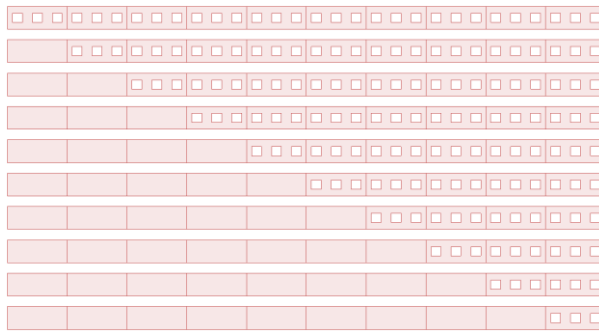


Figure 5.8 Walls studied in the parametric study of number of wall elements with reduced stiffness.

5.2 Analytical calculations

This chapter will explain how the different studies were calculated by hand and what methods that were used. More details about the different methods and how they works can be found in Chapter 4.

5.2.1 Aspect ratio

The aspect ratio study for fixed and cantilever boundary conditions was calculated according to Timoshenko beam theory and equation 4.3-4.4 stated in Chapter 4.2.

5.2.2 Wall elements with openings

These studies were calculated according to *Method 1-3* and the modified version of *Method 2* used in the *Pyramiden* case study, equation 2.4. It should be noted that *Method 3* only was calculated for fixed boundary condition since this method does not work for cantilever wall elements. The stiffness from the other three methods was all calculated for both fixed and free boundary condition.

5.2.3 Interaction between wall elements

For hand calculations the connected wall elements were assumed to act as a solid wall. Therefore the steps were calculated according to Timoshenko beam theory for the entire wall, see equation 4.3-4.4 stated in Chapter 4.2.

The individual wall elements were calculated in the same way as in the *Pyramiden* case study. The stiffness was calculated for each element of the wall individually, and the total stiffness for the wall was equal to the sum of all elements stiffness.

5.2.4 Positions of wall elements with reduced stiffness

The stiffness of each element were calculated according to *Method 1-3* and then summed up in the same way as for the study of “interaction between wall elements” to give the stiffness of the wall.

5.2.5 Number of wall elements with reduced stiffness

The stiffness of a wall element with openings was calculated according to *Method 1-3*. This was summed up for the amount of elements with openings for each step together with the stiffness of the remaining solid wall elements in the wall.

5.3 Numerical calculations

For the numerical calculations in the parametric study *FEM-design* was used. To calculate the stiffness in the different models was the displacement at the top of the wall elements extracted as the mean value of displacements of all elements along the top boundary. This chapter will explain how the FE-models have been done in *FEM-design* and why different assumptions have been taken. For further explanation of the choices made in the sections below the reader is referred to Chapter 2.4.1.

5.3.1 Analysis

It was chosen to perform linear analyses of first order theory. Cracking was not considered.

5.3.2 Element types

The walls were modelled using the *FEM-design* built in object *Plane wall*, which in the *3D-structure* module creates a structural wall consisting of *3D shell elements*.

5.3.3 Material

All walls were assigned the material isotropic concrete C35/45 and the creep and shrinkage factor was set to zero.

The additional wall element that was used to prevent local deformations of the cantilever walls was assigned the material isotropic Steel S 460. The gamma factors were set to the predefined values according to (Eurocode 3, 2005)

5.3.4 Mesh density

The mesh size was chosen to $0.2m$ after a convergence study was performed, this can be found in Appendix B. In the mesh properties it was chosen to use *Accurate* element types instead of *Standard* element types, which increases the number of active nodes.

5.3.5 Supports and boundary condition

The wall elements were assigned the support *Line support group* with the support type *rigid*. In order to model a totally stiff foundation the stiffness against displacement and rotation were set to the maximum allowed stiffness $1 * 10^{15} [kN/m]$ and $1.745 * 10^5 [kNm/^\circ]$ respectively

The fixed boundary conditions at the top of the wall elements were modelled by applying a line support at the top boundary that prevents displacements in global z-direction, see Figure 5.9.a.

Walls with cantilever boundary condition, see Figure 5.9.b, were reinforced at the top boundary with an additional wall element. These elements were supposed to be stiffer than the concrete wall to prevent local deformations at the corners. This was considered a good representation of the walls structural behaviour when connected to a floor diaphragm.

To model the boundary between the wall elements the edge connections were modelled using *rigid* connections with maximum allowed stiffness, which should represent a solid wall element or prefabricated wall elements that were welded together.

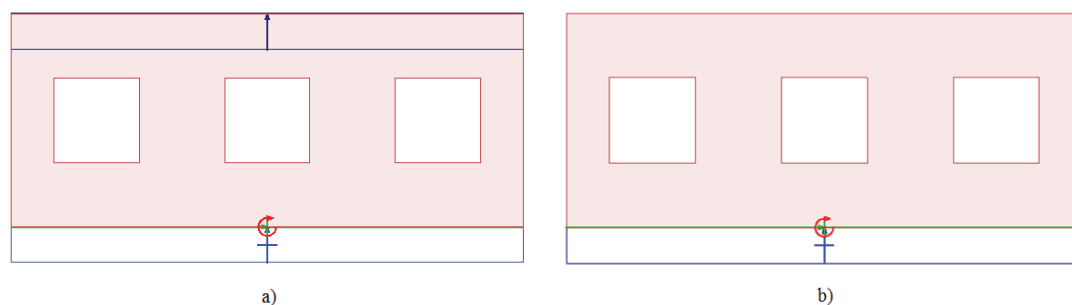


Figure 5.9 a) Fixed boundary condition. b) Cantilever boundary condition.

5.3.6 Loading

The wall was loaded at the top with uniformly distributed load acting along the length of the wall with a magnitude of $138.89 [kN/m]$, which result in a total applied load of $100 [kN/m]$. Self-weight of the building was neglected.

In the case of several connected wall elements and for the wall elements in study of aspect ratio the applied load was $100 [kN/m]$ at each wall element.

5.3.7 Output

The output of the analysis was the mean value of the horizontal displacement at the point of applied load.

5.4 Results

5.4.1 Aspect ratio

The results from the study of the aspect ratio were divided into two parts.

The first part, see Figure 5.10-Figure 5.13, described the relationship between the bending stiffness and the shear stiffness. In these graphs the stiffness against just shear deformations and just bending deformations obtained via analytical calculations was divided by the total stiffness obtained via analytical calculation for each aspect ratio. The lowest values of the curves therefore indicated at which aspect ratio the corresponding deformations were the largest.

It was shown that at low aspect ratios the stiffness against bending was high and the deformations would consequently be dominated by shear deformations. For high aspect ratios the stiffness against shear was high and the deformations would consequently be dominated by bending deformations. The intersection of the curves, at 200%, indicated at which aspect ratio the stiffness against bending and shear was equal. For the fixed boundary condition this intersection occurred at an aspect ratio of approximately 1.8 and for the cantilevered boundary condition at approximately 0.8.

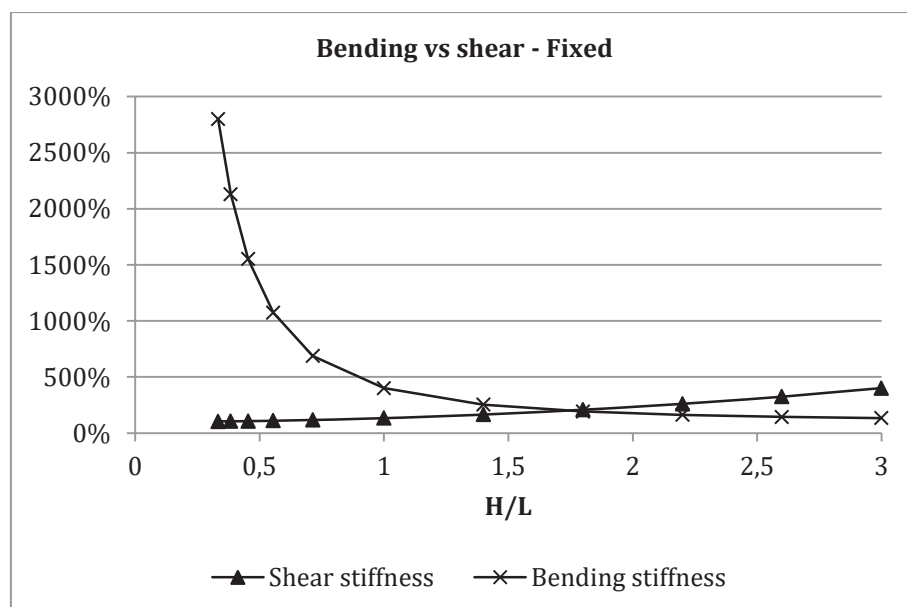


Figure 5.10 Aspect ratios influence on bending and shear stiffness of wall element. Plotted as percentage of total stiffness of each wall element.

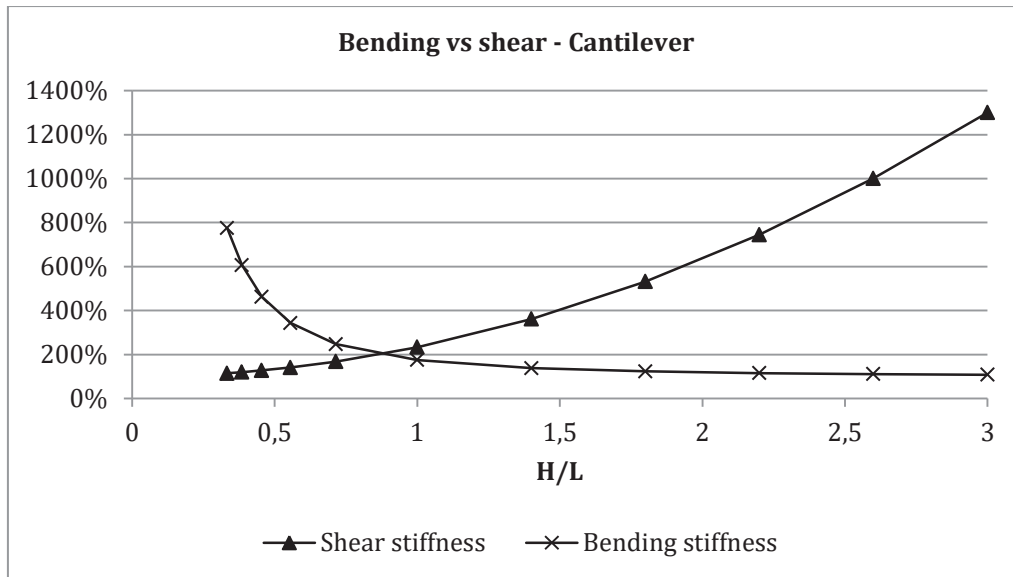


Figure 5.11 Aspect ratios influence on bending and shear stiffness of wall element. Plotted as percentage of total stiffness of each wall element.

The second part, see Figure 5.12-Figure 5.13, described the relationship between the analytical calculations and numerical calculation. The stiffness of the wall element considering both bending deformation and shear deformation were obtained at each aspect ratio and plotted as the percentage of the stiffness compared to the numerical stiffness of the wall element with the lowest aspect ratio.

It was shown that the stiffness of the wall element decreased for both analytical and numerical calculations as the aspect ratio increased. It was also shown that the analytical calculations underestimated the stiffness compared to numerical calculations at low aspect ratio and that this underestimation was larger for the fixed boundary condition.

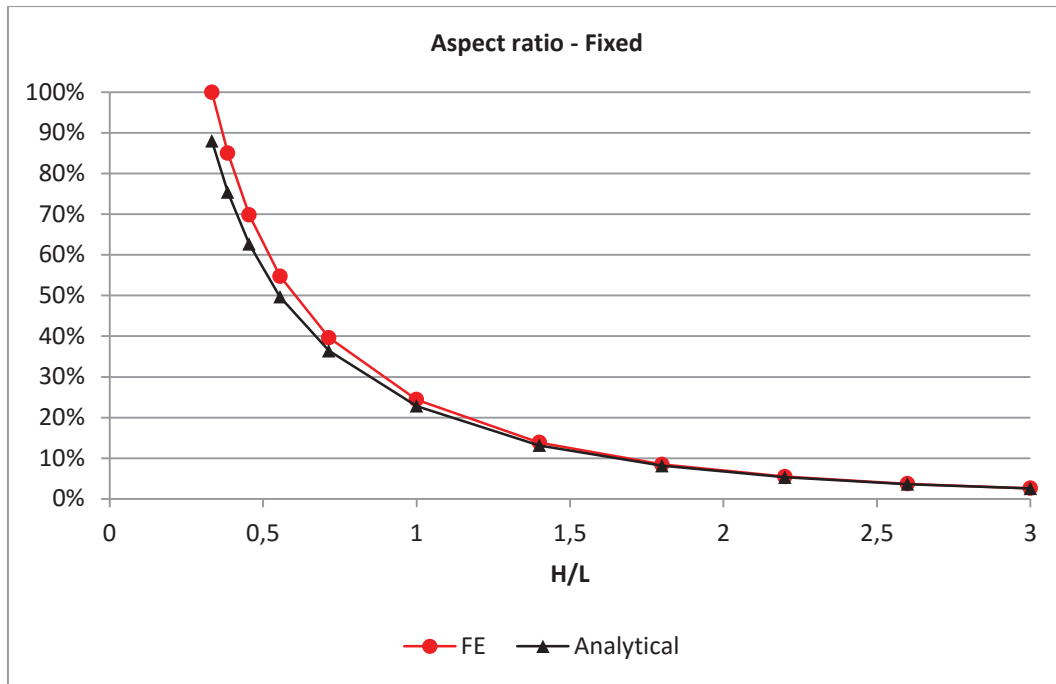


Figure 5.12 Comparison between analytical and numerical stiffness calculations. Plotted as percentage of numerical stiffness of wall element with aspect ratio 1/3 ($K = 7.45 \cdot 10^9$ [N/m]).

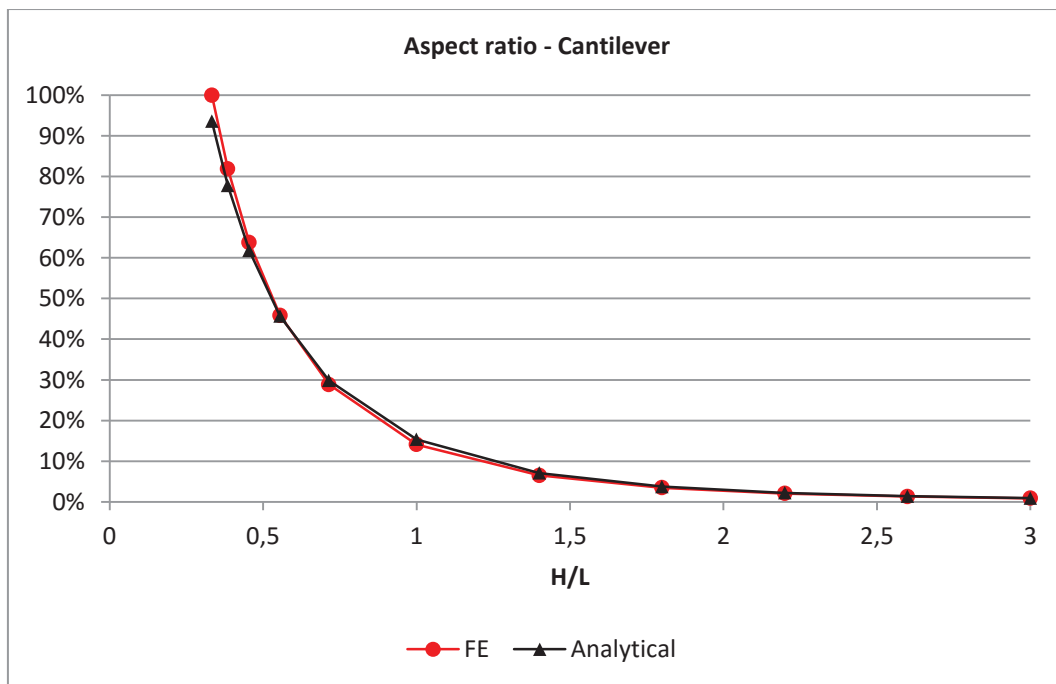


Figure 5.13 Comparison between analytical and numerical stiffness calculations. Plotted as percentage of numerical stiffness of wall element with aspect ratio 1/3 ($K = 6.33 \cdot 10^9$ [N/m]).

5.4.2 Wall elements with openings

The results from the parametric study of wall elements with varying position, height and width of openings were all plotted as curves. For height of opening, as percentage

of solid FE wall element stiffness on y-axis, to amount of opening in total wall element height on x-axis. For width of opening, as percentage of solid FE wall element stiffness on y-axis to amount of opening in total wall element length on x-axis. For position of opening, as percentage of solid FE wall element stiffness on y-axis to position from centre of wall elements on x-axis. These graphs can be found in Appendix C. To better show how the different hand calculation methods treats openings compared to the FE-model the results were summarized as tables in Appendix C.

The result was also displayed as highlighted elements in Figure 5.14-Figure 5.34 to better show how each method treats the different steps in the different studies. The highlighted elements indicate that the method resulted in stiffness within 10 % from the FE result on that specific step.

5.4.2.1 Method 1

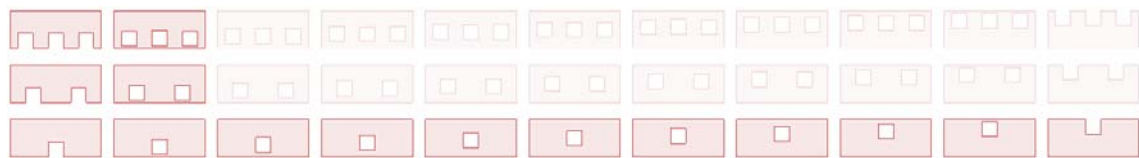


Figure 5.14 Position of openings – Fixed. Wall configuration with stiffness estimation within 10% from numerical calculation.



Figure 5.15 Position of openings - Cantilever. Wall configuration with stiffness estimation within 10% from numerical calculation.

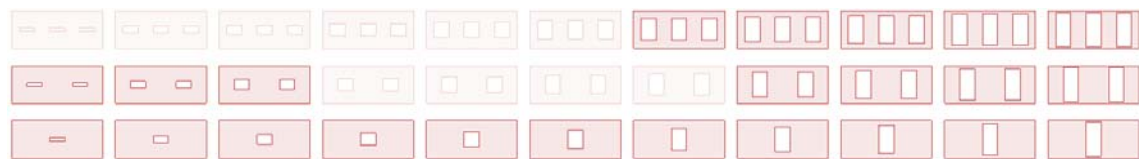


Figure 5.16 Height of openings - Fixed. Wall configuration with stiffness estimation within 10% from numerical calculation.



Figure 5.17 Height of openings - Cantilever. Wall configuration with stiffness estimation within 10% from numerical calculation.

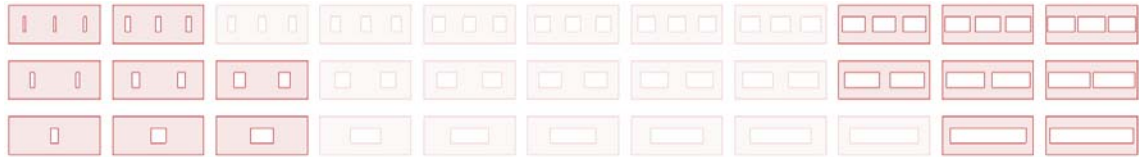


Figure 5.18 Width of openings - Fixed. Wall configuration with stiffness estimation within 10% from numerical calculation.

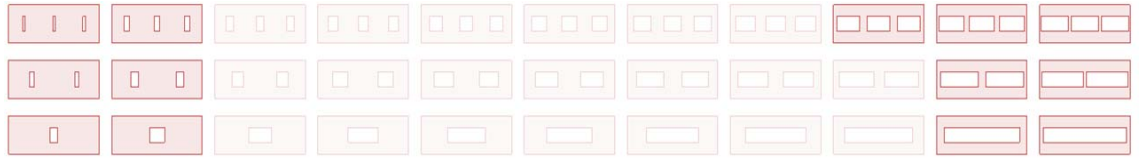


Figure 5.19 Width of openings - Cantilever. Wall configuration with stiffness estimation within 10% from numerical calculation.

5.4.2.2 Method 2



Figure 5.20 Position of openings - Fixed. Wall configuration with stiffness estimation within 10% from numerical calculation.

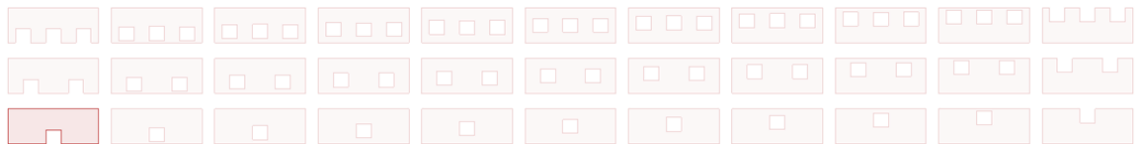


Figure 5.21 Position of openings - Cantilever. Wall configuration with stiffness estimation within 10% from numerical calculation.

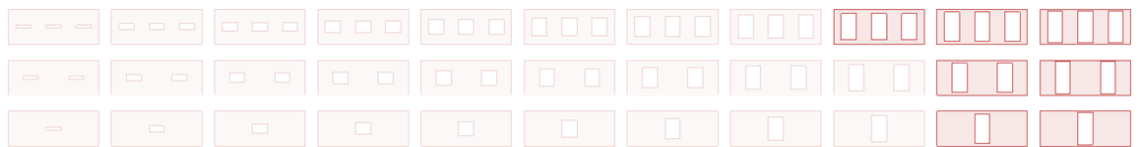


Figure 5.22 Height of openings - Fixed. Wall configuration with stiffness estimation within 10% from numerical calculation.

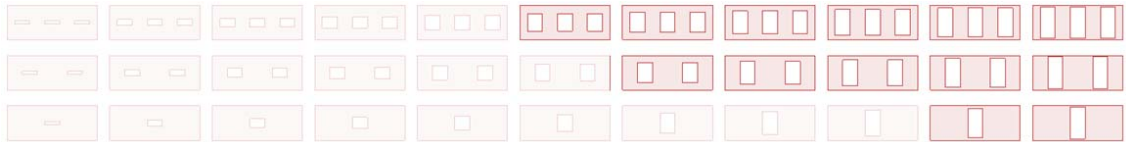


Figure 5.23 Height of openings - Cantilever. Wall configuration with stiffness estimation within 10% from numerical calculation.



Figure 5.24 Width of openings - Fixed. Wall configuration with stiffness estimation within 10% from numerical calculation.

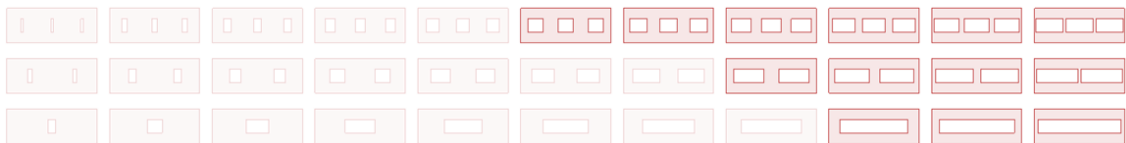


Figure 5.25 Width of openings - Cantilever. Wall configuration with stiffness estimation within 10% from numerical calculation.

5.4.2.3 Method 2 mod

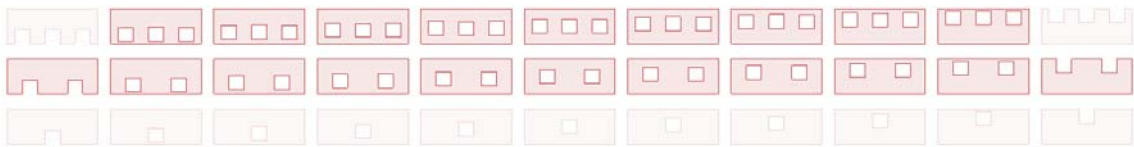


Figure 5.26 Position of openings – Fixed. Wall configuration with stiffness estimation within 10% from numerical calculation.

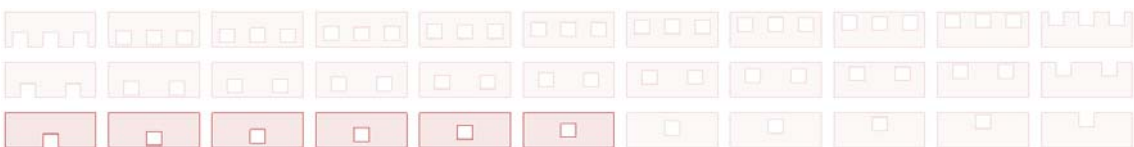


Figure 5.27 Position of openings - Cantilever. Wall configuration with stiffness estimation within 10% from numerical calculation.

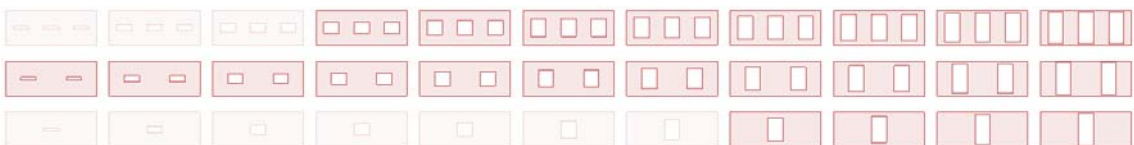


Figure 5.28 Height of openings - Fixed. Wall configuration with stiffness estimation within 10% from numerical calculation.



Figure 5.29 Height of openings - Cantilever. Wall configuration with stiffness estimation within 10% from numerical calculation.

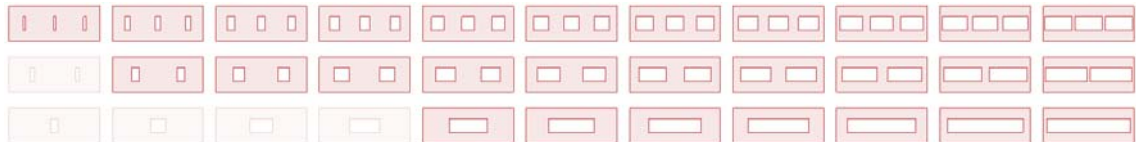


Figure 5.30 Width of openings - Fixed. Wall configuration with stiffness estimation within 10% from numerical calculation.

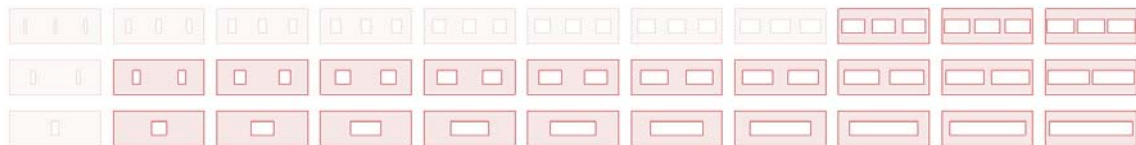


Figure 5.31 Width of openings - Cantilever. Wall configuration with stiffness estimation within 10% from numerical calculation.

5.4.2.4 Method 3

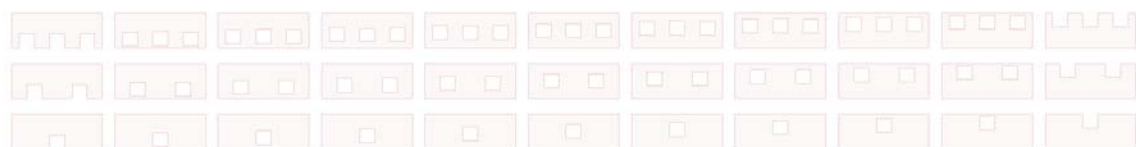


Figure 5.32 Position of openings - Fixed. Wall configuration with stiffness estimation within 10% from numerical calculation.

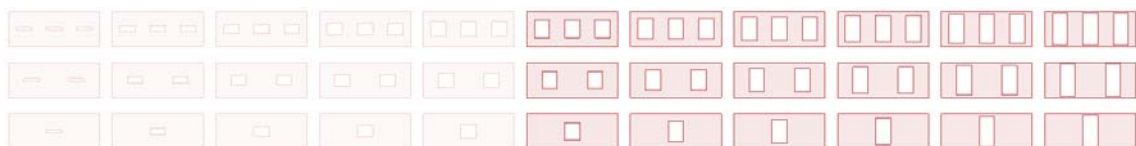


Figure 5.33 Height of openings - Fixed. Wall configuration with stiffness estimation within 10% from numerical calculation.

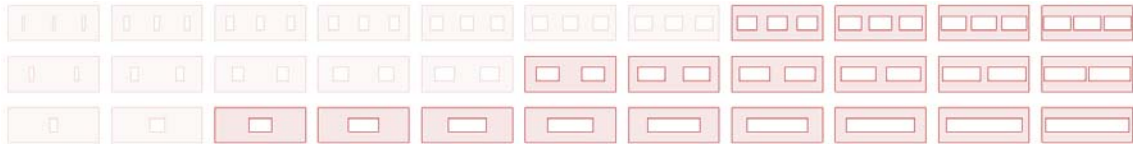


Figure 5.34 Width of openings - Fixed. Wall configuration with stiffness estimation within 10% from numerical calculation.

5.4.3 Distribution of vertical reaction forces

For small dimensions of the openings and when openings were located at the top of the wall elements the distribution of vertical reaction forces was almost linear, see Figure 5.35. As the dimensions of the openings increase or the openings were placed closer to the bottom of the wall element the distribution became increasingly non-linear.

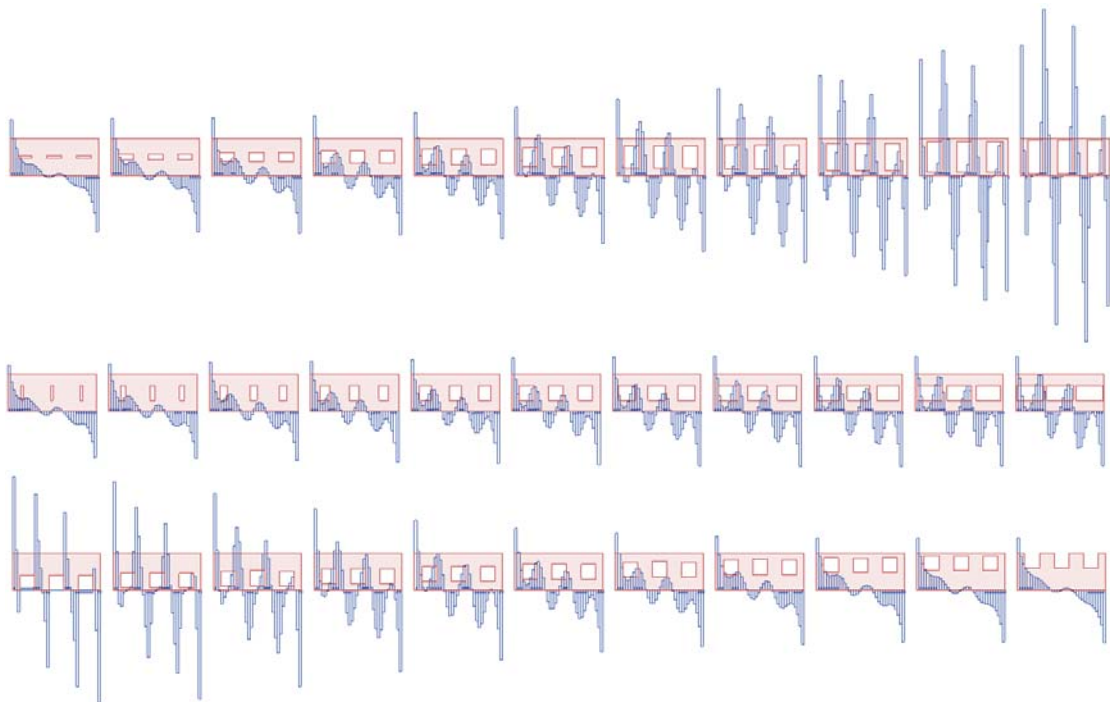


Figure 5.35 Distribution of vertical reaction forces in FEM-design.

5.4.4 Interaction between wall elements

The interaction between wall elements was plotted as two graphs, Figure 5.36 for fixed boundary condition and Figure 5.37 for cantilever. Both graphs show stiffness as percentage of a solid FE element on the y-axis, to the number of wall elements on x-axis.

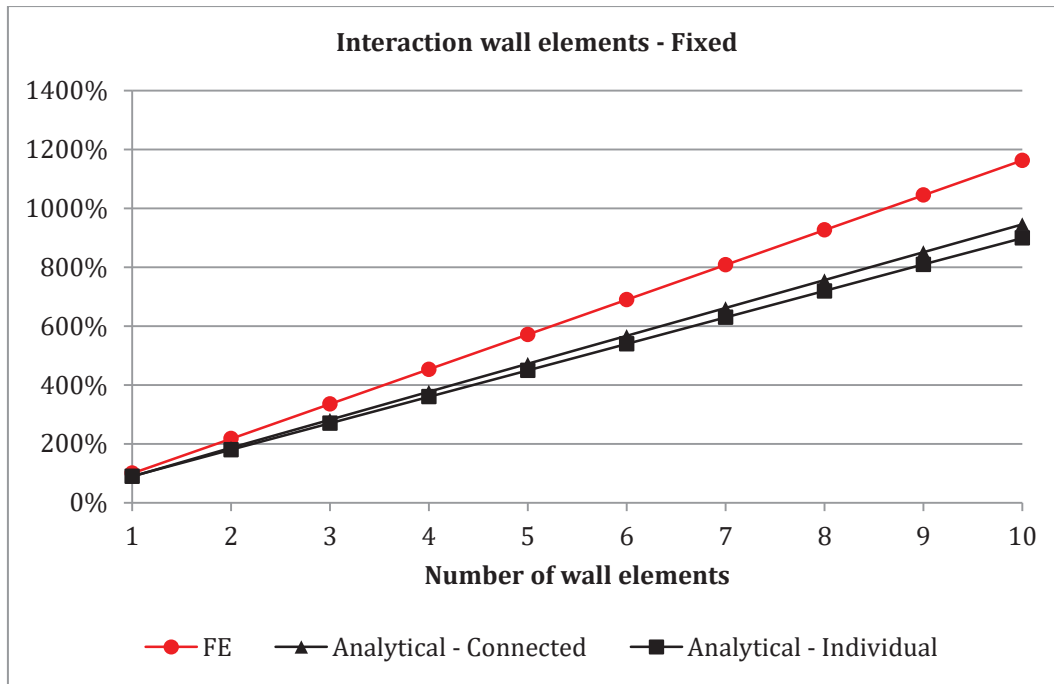


Figure 5.36 Comparison between analytical and numerical stiffness calculations. Plotted as percentage of numerical stiffness of one wall element ($K = 5.75 * 10^9 [N/m]$).

For the fixed boundary condition in Figure 5.36 can a linear behaviour over the number of wall elements be observed for all curves. The linear behaviour was expected since the governing deformation was shear deformation and the shear stiffness increase linearly with the length of the wall. It should be noted that the FE curve has an inclination steeper than one, which indicates that several elements connected are stiffer than just the sum of their individual stiffness. The hand calculation has the same behaviour for connected elements but in the graph the stiffness were plotted as a percentage of solid FE element, giving a slope lower than one since solid FE wall elements are stiffer than hand calculated solid wall elements. The curve representing individual wall elements was lower than the connected since bending deformations decreased the stiffness of the individual wall elements. This curve should of course give a slope of one if plotted against hand calculated solid wall element since the calculation simply was a sum of each elements individual stiffness.

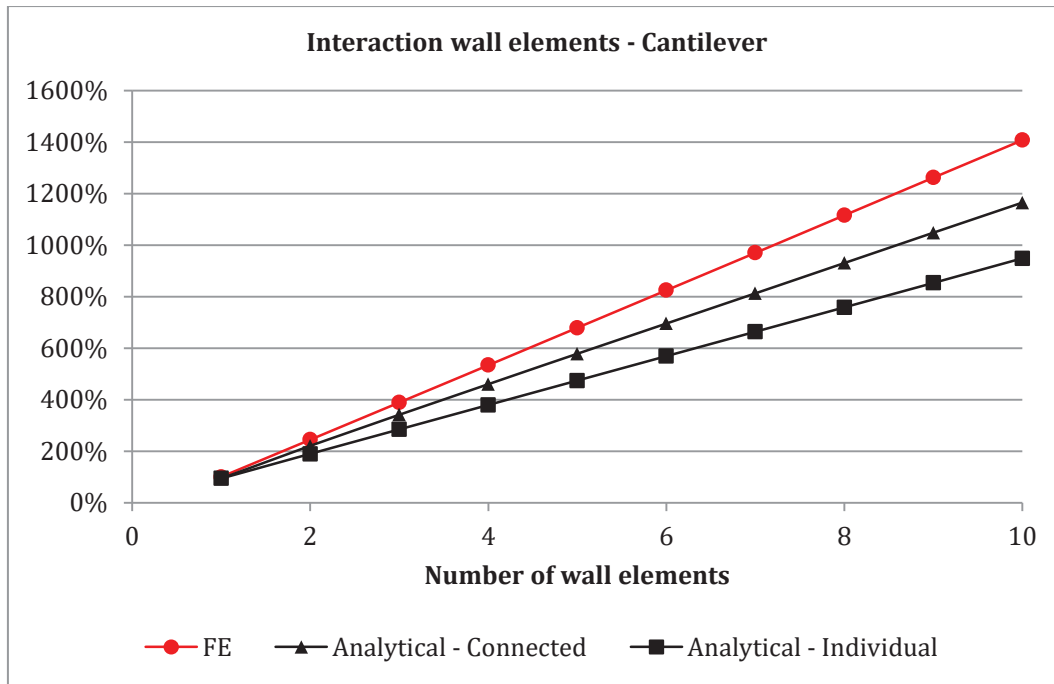


Figure 5.37 Comparison between analytical and numerical stiffness calculations. Plotted as percentage of numerical stiffness of one wall element ($K = 4.66 * 10^9 [N/m]$).

The cantilever boundary condition does also give a linear curve and does in general work in the same way as the fixed boundary. It should be noted that these curve appears to have a higher stiffness than the fixed boundary. For connected wall elements the bending deformations had little effect and the stiffness for the connected wall elements was almost the same for the two boundary conditions. However, the bending deformations had a larger impact on the stiffness of the individual wall element with cantilevered boundary condition. Plotted against a solid FE cantilever element, with much lower stiffness than a fixed one, would therefore give a higher percentage.

5.4.5 Position of wall elements with reduced stiffness

The position of the wall elements with reduced stiffness were plotted as two graphs, Figure 5.38 and Figure 5.39. All curves were plotted with stiffness as percentage of FE configuration 1 on the y-axis and placement one-five, according to Figure 5.7, on the x-axis. All hand calculation curves have a constant value for every configuration since the method with summing up the stiffness of individual elements does not take placement into consideration. It should be noted that the FE curves also have a very constant behaviour which indicates that placement have a minor influence on the total stiffness of the wall.

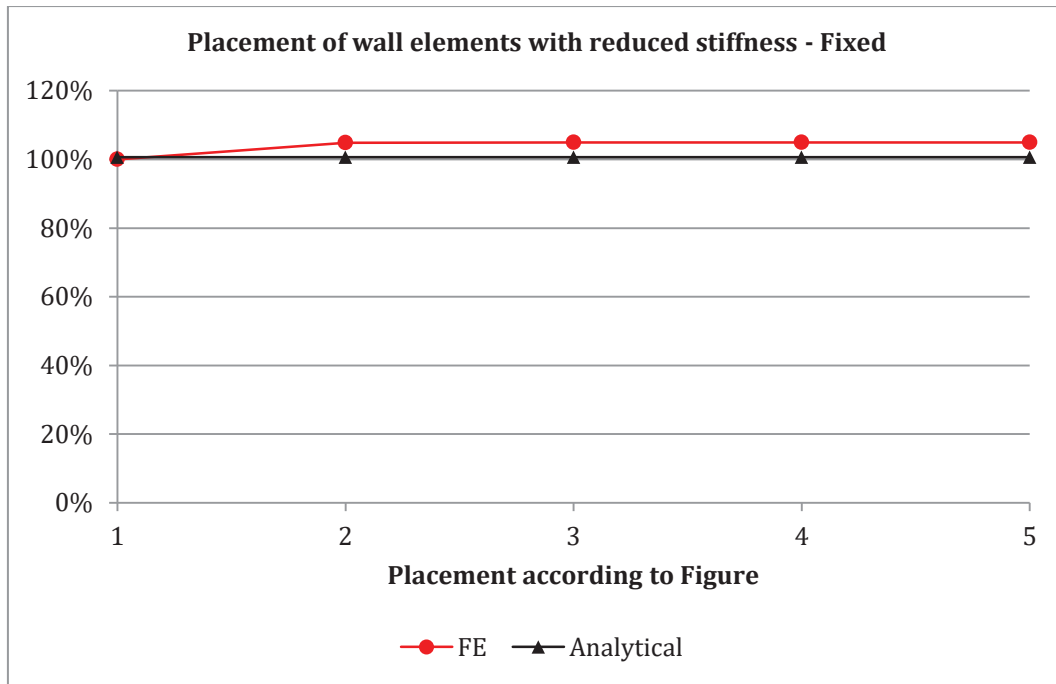


Figure 5.38 Comparison between analytical and numerical stiffness calculations. Plotted as percentage of numerical stiffness of wall ($K = 4.43 * 10^{10}$ [N/m]).

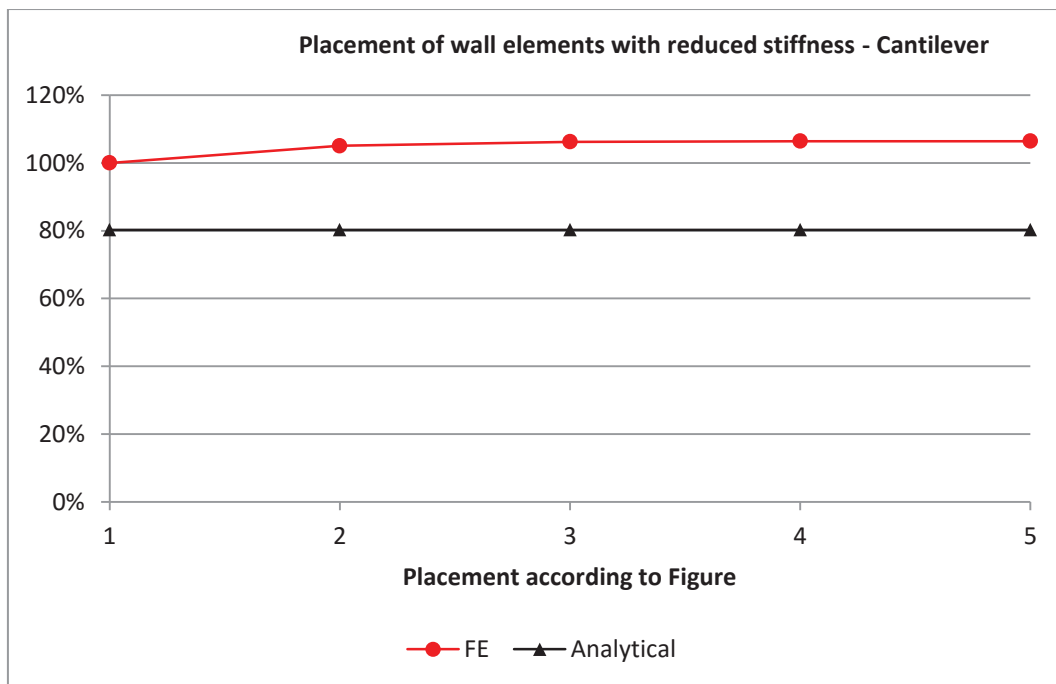


Figure 5.39 Comparison between analytical and numerical stiffness calculations. Plotted as percentage of numerical stiffness of wall ($K = 4.49 * 10^{10}$ [N/m]).

5.4.6 Number of wall elements with reduced stiffness

The influence of the number of elements with reduced stiffness is shown in Figure 5.40 and Figure 5.41. All curves were plotted as stiffness as percentage of FE wall

with one reduced element on the y-axis and how big part of the wall that consists of elements with reduced stiffness on the x-axis. All hand calculation curves give a linear behaviour where the stiffness of the wall was reduced when the number of elements with reduced stiffness was increased. The FE curves have a steeper slope in the beginning but converge towards a linear behaviour when the amount of elements with reduced stiffness was increased.

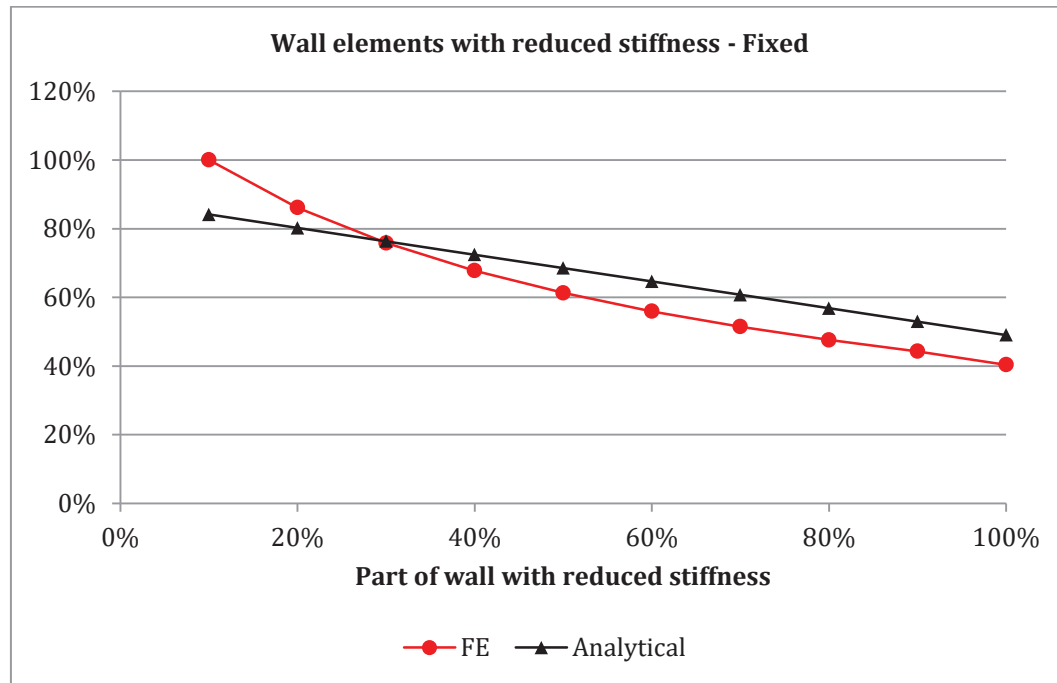


Figure 5.40 Comparison between analytical and numerical stiffness calculations. Plotted as percentage of numerical stiffness of wall ($K = 5.84 * 10^{10}$ [N/m]).

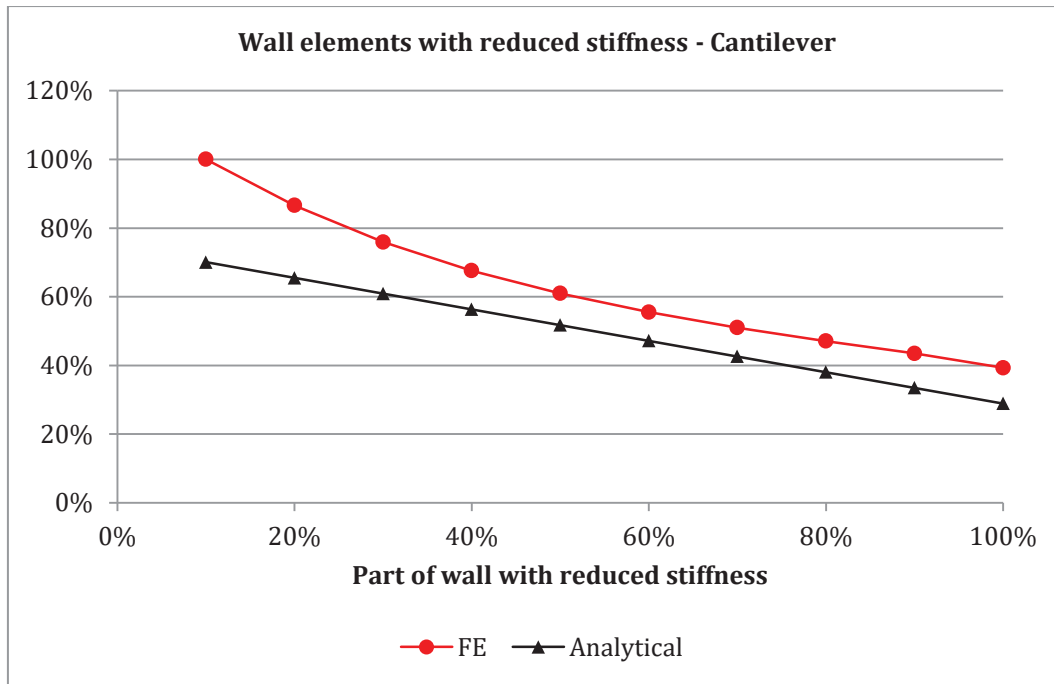


Figure 5.41 Comparison between analytical and numerical stiffness calculations. Plotted as percentage of numerical stiffness of wall ($K = 5.92 * 10^{10}$ [N/m]).

5.5 Discussion

5.5.1 Aspect ratio

No apparent reason could be identified for the analytical underestimation of stiffness for low aspect ratios.

5.5.2 Individual wall elements

In the parametric study of the wall element where the dimensions and location of the openings were altered it was chosen to present the results as the configurations which stiffness deviated 10% or less from the FE-analysis. Whether the stiffness was over- or underestimated was not considered in the results presented in this thesis with the motivation that both over- and underestimations influences the load distribution on a global structural level.

For all the investigated methods, including the FE-analysis, the stiffness converged towards a common value as the dimensions of the openings were increased. For the wall elements with wide openings large deformations occurred resulting in stiffness close to zero and for wall elements with high openings the structural behaviour was similar to that of a system of columns. Thus, it could be argued that the most reliable results of the investigation were those of wall elements with reasonable sized openings. This argument is strengthened by the limitations of the hand calculations referred to as *Method 1* and *Method 3* and the recommendations to not apply for wall elements with openings where the openings have large effect on the stress distribution. Some problems occurred with preventing rotation along the top of the wall elements when modelling the fixed boundary condition in the FE-software which were solved by also preventing axial deformations along the height of the wall element. This

boundary condition should be a good representation of the analytical boundary condition under the assumption of small deformations. Considering the mentioned uncertainties and that the parametric study only has been performed on wall elements with a specific dimension the results should not be considered general.

Cracking was not taken into consideration in this parametric study. For *Method 1-3* cracking of the concrete could have been considered by reducing the bending stiffness in the cracked sections. In (Boverket, 2004) it was stated that stiffness calculations of bracing members should consider cracking and two approaches were presented.

However, one of the challenges with initial calculations of wall elements with openings was to estimate the stress distribution through the wall element and it was therefor also problematic to determine which sections that were cracked and should be reduced. Including cracking in the analysis was also considered to counteract the purpose of the parametric study since the effect of the other parameters probably would be less distinct. For a more realistic investigation of the effects of openings in wall elements cracking and long term effects should be taken into consideration and studied in detail using more advanced FE-software.

In (Balasubramanian, et al., 2011) *Method 3* was introduced as a stiffness estimation of brick masonry wall elements with openings. The used discretization schema and the derivation of the boundary conditions for each pier type were assumed to be valid also for concrete wall elements with openings.

From the results presented in Figure 5.14-Figure 5.34 it could be seen that the stiffness obtained by *Method 1* agreed well with FE-analysis for wall elements with fixed boundary conditions and one opening with a width of 1.2 meters for all studied heights and positions. This agreed with (Balasubramanian, et al., 2011) that presented *Method 1* as a highly approximate method that often overestimates the stiffness since the failure was confined to the piers. The results obtained in this study do not agree with the recommendation to only consider the cantilevered boundary conditions for *Method 1*. However, it was also recommended to not use this approach for wall elements with large openings, which was considered an indication of the uncertainties with this approach.

Method 2 showed an overall poor estimation of the stiffness. It was most reliant for cantilevered boundary condition of wall element with three openings with large dimensions where the wall elements act similar to a system of columns. The calculations performed by (Dickey & Schnider, 1994) also indicated that *Method 2* generally overestimates the stiffness of the wall element.

The stiffness estimation obtained from *Method 3* agrees well with FE-analysis compared to *Method 1* and *Method 2*, as were suggested in (Balasubramanian, et al., 2011). The underestimation of the stiffness compared to FE-analysis also agrees with the observed differences in (Balasubramanian, et al., 2011) and are explained by the methods inability to consider the shear forces along the vertical interface of adjacent piers.

Method 2 with modified height agreed overall very well with the FE-analysis. It could be seen in Figure 5.26-Figure 5.31 that the most reliant stiffness estimations occurred for configurations with two or three openings and with fixed boundary conditions. It should be noted that deviation compared to FE-analysis was within 0-50% for all the studied wall configurations, which could be considered a sufficient estimation in the initial calculations.

The non-linear distribution of vertical reaction forces observed in the parametric study indicated that the parts of the wall located in-between openings obtained an almost linear distribution of vertical reaction forces.

5.5.3 Connected wall elements

A brief investigation of how individual wall elements interact when connected longitudinally was carried out with the stiffest possible boundary condition applied in the FE-analysis. For boundary conditions with a sufficiently large stiffness the connected wall elements were assumed to act as a solid wall and adding additional wall elements therefore results in behaviour similar to the one observed in the aspect ratio study for low aspects. As the number of wall elements was increased the bending deformations had lower impact and the wall consisting of ten wall elements therefore obtained stiffness larger than ten times the stiffness of the individual wall element for the numerical calculations. It was also observed that the difference between summarization of the individual wall elements stiffness and the stiffness of an equally long solid wall diverged in the analytical calculations as the number of wall elements increase, which also could be explained by the reduced impact of bending deformation for the solid wall. The difference between the analytical methods was therefore larger for the cantilever boundary condition where the bending deformations had larger impact compared to fixed boundary conditions.

When studying the influence of the location of the wall element with reduced stiffness within the wall it was observed that the analytical and numerical methods obtain the same stiffness regardless of the placement except for when the wall elements were located at the end of the wall in the numerical calculations. This reduced stiffness originated from local deformations of the wall element with reduced stiffness and was therefore considered to be negligible. However, it was found that the stiffness of the wall varied non-linear as the number of wall elements with reduced stiffness increased in the numerical calculations, a behaviour that was not observed in the analytical calculations. As the number of wall elements with reduced stiffness increased the behaviour of the total stiffness became linear. It was therefore assumed that the observed non-linearity occurred due to local deformations.

6 Parametric Study – Load Distribution

The study intends to investigate how different calculation methods for global stability works when the rotation centre of the building is not located in the centre, i.e. the building is subjected to torsion. This is the case when the walls and their stiffness are not symmetrical.

6.1 Method of study

The study was performed by decreasing the thickness of *Wall 4* in the simplified building used in Chapter 3. All walls were designed as solid walls to better capture the differences in stabilizing calculations. The thickness was decreased from $0.2m$, same thickness as the other walls in the building, to $0.02 m$. This was done over ten steps with a change of 0.02 per step. This means that the walls were symmetrical in the first step and no torsion was present in the building, i.e. only walls parallel to load direction were subjected to force. When the thickness of *Wall 4* starts to decrease the building would start to turn and walls perpendicular to the load direction will be subjected to load.

The resulting moment in each wall was calculated with *FEM-design* and *Rymdknäckning*.

6.2 Analytical calculations

Analytical calculations were performed in *Rymdknäckning*. The input in *Rymdknäckning* was the same as for the solid simplified building in Chapter 3.2 but with all eight walls designed separately, see Figure 6.1.

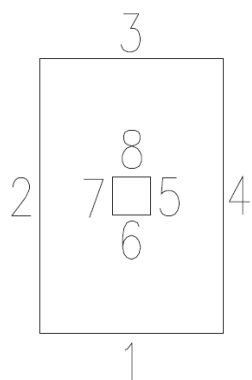


Figure 6.1 Configuration of stabilizing walls in *Rymdknäckning*

6.3 Numerical calculations

The numerical calculations were performed with *FEM-design* with the same configuration as for the solid simplified building in Chapter 3.3

6.4 Results

On global level each of the eight walls in the building was plotted in Figure 6.2- Figure 6.9 as percentage of total reaction moment on y-axis, to width of *Wall 4* on x-axis.

It was discovered that the distribution of load in the eight walls were very close between *FEM-design* and *Rymdknäckning* when *Wall 4* had the same thickness as the other walls. When the thickness of *Wall 4* was reduced were differences in the two calculations discovered. For *Rymdknäckning* when the moment in *Wall 4* was reduced, the amount of moment in *Wall 2* stayed almost constant while *Wall 1* and *Wall 3* increased. The results from the FE calculation showed that the amount of moment in *Wall 4* decreased faster than for *Rymdknäckning* while the amount of moment in *Wall 2* increased in contrary to *Rymdknäckning*. The results also indicates that the increase of moment in *Wall 1* and *Wall 3* were lower for *FEM-design* than *Rymdknäckning*.

It should be noted that the result of the internal walls represent small amount of the total moment and when plotted showed some round off problems from both *Rymdknäckning* and *FEM-design* results.

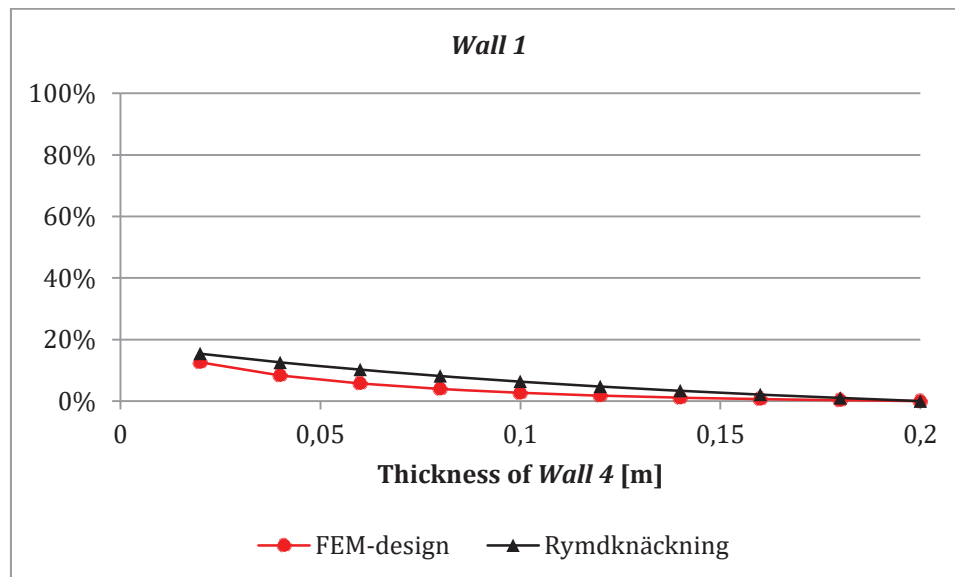


Figure 6.2 Comparison between analytical and numerical moment calculations. Plotted as percentage of total distributed moment.

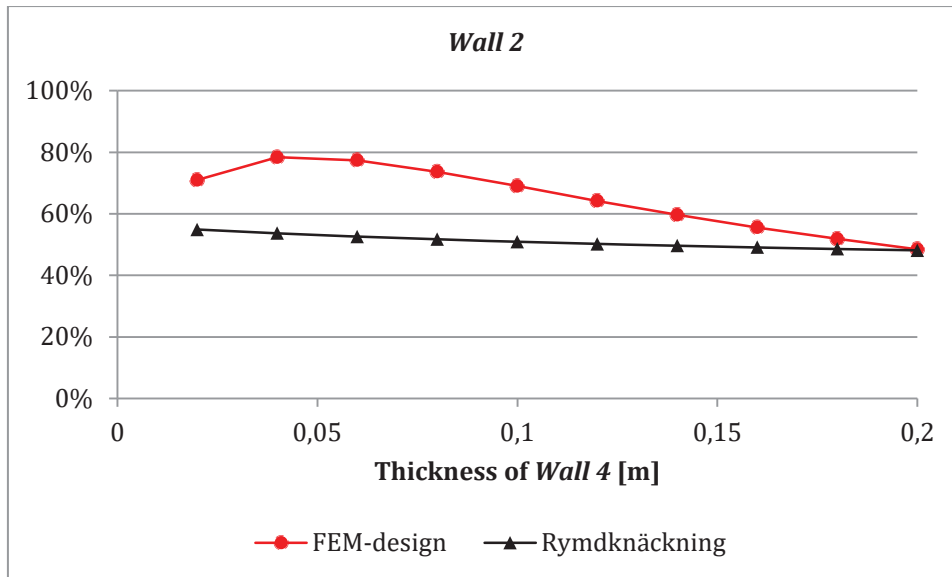


Figure 6.3 Comparison between analytical and numerical moment calculations. Plotted as percentage of total distributed moment.

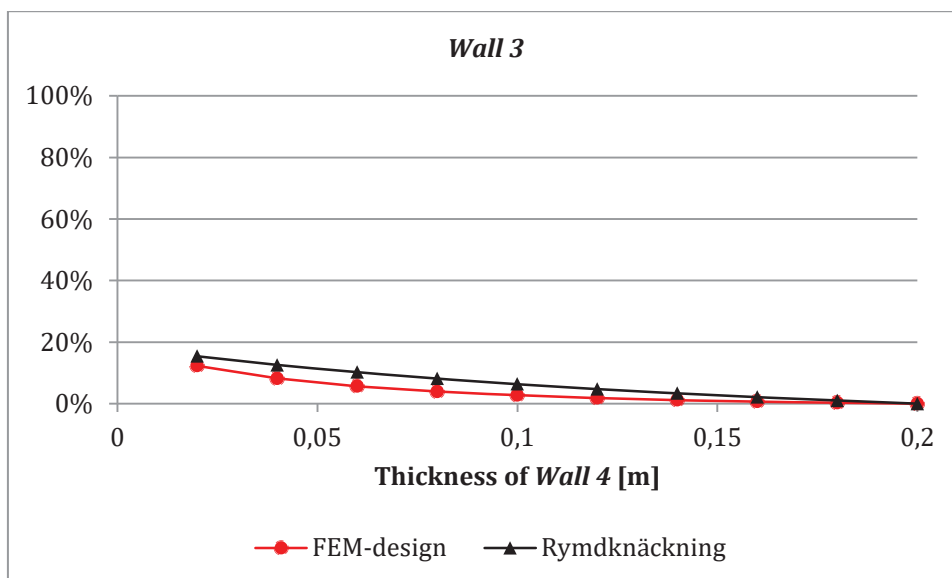


Figure 6.4 Comparison between analytical and numerical moment calculations. Plotted as percentage of total distributed moment.

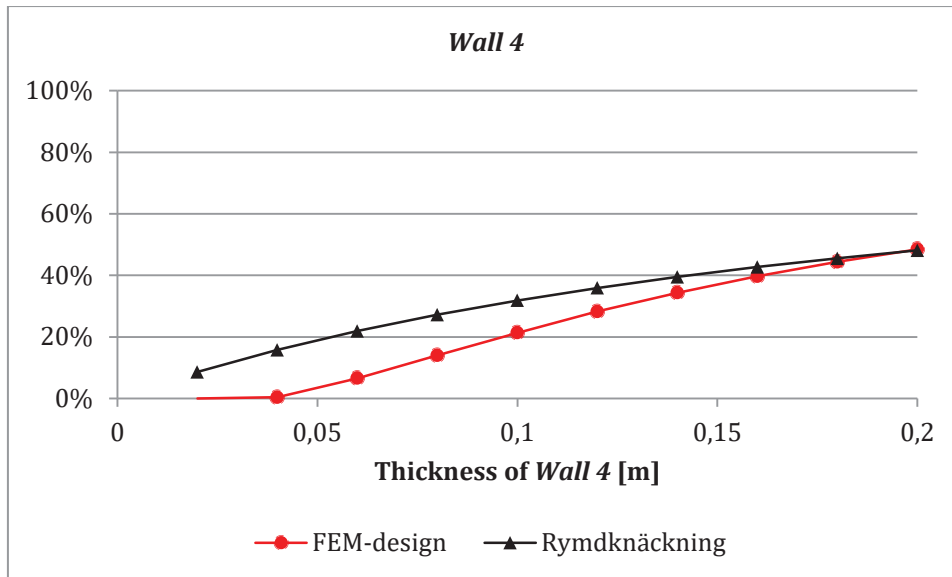


Figure 6.5 Comparison between analytical and numerical moment calculations. Plotted as percentage of total distributed moment.

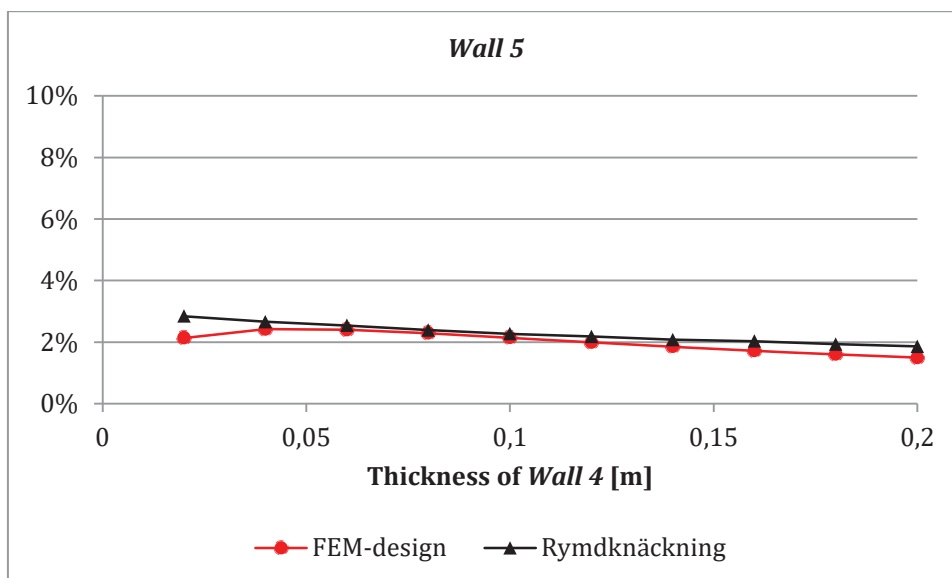


Figure 6.6 Comparison between analytical and numerical moment calculations. Plotted as percentage of total distributed moment.

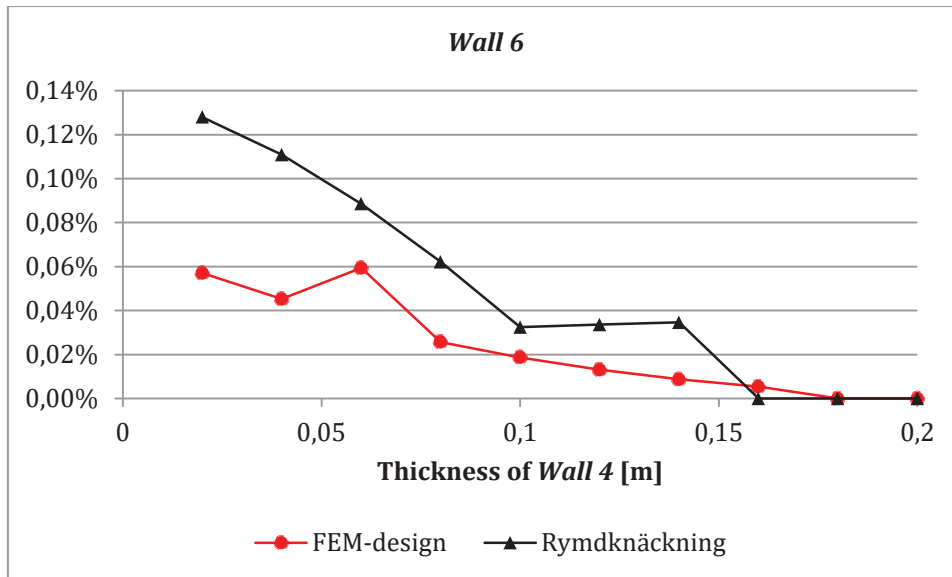


Figure 6.7 Comparison between analytical and numerical moment calculations. Plotted as percentage of total distributed moment.

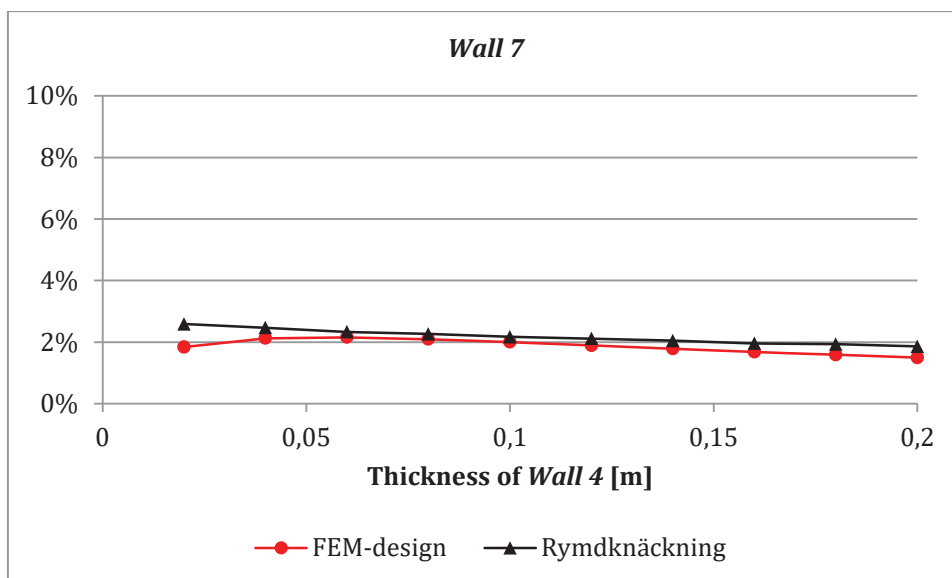


Figure 6.8 Comparison between analytical and numerical moment calculations. Plotted as percentage of total distributed moment.

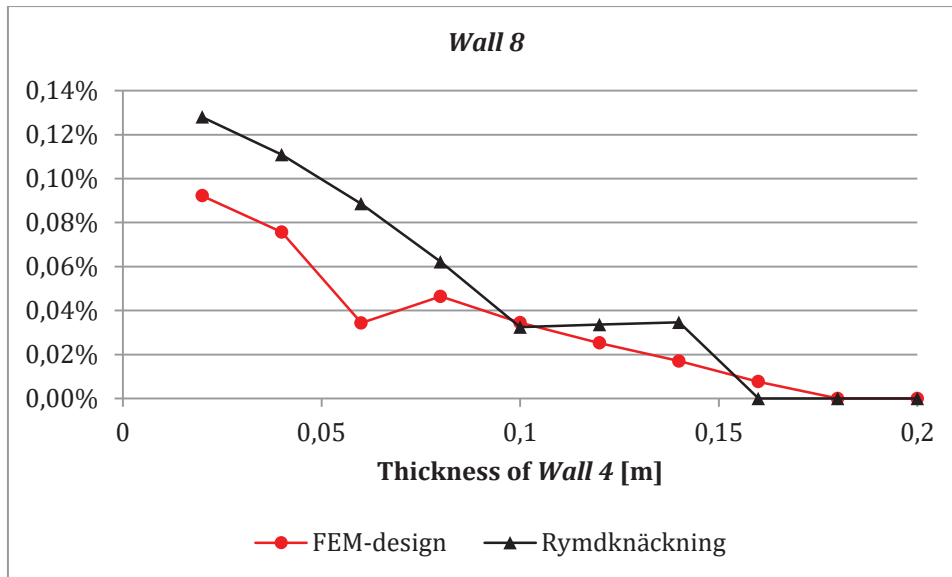


Figure 6.9 Comparison between analytical and numerical moment calculations. Plotted as percentage of total distributed moment.

6.5 Discussion

In the parametric study on structural level the stiffness was reduced in one of the exterior walls parallel to the applied load by reducing the thickness of the wall. This method of reducing the stiffness was considered to provide a more accurate comparison of the load distribution between the wall elements than the one carried out in the case study of the simplified building since the error in estimating the stiffness of wall elements with openings was eliminated.

Due to the limited possibility of applying a specific deviation load in *Rymdknäckning* differences occurred in the applied deviation loads for FE-analyses compared to calculations in *Rymdknäckning*. These differences were small enough to assume that their influence on the load distribution would be limited, which were confirmed by that the differences in the total resulting moment were sufficiently small. In the graphs of the moment distribution between the walls the correlation between the moment in each wall for FE-analysis and *Rymdknäckning* were the highest for equally stiff exterior walls and were considered sufficiently equal to suggest that the differences in the applied load could be accepted. As a precaution it was chosen to not compare the actual values of the graphs but the overall behaviour of the curves. That the moment for the different calculation methods coincides in each wall for equally stiff exterior walls and deviates more as the reduction of stiffness increases was interpreted as that *Rymdknäckning* and FE-analysis manages the load distribution differently. This implied that no matter how small the difference was in the stiffness calculation between the initial and final calculation of the individual walls there would always be a difference in the global load distribution when using the studied software.

The observed difference could probably, to some extent, be explained by how the two different software consider the connections between the exterior walls. As discussed in Chapter 3.5 the exterior walls are not connected in *Rymdknäckning* resulting in individual deformation of each wall. *FEM-design* treats the building as a box-structure where a deformation in one of the walls also influences the formation of adjacent walls. This connection between exterior walls entails a global rotation around the centre of gravity of the building and thereby an additional load distribution that is

not considered in *Rymdknäckning*. The additional global rotation could also be seen by studying the moment distribution between *Wall 1* and *Wall 3*. In *Rymdknäckning* the two walls attracted the same amount of the total moment as the stiffness decrease while *Wall 1* was subjected to a larger amount of the total stiffness compared to *Wall 3* in FE-analysis.

7 Conclusion

From the case study of *Pyramiden* it could be concluded that in the initial design of the structural system there exist uncertainties in how to treat horizontally loaded bracing members. Assumption had to be made regarding stiffness estimations of wall elements with openings and interactions between wall elements. By reducing the stiffness of the wall the presence of openings will reduce the portion of the horizontal load attracted by the wall and thereby the load distribution of the building.

The applicability of methods suggested in literature to estimate the stiffness of wall elements with openings was limited and there existed uncertainties for which dimensions of the openings they were valid. Through the parametric study of various configurations of wall elements it was concluded that treating a wall element with openings as a system of columns were the most reliable of the studied methods.

For a wall consisting of connected wall elements the presence of wall elements with reduced stiffness, if assuming stiff connections, reduced the total stiffness of the wall. It was shown that the number and the placement of wall elements with reduced stiffness had negligible effect on the stiffness comparison between analytical and numerical calculations. Besides reducing the stiffness of the wall element the presence of openings influences the stress distribution within the wall and thereby the distribution of vertical and horizontal reaction forces along the bottom of the wall.

It could also be concluded that for low aspect ratios the analytical calculations underestimated the stiffness of a solid wall element compared to FE-analysis. The same effect was shown as the number of wall elements increased in a wall consisting of connected wall elements under the assumption of stiff connections.

When comparing the load distribution of a horizontally loaded structural system in *Rymdknäckning* and *FEM-design* it was shown that load distribution between the walls differed as the stiffness was reduced in one of the exterior walls. The difference most likely arose due to *Rymdknäcknings* inability to consider the connection between exterior walls and 2nd order rotational deformations of the building.

The differences in the stiffness estimation observed in this thesis should be considered when calculating the horizontal load distribution. The results of the parametric study could be used by the structural engineer as guidance how to estimate the stiffness for various configurations of wall elements with openings and the behaviour of connected wall elements. However, the problem with differences of the load distribution between *Rymdknäckning* and *FEM-design* would still remain and needs to be investigated further.

Even if the results of the parametric study showed concordance with FE-analysis for the studied wall configurations it was not possible to draw general conclusions and recommendations that were valid for all possible wall configurations. FE-analysis provided accurate stiffness estimation of wall configurations with complex geometries but was time consuming when changes had to be done on a structural level. *Rymdknäckning* provided the possibility to change material and geometrical properties of the structural system without changing the actual model. The feasibility of using the accuracy of the FE-analysis to estimate stiffness of wall configurations

together with the time efficient design process of *Rymdknäckning* should be considered.

7.1 Recommendations

The authors would also like to emphasize the problems with the building process. A lot of the uncertainties that occurred during the design process was mainly the result of a too short timespan and the involvement of different parties rather than the lack of knowledge of the structural engineer. Instead of focusing on reducing the differences between assumptions made in the initial and the final calculation it would be favourable for the design process to increase the collaboration between the involved parties and clarify the mutual responsibilities. Uncertainties in the calculations and the assumptions that has been discussed in this thesis could probably have been diminished or avoided by adopting some of the following changes in the building process:

- Implementing conceptual design where the involved parties work together continuously through the design process of the structural system.
- Designate one party that is responsible for the overall assessment and the quality control of the structural design, which also entails demands on compiled documentation from the involved parties of the structural system's capacity. The focus of the additional control should be on avoiding major errors.
- Involving the prefabricator manufacturer in the design process in the initial design phase.
- Increasing the collaboration between the structural engineer and the prefabricator manufacturer to make sure that assumptions made regarding material properties and the structural behaviour are the same in the initial and the final design.

8 References

- Balasubramanian, S. et al., 2011. An improved method for estimation of elastic lateral stiffness of brick masonry shear walls with openings. *KSCE Journal of Civil Engineering*, 15(2), pp. 281-293.
- Betongelementföreningen, 1998. *Bygga med prefab: en handbok i teknik, estetik, kvalitet, ekonomi, miljö*. 1:st ed. Bromma: Betongelementföreningen.
- Boverket, 2004. *Boverkets handbok om betongkonstruktioner, BBK 04*. ed. : Boverket.
- Broo, H., Lundgren, K. & Plos, M., 2008. *A guide to non-linear finite element modelling of shear and torsion in concrete bridges*, Göteborg: Chalmers University of technology.
- Bulleit, W. M., 2008. Uncertainty in Structural Engineering. *Practice Periodical on Structural Design and Construction*, Volume 13.
- Dickey, W. L. & Schnider, R. R., 1994. *Reinforced masonry design*. 3 ed. Englewood Cliffs: Prentice Hall.
- ELU konsult AB, 2015. *KV. Pyramiden 3-4 Hus 3 Belastningar - Horisontallaster [internal material]*. Göteborg: s.n.
- ELU konsult AB, 2015. *Teknisk beskrivning och föreskrifter för prefabricerad stomme [internal document]*. Göteborg: s.n.
- Eurocode 1, 2002. *SS EN 1991 Eurocode 1: Actions on structures*. : .
- Eurocode 2, 2005. *SS EN 1992 Eurocode 2: Concrete structures*. s.l.:s.n.
- Eurocode 3, 2005. *SS EN 1993 Eurocode 3: Design of steel structures*. s.l.:s.n.
- Neuenhofer, A., 2006. Lateral stiffness of shear walls with openings. *Journal of structural engineering*, 132(11).
- Nordstrand, U., 2008. *Byggprocessen*. Stockholm: Liber.
- Quamaruddin, M., 1999. In-plane stiffness of shear walls with openings. *Building and environment*, 34(2), pp. 109-127.
- Schramm, M., 2014. *Planbeskrivning - Detaljplan för kv. Pyramiden m.fl*, Solna: Solna stad - Stadsbyggnadsförvaltningen.
- SSI Byggkonsult, ., n.d. *Rymdknäckning [internal software]*. s.l.:s.n.
- Strusoft, 2009. *Frame Analysis (Version 6) [software]*. : <http://www.strusoft.com/products/win-statik>.

Strusoft, 2015. *Strusoft FEM-design 3D Structure (Version 14.00.007) [software]*.
<http://www.strusoft.com/products/fem-design>: .

Westerberg, B., 1997. *Stabilisation of buildings [lecture at Chalmers university of technology]*. Göteborg: s.n.

Verbal references:

Granberg, E., 2016. [Interview] (26 04 2016).

Granberg, E., 2016. [Interview] (28 04 2016).

Jansson, B., 2016. *Byggprocessen* [Interview] (26 01 2016).

Lindewald, H., 2016. *Byggprocessen* [Interview] (10 02 2016).

Sagemo, A., 2016. *Byggprocessen* [Interview] (08 02 2016).

Appendix A: Theory

Appendix A presents addition theory not presented in the thesis.

A.1 Beam theory

To calculate the deformations in walls and columns beam theory needs to be applied. The following chapter describes the theories of Euler-Bernoulli and Timoshenko.

A.1.1 Euler-Bernoulli beam theory

The Euler-Bernoulli beam theory assumes that the shear deformation can be neglected in relation to the curvature of the beam. This assumption works for slender beams with small deformations. Equation A.1 describes the Euler-Bernoulli beam with constant stiffness along the beam.

$$EI \frac{d^4 w}{dx^4} = q \quad (\text{A.1})$$

Where $E = \text{Modulus of elasticity}$
 $I = \text{Moment of inertia}$
 $q = \text{Distributed load}$
 $w = \text{Deflection}$

Or as moment and shear force, see equation A.2-A.3

$$M(x) = -EI \frac{d^2 w}{dx^2} \quad (\text{A.2})$$

$$T(x) = -EI \frac{d^3 w}{dx^3} \quad (\text{A.3})$$

Where $M = \text{Moment}$
 $T = \text{Shear force}$
 $x = \text{Position within a structural member}$

If equation A.1 is solved for a case of a cantilever beam with a point load at the free end, see Figure A.1, the maximum deflection is given according to equation A.4.

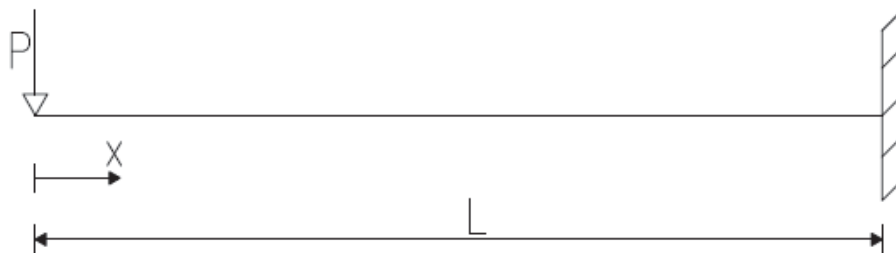


Figure A.1 Cantilever beam subjected to point load

$$w = \frac{PH^3}{3EI} \quad (\text{A.4})$$

Where $H = \text{Height of structural member}$
 $P = \text{Applied point load}$

A.1.2 Timoshenko beam theory

In contrary to the Euler-Bernoulli beam theory the Timoshenko beam takes shear deformations into account. The theory is described by two uncoupled differential equation, see equation A.5-A.6, assuming a constant cross-section.

$$EI \frac{d^3\theta}{dx^3} = q \quad (\text{A.5})$$

$$EI \frac{d^4w}{dx^4} = q - \frac{EI}{GAK} \frac{d^2q}{dx^2} \quad (\text{A.6})$$

Where $A = \text{Cross - sectional area}$
 $G = \text{Shear modulus}$
 $K = \text{Timoshenko shear coefficient}$
 $\theta = \text{Rotation}$

The bending moment and shear force for a linear elastic Timoshenko beam are described by equation A.7-A.8.

$$M(x) = -EI \frac{d\theta}{dx} \quad (\text{A.7})$$

$$T(x) = GAK \left(-\theta + \frac{dw}{dx} \right) \quad (\text{A.8})$$

If equation A.1-A.8 are solved for a case of a cantilever beam loaded with a point load at free end, see Figure A.1, the maximum deflection is given according to equation A.16. Equation A.9-A.15 describes the derivation of equation A.16.

A free body diagram gives:

$$-Px - M(x) = 0 \quad (\text{A.9})$$

$$P + T(x) = 0 \quad (\text{A.10})$$

Combining equation A.7 with equation A.9 and equation A.8 with equation A.10 gives:

$$Px = EI \frac{d\theta}{dx} \quad (\text{A.11})$$

$$-P = GAK \left(-\theta + \frac{dw}{dx} \right) \quad (\text{A.12})$$

Integration of equation A.11 with the boundary condition $\theta = 0$ at $x = L$ gives:

$$\theta = \frac{P(x^2-L^2)}{2EI} \quad (\text{A.13})$$

Equation A.13 inserted into equation A.12 leads to:

$$\frac{-P}{GAK} + \frac{P(x^2-L^2)}{2EI} = \frac{dw}{dx} \quad (\text{A.14})$$

Integration of equation A.14 with the boundary condition $w = 0$ at $x = L$ gives the expression for the deflection:

$$w = \frac{P}{GAK}(L-x) - \frac{Px\left(L^2 + \frac{x^2}{3}\right)}{2EI} + \frac{PL^3}{3EI} \quad (\text{A.15})$$

The maximum deflection at the free end ($x=0$) is:

$$w = \frac{PH^3}{3EI} + \frac{PH}{GAK} \quad (\text{A.16})$$

The equation can in a similar way be solved for a case where instead of a free end, rotation is forbidden and only translation at free end is possible. This results in equation A.17.

$$w = \frac{PH^3}{12EI} + \frac{PH}{GAK} \quad (\text{A.17})$$

In this case the bending stiffness is increased by a factor four while shear deformations are the same as for a cantilever beam.

A.2 Trusses

A truss element consists of a beam-column frame system with moment free joints that are stabilized by one or two diagonal bar elements, see Figure A.2. The load resistance of the truss element is only dependent of the axial response of the members. In order to achieve moment free joints at the connections the centre axis of each member must be connected without eccentricity to the centre of the joint

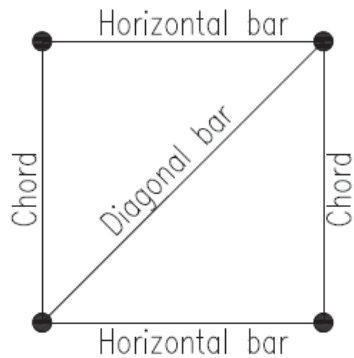


Figure A.2 Members of a truss element

The lateral load transferring response of a truss element is comparable to that of an I-beam. Shear forces are transferred by the horizontal bars and the diagonal bar, similar to the web of an I-beam. The two vertical bars act as the flanges of an I-beam transferring moment by tension and compression

Hand calculations of deformations of truss elements subjected to lateral load are normally carried out under the assumption of small deformations. The truss structure is simplified to a triangular system, see Figure A.3, and the displacement is limited to axial deformations of the diagonal bar and is determined according to equation A.18. (Lorentsen, et al., 1995).

$$\Delta = \frac{PL_{truss}^3}{EA_{truss}L^2} \quad (A.18)$$

Where A_{truss} = Cross – sectional area of diagonal bar
 L = Length of horizontal bar
 L_{truss} = Length of diagonal bar
 Δ = Horizontal deformation

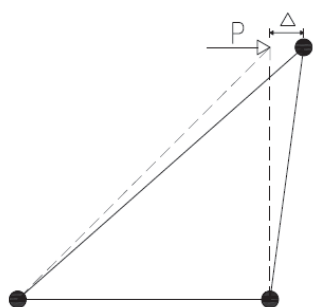


Figure A.3 Assumed deformation of truss element

The deflection of a truss element can also be derived by calculating the second moment of area according to equation A.19 and implementing it in the formula for beam deflection.

$$I = 2 * A_{chord} * d_{gravity}^2 \quad (A.19)$$

Where A_{chord} = Cross – sectional area of chord
 $d_{gravity}$ = Distance to the centre of gravity

A.3 Elevator shafts

In a preliminary estimation of horizontal load distribution the stiffness of slender members, where bending deformation is dominant, can be treated approximately. For stabilizing cores this means that shear deformations general can be ignored. However, if the stabilizing core has openings, which is the case for elevator shafts, the openings can have a substantial influence on the deformations and shear deformations needs to be considered. (Westerberg, 1997)

In (Westerberg, 1997) a method for evaluating the bending and shear deformations of an elevator shaft, see Figure A.4 at each storey is presented.

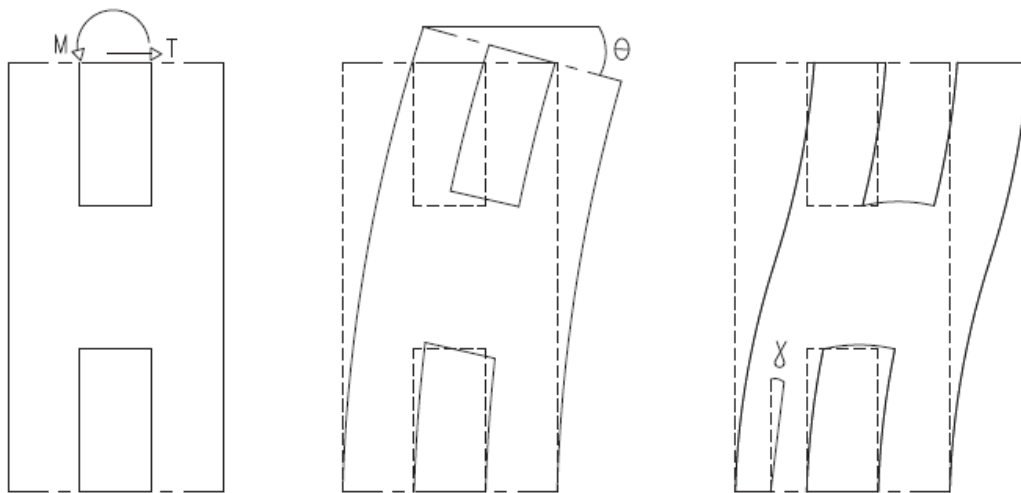


Figure A.4 Global bending and shear deformation of elevator shaft

The global bending deformation of an elevator shaft is calculated in the same way as for members without openings using a reduce value of the moment of inertia for the cross-section, see equation. Full interaction is assumed between the two parts of the cross-section.

$$\theta = \left(M + \frac{TH}{2} \right) \frac{T}{EI} \quad (A.20)$$

The global shear deformation of an elevator shaft is the result of local bending and shear deformations of the horizontal and vertical members of the structure, see

equation A.21-A.24, and can consequently not be calculated as easily. An expression for the global shear deformation of an equivalent frame can be derived under the assumption of symmetry of the placement of openings and hinges in the midpoints of the vertical and horizontal parts, see equation A.25.

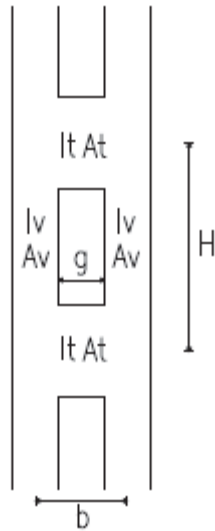


Figure A.5 Notations of elevator shaft

Bending deformation of the transverse parts

$$\gamma_{tb} = \frac{Hg^3}{12b^2EI_t} \quad (\text{A.21})$$

Bending deformation of the vertical parts

$$\gamma_{vb} = \frac{H^2}{24EI_v} \quad (\text{A.22})$$

Shear deformation of transverse parts

$$\gamma_{ts} = \frac{Hg}{b^2GA_t} \quad (\text{A.23})$$

Shear deformation of vertical member

$$\gamma_{vs} = \frac{1}{2GA_v} \quad (\text{A.24})$$

Global shear deformation

$$\gamma = \frac{Hg^3}{12b^2EI_t} + \frac{H^2}{24EI_v} + \frac{Hg}{b^2GA_t} + \frac{1}{2GA_v} \quad (\text{A.25})$$

In (Lorentsen, et al., 1995) the same approach is presented in a similar way but under the assumption that the transverse members are infinitely stiff in the connections to the vertical members, see Figure XX. It is stated that the expression for the global

shear deformation only is valid if the vertical parts has a sufficiently large stiffness to prevent deflection of 2nd order. It is further stated that the difference between treating the elevator shaft as a frame or as a core with openings has to be evaluated for each specific building, but that this approach generally only is valid for buildings with a number of storeys larger than 4. Otherwise the structure needs to be treated as a frame by neglecting the shear deformations in the horizontal and vertical members. The global shear deformation is obtained according to equation A.26

$$\gamma = \frac{Hc^3}{12b^2EI_t} + \frac{H^2}{24EI_v} + \xi \frac{Hc}{b^2GA_t} + \xi \frac{1}{2GA_v} \quad (\text{A.26})$$

Where $c = \text{width of opening} + \text{height of vertical member}$

A.4 References

Lorentsen, M., Petersen, T. & Sundquist, H.,1995. *Stabilisering av byggnader*, Stockholm: Institutionen för byggkonstruktion Kungl Teknisk Högskolan

Westerberg, B., 1997. *Stabilisation of buildings [lecture at Chalmers university of technology]*. Göteborg: s.n.

Appendix B: Convergence study

A convergence study was carried out on four different configurations of wall elements with openings, see Figure B.1, in order to identify a sufficiently dense mesh for the parametric study. The four wall elements represented different configurations of locations and dimensions of openings and were considered to provide enough information to motivate the choice of element size in the FE-analysis.

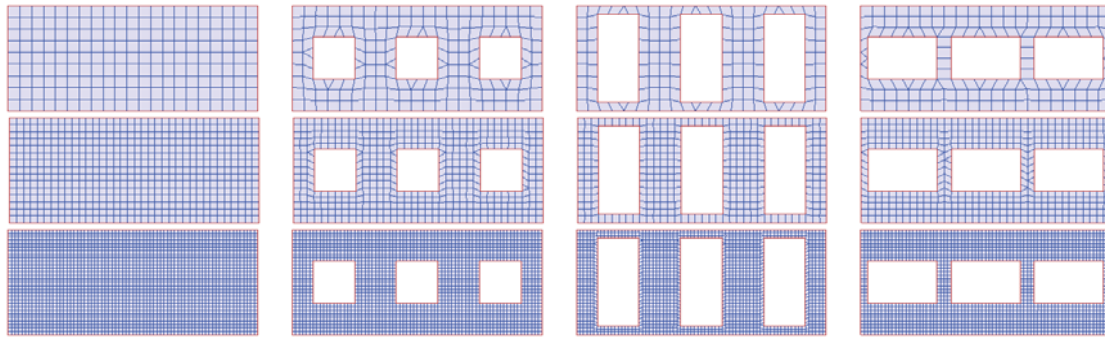


Figure B.1 Configuration of Wall 1, Wall 2 , Wall 3 and Wall 4 with increased mesh density.

Table.B.1 presents the average displacement at the top of the wall element for three different mesh densities and the corresponding percentage of difference as the elements size decreased. The initial mesh size was obtained from the function *prepare* in *FEM-design*. It is chosen to also consider the element sizes $0.2m$ and $0.1 m$.

Table B.1 Mesh density and the corresponding displacement.

	Wall 1		Wall 2		Wall 3		Wall 4	
Mesh size [m]	Disp. [mm]	Diff. [%]	Disp. [mm]	Diff. [%]	Disp. [mm]	Diff. [%]	Disp. [mm]	Diff. [%]
0.32396	0.1251		0.3671		0.8981		2.5757	
0.2	0.1252	0.03	0.3730	1.59	0.9066	0.94	2.7723	7.63
0.1	0.1251	-0.03	0.3773	1.15	0.9148	0.90	2.8588	3.12

Based on the result presented in Table B.1 it was chosen to consider the results to be converged at an element size of $0.2 m$. The displacement of *Wall 4* increase with 3% as the element size decreases from $0.2m$ to $0.1m$, which could be considered an un-converged result. However, this was neglected in this thesis since the deformation of *Wall 4* obtained very low values of stiffness for all element sizes compared to the other configurations. It should also be noted that the chosen element size reduced the computational time significantly.

Appendix C: Results of parametric study

C.1 Graphs

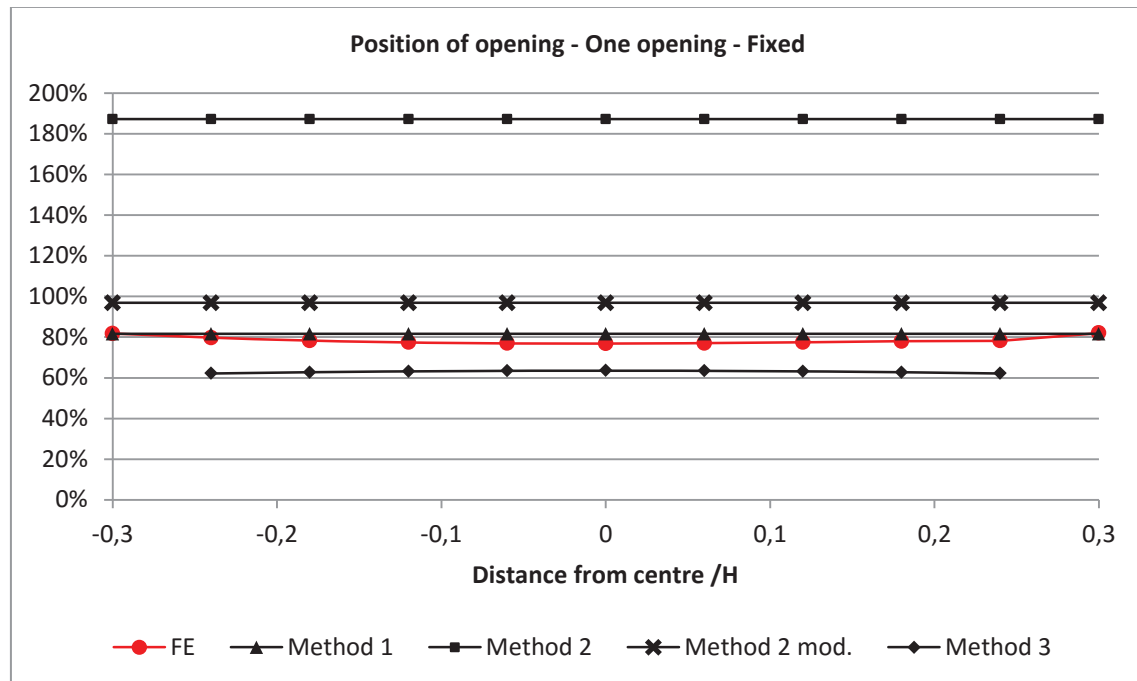


Figure C.10 Comparison between analytical and numerical stiffness calculations. Plotted as percentage of numerical stiffness of one wall element ($K = 5.75 \cdot 10^9$ [N/m]).

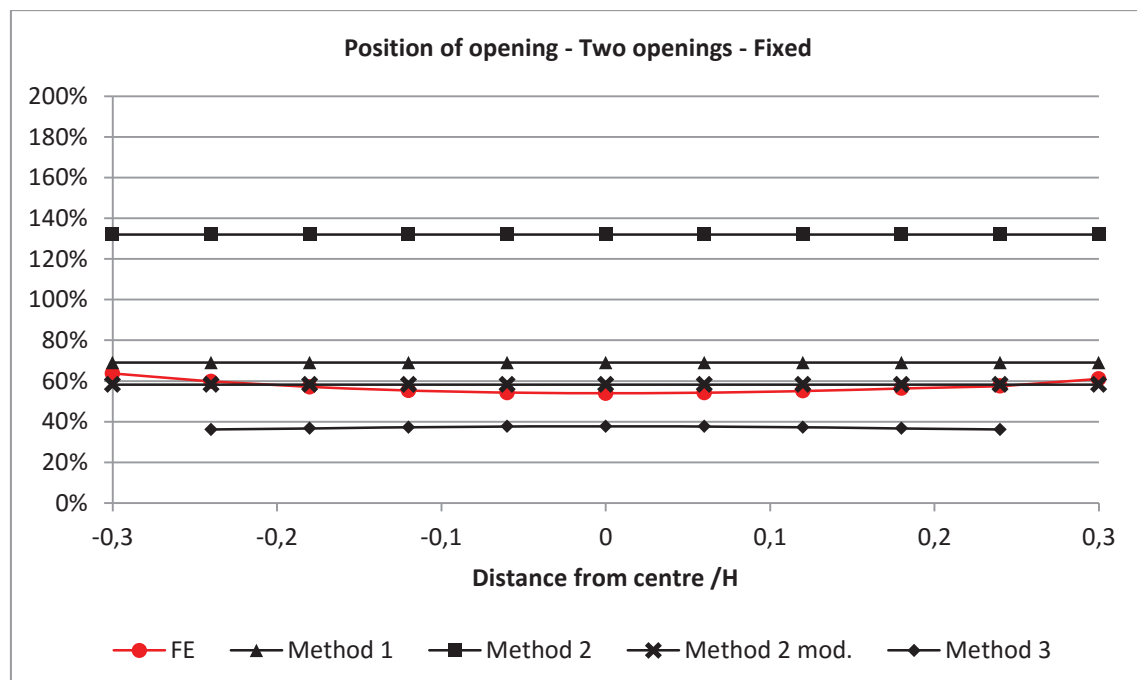


Figure C.11 Comparison between analytical and numerical stiffness calculations. Plotted as percentage of numerical stiffness of one wall element ($K = 5.75 \cdot 10^9$ [N/m]).

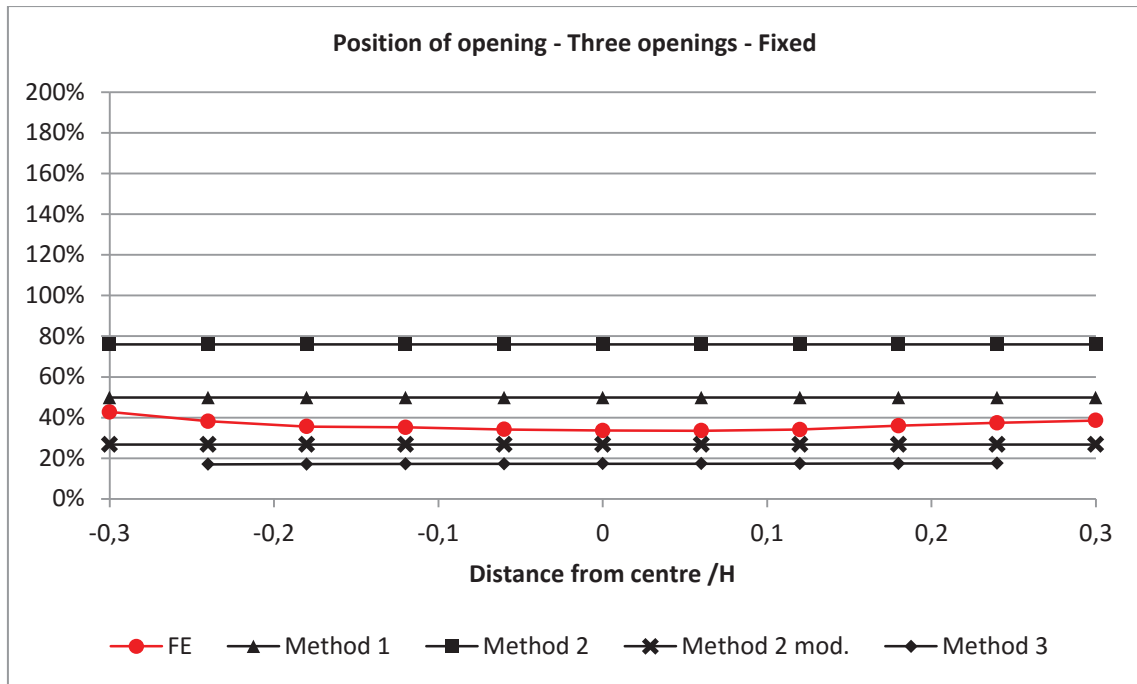


Figure C.12 Comparison between analytical and numerical stiffness calculations. Plotted as percentage of numerical stiffness of one wall element ($K = 5.75 \cdot 10^9$ [N/m]).

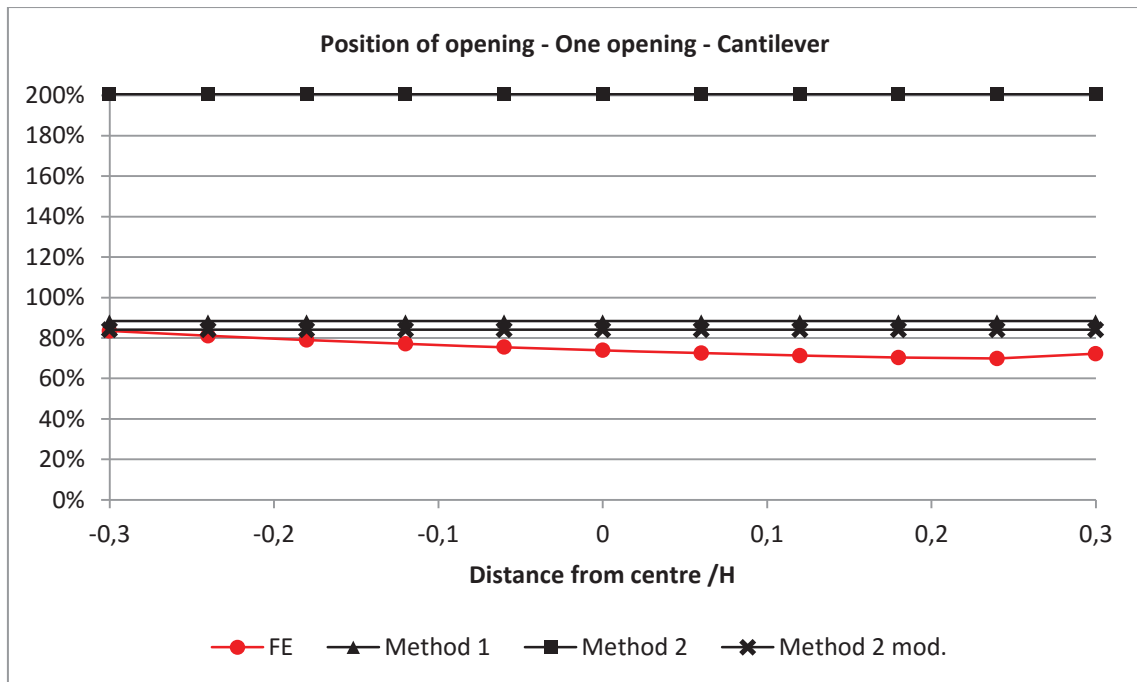


Figure C.13 Comparison between analytical and numerical stiffness calculations. Plotted as percentage of numerical stiffness of one wall element ($K = 4.66 \cdot 10^9$ [N/m]).

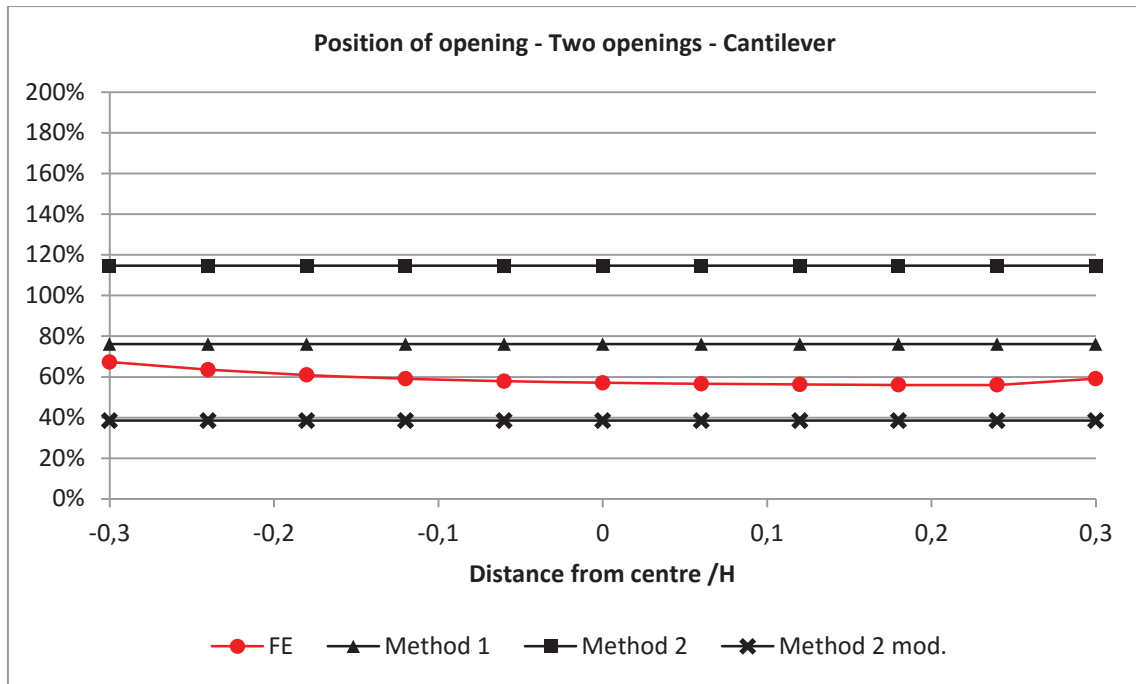


Figure C.14 Comparison between analytical and numerical stiffness calculations. Plotted as percentage of numerical stiffness of one wall element ($K = 4.66 \cdot 10^9$ [N/m]).

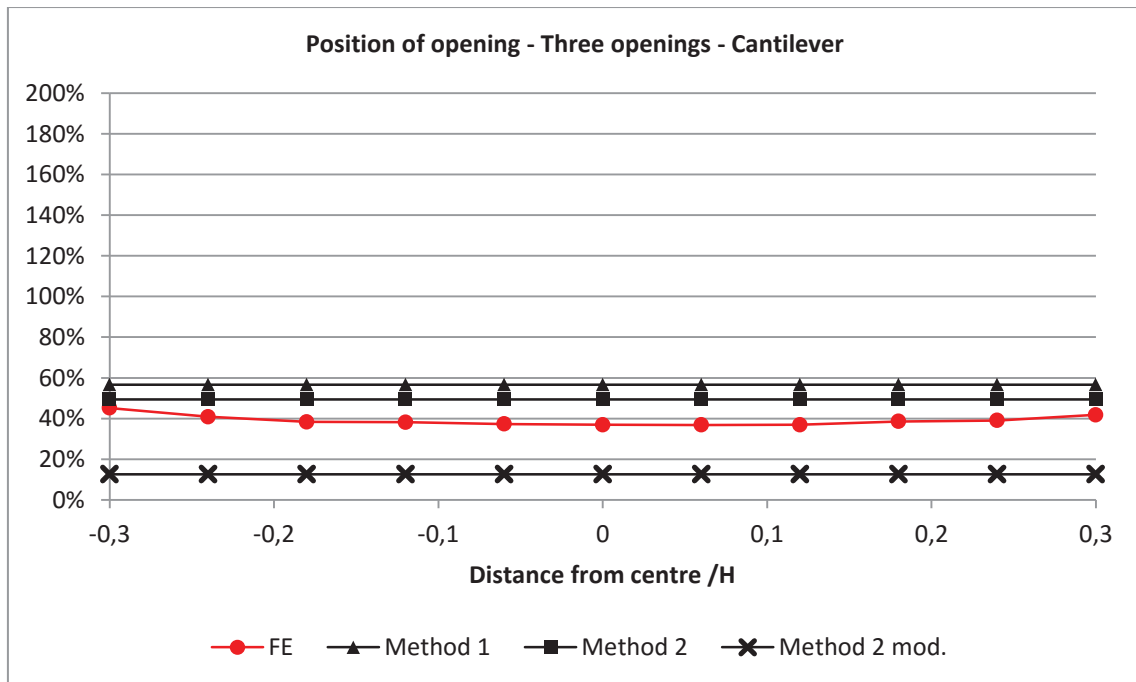


Figure C.15 Comparison between analytical and numerical stiffness calculations. Plotted as percentage of numerical stiffness of one wall element ($K = 4.66 \cdot 10^9$ [N/m]).

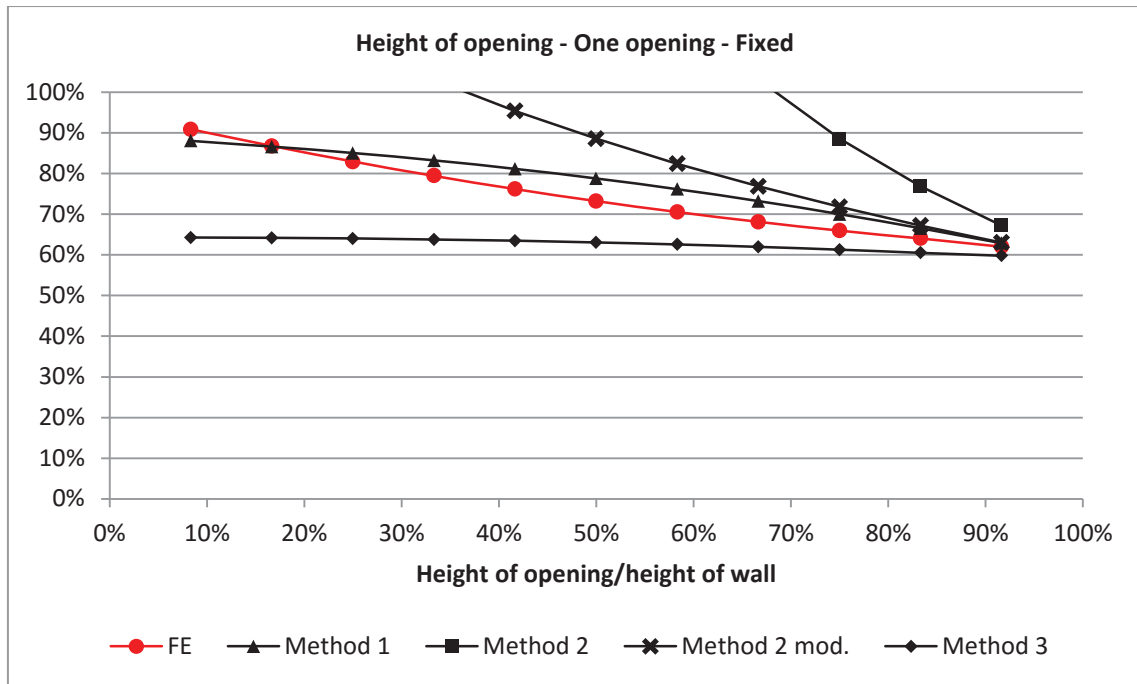


Figure C.16 Comparison between analytical and numerical stiffness calculations. Plotted as percentage of numerical stiffness of one wall element ($K = 5.75 \cdot 10^9$ [N/m]).

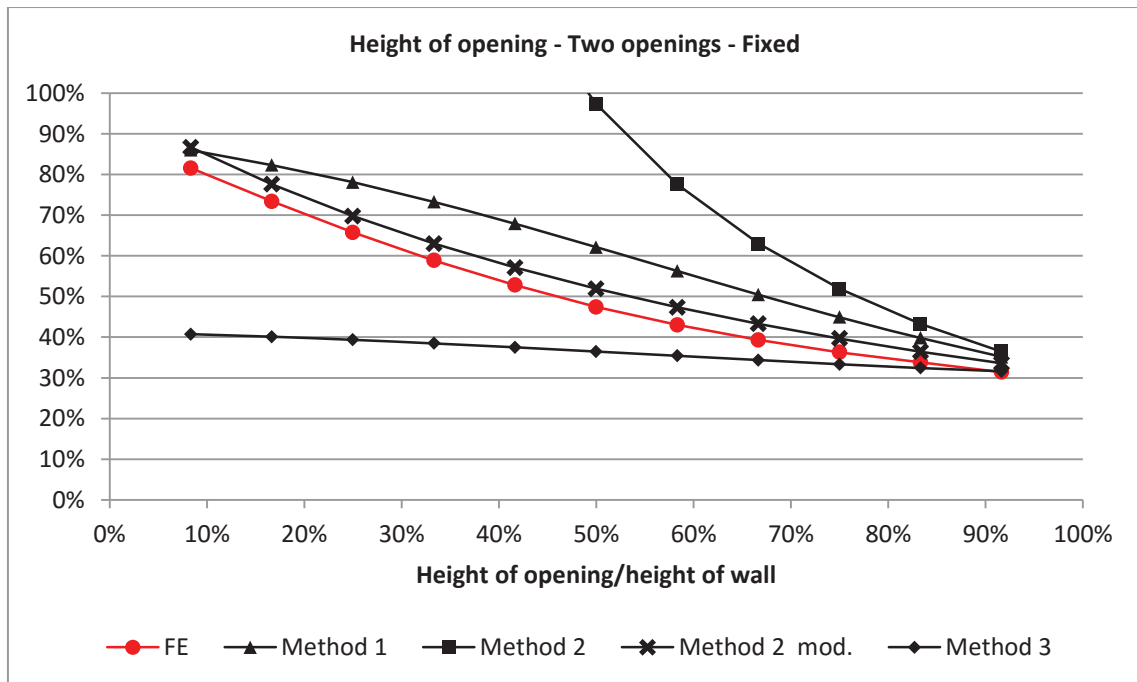


Figure C.17 Comparison between analytical and numerical stiffness calculations. Plotted as percentage of numerical stiffness of one wall element ($K = 5.75 \cdot 10^9$ [N/m]).

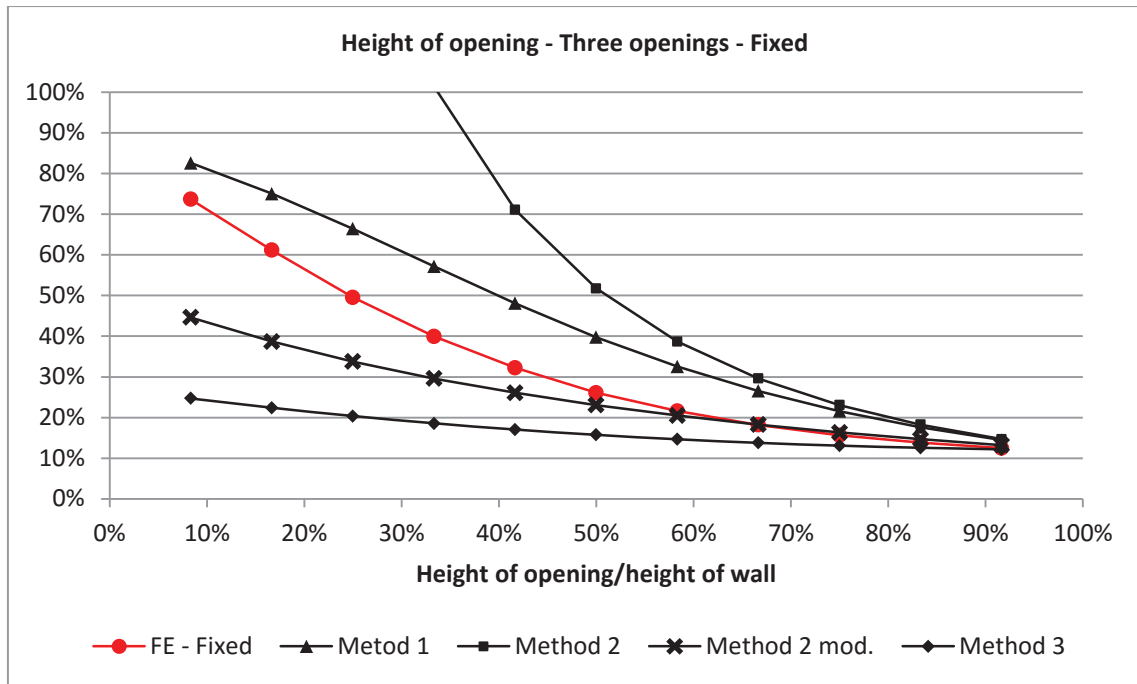


Figure C.18 Comparison between analytical and numerical stiffness calculations. Plotted as percentage of numerical stiffness of one wall element ($K = 5.75 \cdot 10^9$ [N/m]).

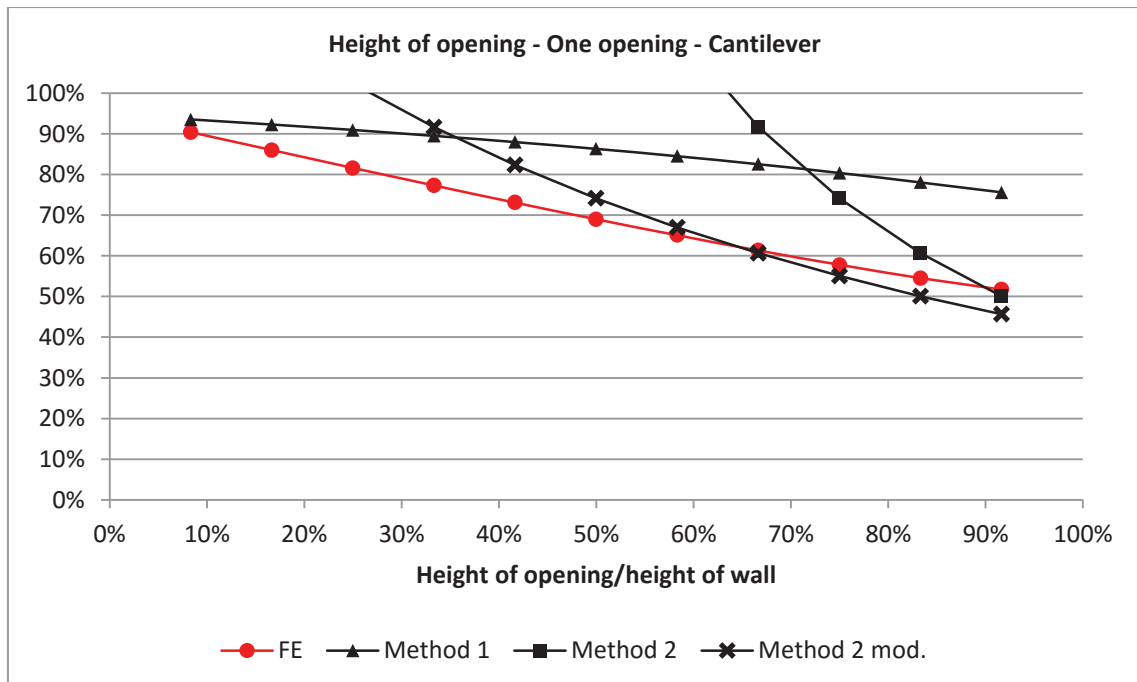


Figure C.19 Comparison between analytical and numerical stiffness calculations. Plotted as percentage of numerical stiffness of one wall element ($K = 4.66 \cdot 10^9$ [N/m]).

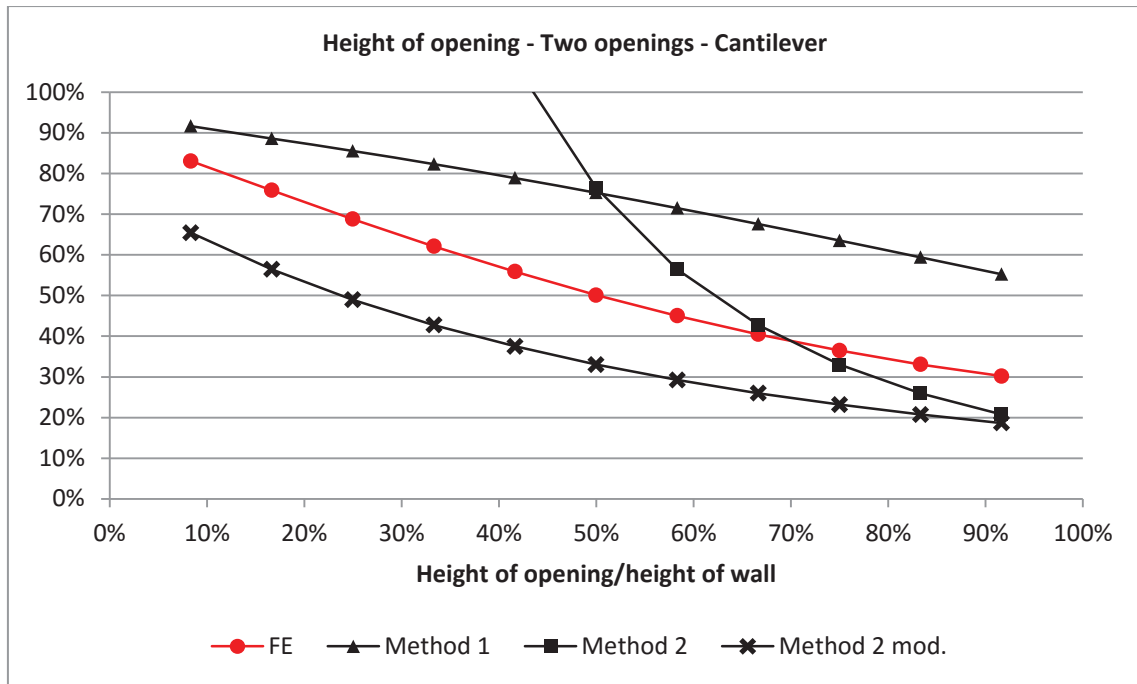


Figure C.20 Comparison between analytical and numerical stiffness calculations. Plotted as percentage of numerical stiffness of one wall element ($K = 4.66 \cdot 10^9$ [N/m]).

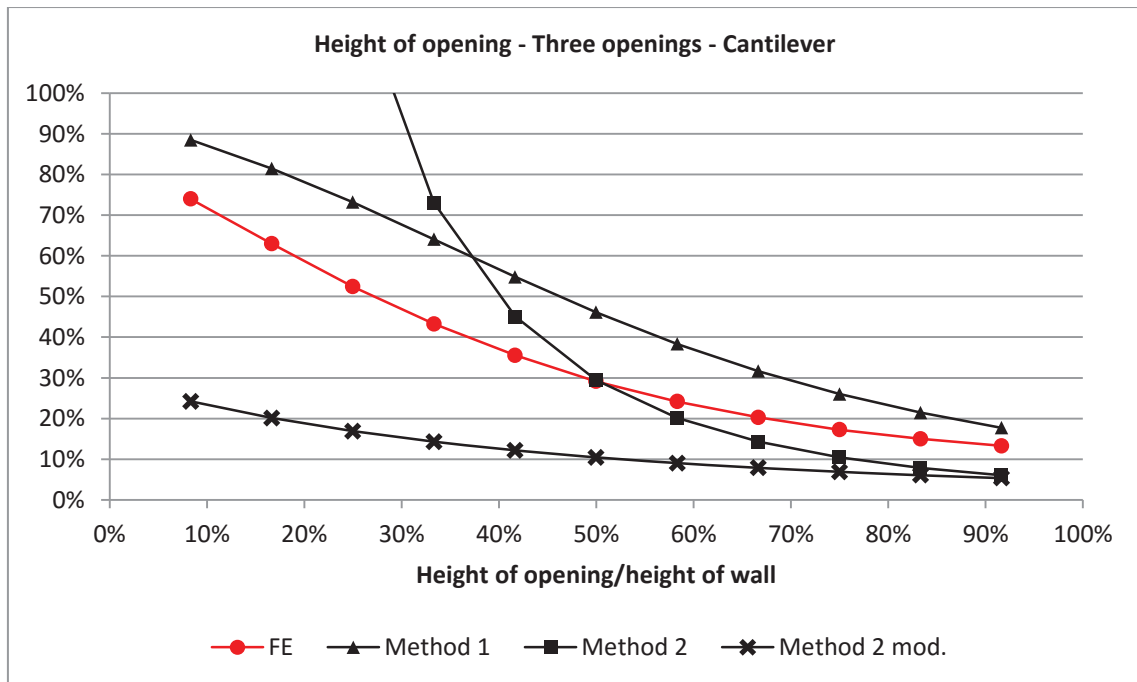


Figure C.21 Comparison between analytical and numerical stiffness calculations. Plotted as percentage of numerical stiffness of one wall element ($K = 4.66 \cdot 10^9$ [N/m]).

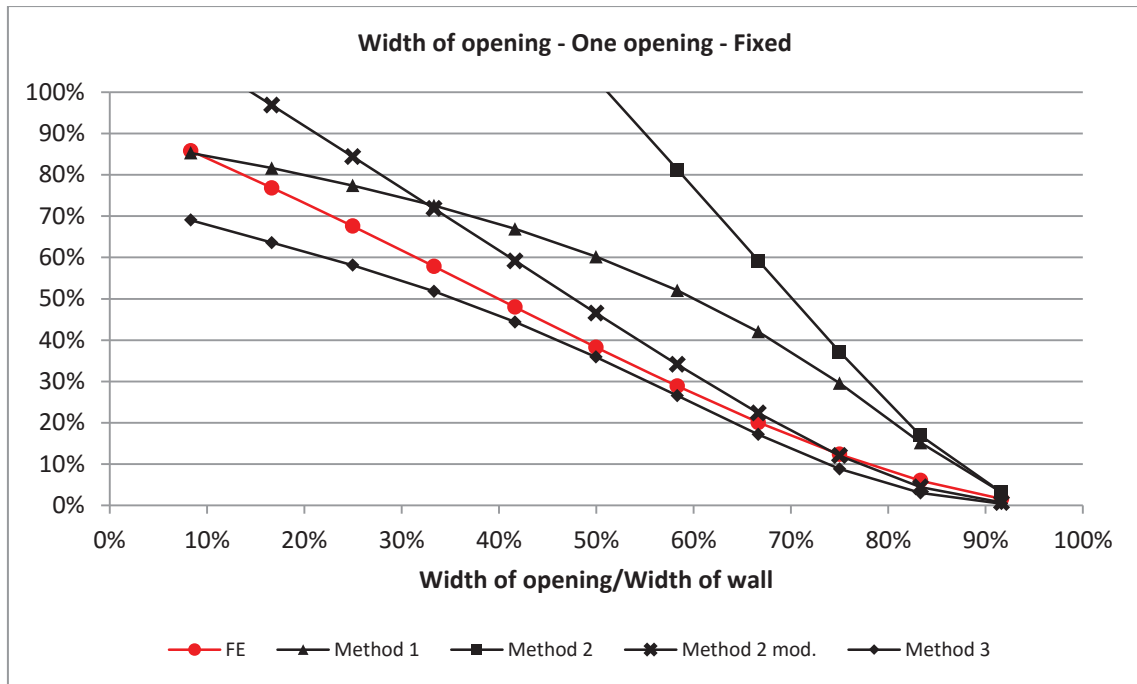


Figure C.22 Comparison between analytical and numerical stiffness calculations. Plotted as percentage of numerical stiffness of one wall element ($K = 5.75 \cdot 10^9$ [N/m]).

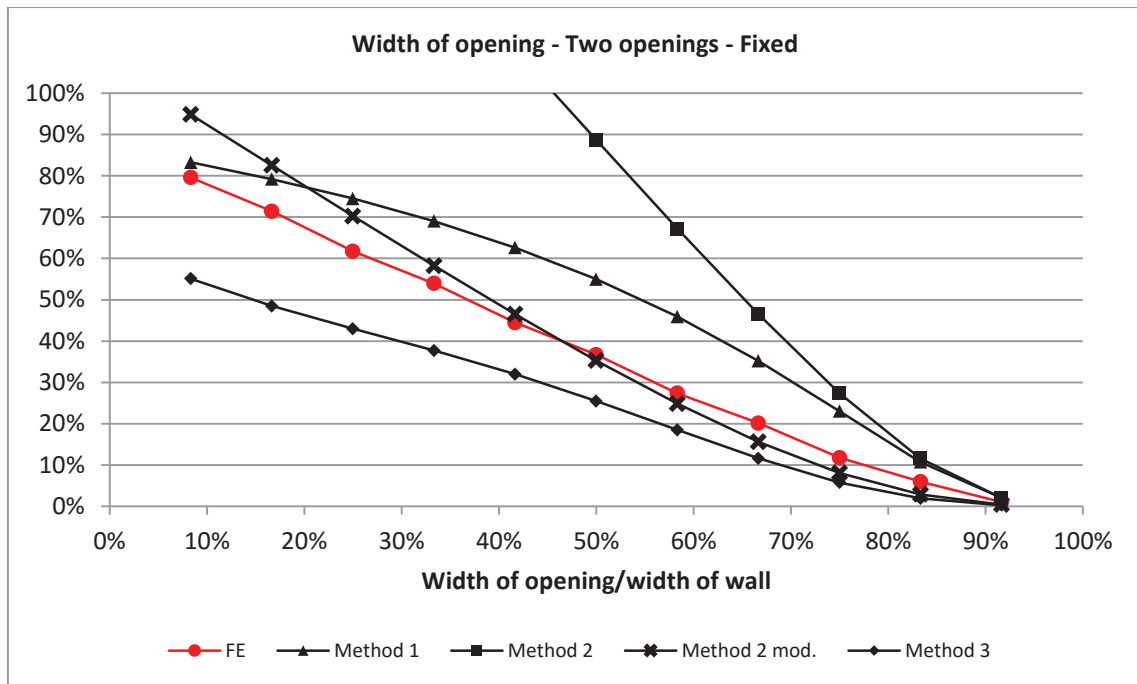


Figure C.23 Comparison between analytical and numerical stiffness calculations. Plotted as percentage of numerical stiffness of one wall element ($K = 5.75 \cdot 10^9$ [N/m]).

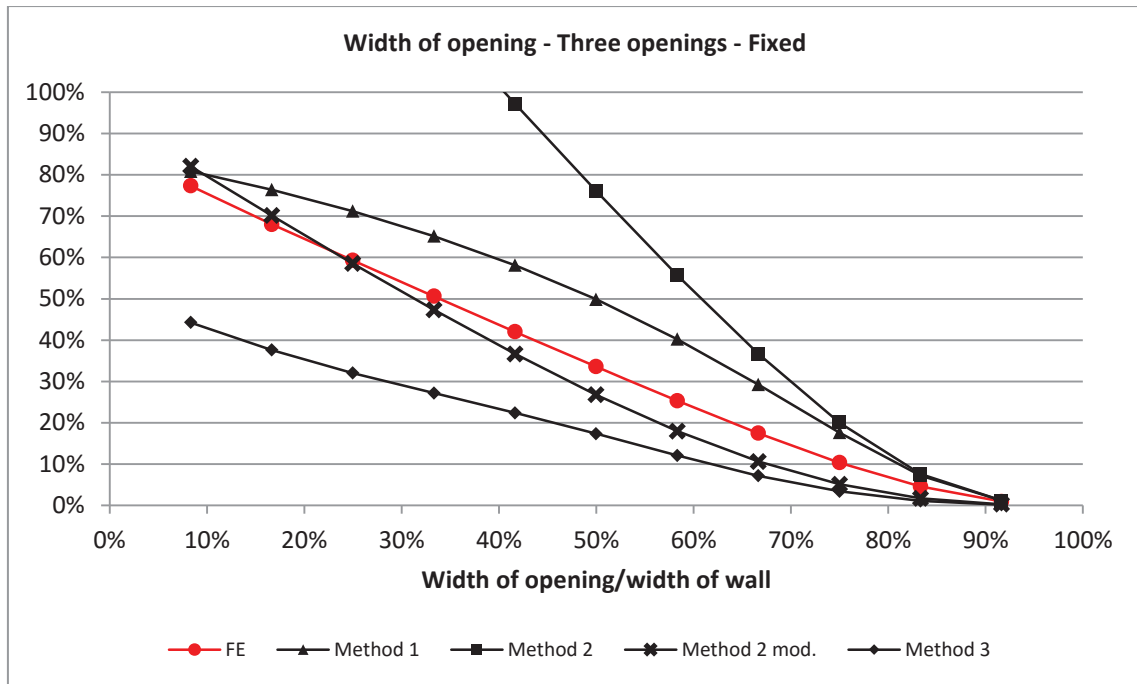


Figure C.24 Comparison between analytical and numerical stiffness calculations. Plotted as percentage of numerical stiffness of one wall element ($K = 5.75 \cdot 10^9$ [N/m]).

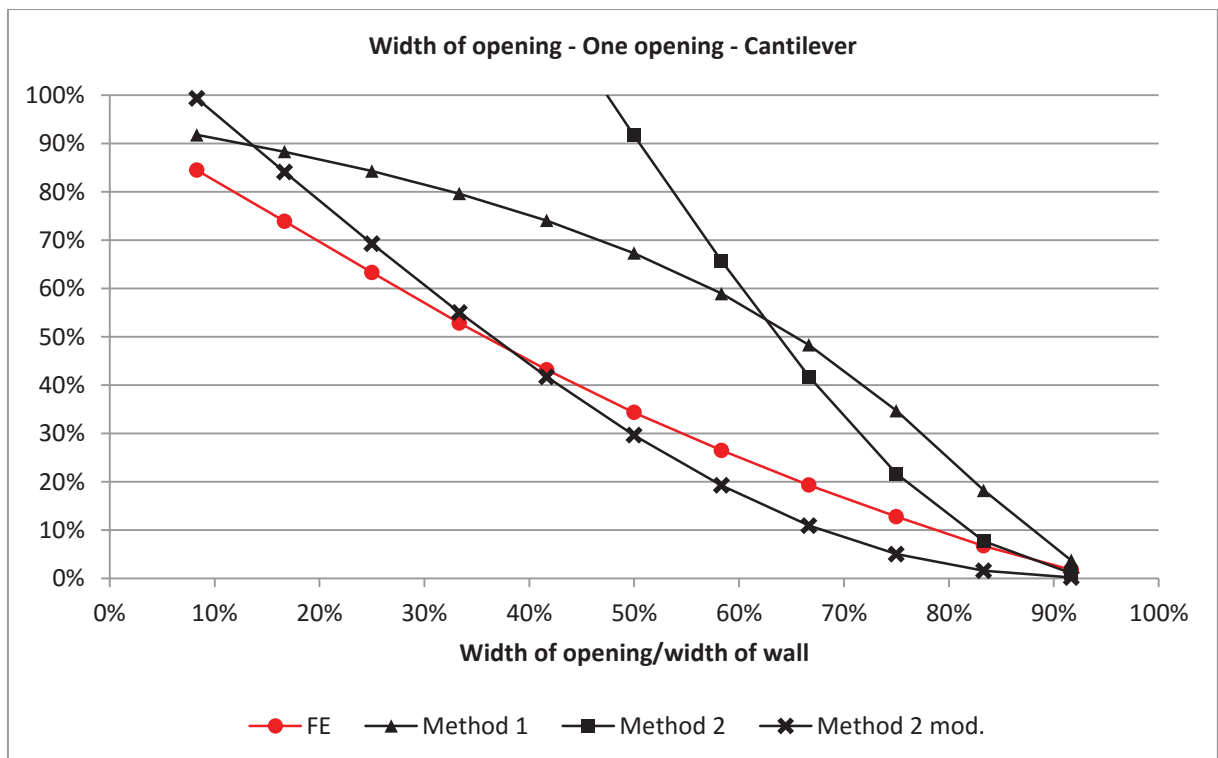


Figure C.25 Comparison between analytical and numerical stiffness calculations. Plotted as percentage of numerical stiffness of one wall element ($K = 4.66 \cdot 10^9$ [N/m]).

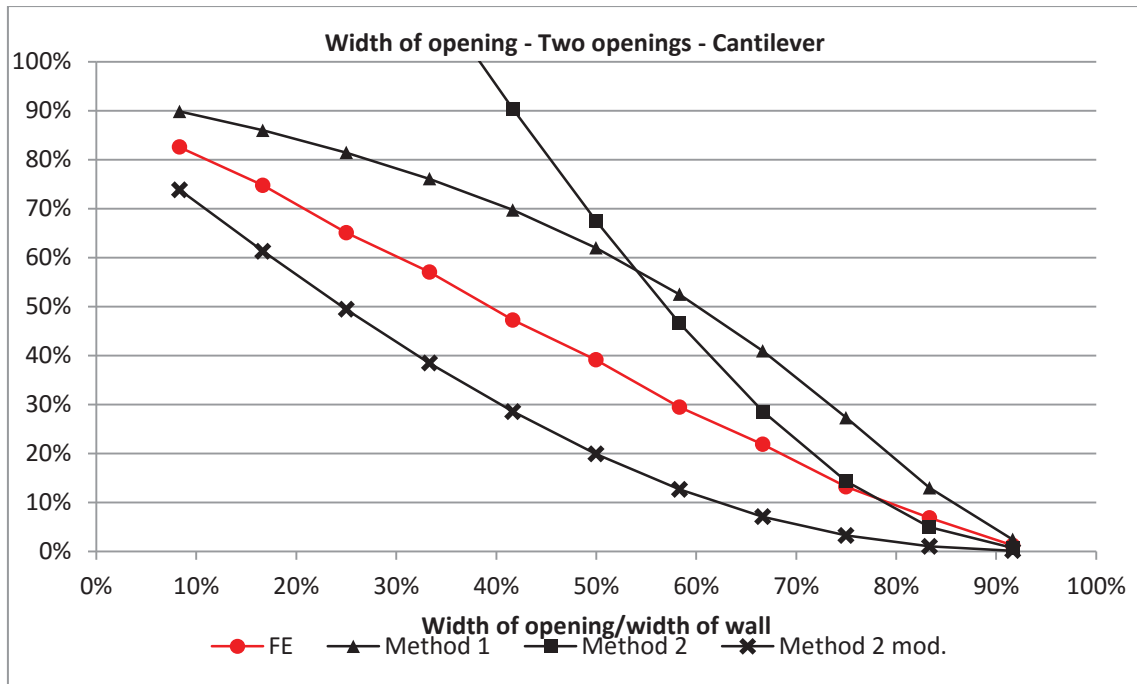


Figure C.26 Comparison between analytical and numerical stiffness calculations. Plotted as percentage of numerical stiffness of one wall element ($K = 4.66 \cdot 10^9$ [N/m]).

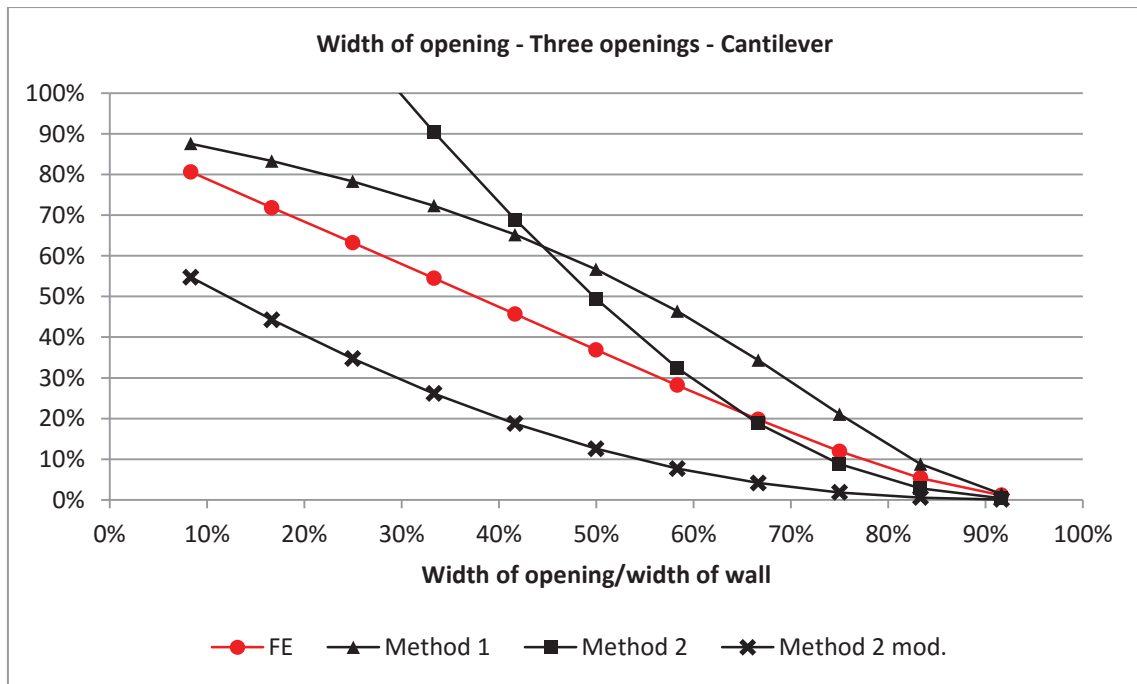


Figure C.27 Comparison between analytical and numerical stiffness calculations. Plotted as percentage of numerical stiffness of one wall element ($K = 4.66 \cdot 10^9$ [N/m]).

C.2 Tables

The tables show how many percentages each hand calculation method was of-set from the FE curve. The table also indicate with a green colour when the stiffness from a method was 0-10% from FE, and in which interval this happens.

		Method 1			
		Fixed		Cantilever	
		%	Span	%	Span
Position:					
	1	0-4 %	(-0,3 : 0,3)	0-10%, 10-18%	(-0,3 : -1,8),(-1,8 : 0,3)
	2	5-10 % , 10-15 %	(-0,3 : -0,25), (-0,25 : 0,3)	10-20%	(-0,3 : 0,3)
	3	8-10 % , 10-16%	(-0,3 : -0,275), (-0,275 : 0,3)	10-20%	(-0,3 : 0,3)
Height:					
	1	0-6 %	(0,1:0,9)	0-10 % ,10-20%	(0,1:0,25),(0,25:0,9)
	2	5-10%, 10-15%	(0,1:0,25 and 0,67:0,9),(remain)	10-25%	(0,1:0,9)
	3	0-10 % , 10-18 %	(0,58:0,9),(0,1:0,58)	0-10 % , 10-20%	(0,75:0,9),(0,1:0,75)
Width:					
	1	0-10%,10-23%	(0,1:0,25 and 0,83:0,9),(remain)	0-10%,10-33%	(0,1:0,17 and 0,83:0,9),(remain)
	2	0-10%,10-19%	(0,1:0,2 and 0,75:0,9),(remain)	0-10%,10-23%	(0,1:0,17 and 0,79:0,9),(remain)
	3	0-10%,10-14%	(0,1:0,17 and 0,7:0,9),(remain)	0-10%,10-20%	(0,1:0,17 and 0,75:0,9),(remain)

Figure C.28

		Method 2			
		Fixed		Cantilever	
		%	Span	%	Span
Position:					
	1	110%	(-0,3 : 0,3)	120%	(-0,3 : 0,3)
	2	60%	(-0,3 : 0,3)	40%	(-0,3 : 0,3)
	3	33-42 %	(-0,3 : 0,3)	0-10 % , 10-14 %	(-0,3:-0,25),(-0,25:0,3)
Height:					
	1	0-10 % , 10-940 %	(0,83:0,9),(0,1:0,83)	0-10 % , 10-1000 %	(0,8:0,9),(0,1:0,8)
	2	0-10 % , 10-750 %	(0,83:0,9),(0,1:0,83)	0-10 % , 10-900 %	(0,58:0,9),(0,1:0,58)
	3	0-10 % , 10-550 %	(0,7:0,9),(0,1:0,7)	0-10 % , 10-630 %	(0,42:0,9),(0,1:0,42)
Width:					
	1	0-10%,10-110%	(0,83:0,9),(0,1:0,83)	0-10%,10-130%	(0,72:0,9),(0,1:0,72)
	2	0-10%,10-100%	(0,75:0,9),(0,1:0,75)	0-10%,10-90%	(0,62:0,9),(0,1:0,62)
	3	0-10%,10-80%	(0,75:0,9),(0,1:0,75)	0-10%,10-60%	(0,5:0,9),(0,1:0,5)

Figure C.29

		Method 2 mod.			
		Fixed		Cantilever	
		%	Span	%	Span
Position:					
1	16-20 %		(-0,3 : 0,3)	0-10%, 10-14%	(-0,3 : 0),(0 : 0,3)
2	0-6 %		(-0,3 : 0,3)	18-29%	(-0,3 : 0,3)
3	7-10 %, 10-16 %		(-0,225 : 0,225), (remain)	24-33 %	(-0,3 : 0,3)
Height:					
1	0-10 %, 10-42 %		(0,65:0,9),(0,1:0,65)	0-10%, 10-39 %	(0,42:0,9),(0,1:0,42)
2	2-5%		(0,1:0,9)	12-19 %	(0,1:0,9)
3	0-10 %, 10-30 %		(0,33:0,9),(0,1:0,33)	8-10%, 10-50%	(0,75:0,9),(0,1:0,75)
Width:					
1	0-10%, 10-24%		(0,42:0,9),(0,1:0,42)	0-10 %, 10-15 %	(0,17:0,9),(0,1:0,17)
2	0-10%, 10-14%		(0,17:0,9),(0,1:0,17)	0-10 %, 10-19 %	(0,17:0,9),(0,1:0,17)
3	0-8%		(0,1:0,9)	0-10 %, 10-28 %	(0,75:0,9),(0,1:0,75)

Figure C.30

		Method 3	
		Fixed	
		%	Span
Position:			
1	13-20 %		(-0,3 : 0,3)
2	16-26 %		(-0,3 : 0,3)
3	16-26 %		(-0,3 : 0,3)
Height:			
1	3-10% , 10-26 %		(0,5:0,9),(0,1:0,5)
2	0-10%, 10-41 %		(0,5:0,9),(0,1:0,5)
3	0-10 %, 10-50 %		(0,5:0,9),(0,1:0,5)
Width:			
1	0-10 %, 10-16 %		(0,25:0,9),(0,1:0,25)
2	0-10 %, 10-25 %		(0,5:0,9),(0,1:0,5)
3	0-10 %, 10-33 %		(0,67:0,9),(0,1:0,67)

Figure C.31